ANTI-PROLIFERATIVE METABOLITES FROM THE ROOT OF *Calophyllum inophyllum* L.

Miss Syahadatain Nor Haerani

จุฬาลงกรณ์มหาวิทยาลัย
CHULALONGKORN UNIVERSITY

A Thesis Submitted in Partial Fulfillment of the Requirements

for the Degree of Master of Science in Chemistry

Department of Chemistry

FACULTY OF SCIENCE

Chulalongkorn University

Academic Year 2020

Copyright of Chulalongkorn University

เมทาบอไลต์จากรากของกระทิง *Calophyllum inophyllum* L.ที่มีฤทธิ์ยับยั้งการเจริญเติบโตของเซลล์

น.ส.ซาฮาดาเทน นอร์ เฮรานี

จุฬาลงกรณ์มหาวิทยาลัย
CHULALONGKORN UNIVERSITY

วิทยานิพนธ์นี้เป็นส่วนหนึ่งของการศึกษาตามหลักสูตรปริญญาวิทยาศาสตรมหาบัณฑิต
สาขาวิชาเคมี ภาควิชาเคมี
คณะวิทยาศาสตร์ จุฬาลงกรณ์มหาวิทยาลัย
ปีการศึกษา 2563
ลิขสิทธิ์ของจุฬาลงกรณ์มหาวิทยาลัย

Thesis Title	ANTI-PROLIFERATIVE METABOLITES FROM THE ROOT OF *Calophyllum inophyllum* L.
By	Miss Syahadatain Nor Haerani
Field of Study	Chemistry
Thesis Advisor	Professor KHANITHA PUDHOM, Ph.D.

Accepted by the FACULTY OF SCIENCE, Chulalongkorn University in Partial Fulfillment of the Requirement for the Master of Science

..... Dean of the FACULTY OF SCIENCE
(Professor POLKIT SANGVANICH, Ph.D.)

THESIS COMMITTEE

..... Chairman
(Associate Professor VUDHICHAI PARASUK, Ph.D.)

..... Thesis Advisor
(Professor KHANITHA PUDHOM, Ph.D.)

..... Examiner
(Associate Professor NATTAYA NGAMROJANAVANICH, Ph.D.)

..... External Examiner
(Assistant Professor Thanesuan Nuanyai, Ph.D.)

จุฬาลงกรณ์มหาวิทยาลัย
Chulalongkorn University

ซาฮาดาเทน นอร์ เฮรานี : เมทาบอไลต์จากรากของกระทิง *Calophyllum inophyllum* L.ที่มีฤทธิ์ยับยั้งการเจริญเติบโตของเซลล์. (ANTI-PROLIFERATIVE METABOLITES FROM THE ROOT OF *Calophyllum inophyllum* L.) อ.ที่ปรึกษาหลัก : ศ. ดร.ขนิษฐา พุดหอม

งานวิจัยนี้ศึกษาการแยกสารเมทาบอไลต์จากรากของ *C. inophyllum* L. และฤทธิ์ในการยับยั้งการเจริญของเซลล์มะเร็งตับและลำไส้ของสารที่แยกได้ จากการนำส่วนสกัดหยาบเฮกเซนและเอทิลอะซิเตทมาแยกด้วยเทคนิคทางโครมาโทกราฟีได้สารประกอบแซนโทนชนิดใหม่ 2 ชนิด (1 และ 2) และที่มีการรายงานแล้วอีก 12 ชนิด (3-14) นอกจากนี้พบว่าสาร 4 6 และ 8 แยกได้จากพืชสกุล *Calophyllum* เป็นครั้งแรก เมื่อนำสารเมทาบอไลต์ที่แยกได้มาทดสอบฤทธิ์ในการยับยั้งการเจริญของเซลล์มะเร็งตับ Hep-G2 และมะเร็งลำไส้ HCT-116 พบว่า สาร 5 และ 14 มีฤทธิ์ดีที่สุดในการยับยั้งเซลล์มะเร็งทั้งสองชนิด โดยสารทั้งสองสามารถยับยั้งการเจริญของเซลล์มะเร็งลำไส้ HCT-116 ได้ดีด้วยค่า IC_{50} 3.04 μM นอกจากนี้ยังพบว่าสาร 5 และ 14 มีฤทธิ์ยับยั้งเซลล์มะเร็งตับ Hep-G2 ได้ดีด้วยโดยมีค่า IC_{50} 6.07 และ 5.94 μM ตามลำดับ ดังนั้นจึงนำสาร 14 มาศึกษากลไกการออกฤทธิ์ต่อเซลล์ Hep-G2 ด้วยวิธี western blot ซึ่งพบว่าสาร 14 สามารถเหนี่ยวนำให้เซลล์ตายแบบอะพอพโทซิสได้โดยกดการแสดงออกของทั้งโปรตีน Bcl-2 และ Bcl-XL ตามลำดับความเข้มข้นของสาร

จุฬาลงกรณ์มหาวิทยาลัย
CHULALONGKORN UNIVERSITY

สาขาวิชา เคมี ลายมือชื่อนิสิต .....

ปีการศึกษา 2563 ลายมือชื่อ อ.ที่ปรึกษาหลัก .....

6172176423 : MAJOR CHEMISTRY

KEYWORD: Calophyllum inophyllum L., Xanthones, Anti-proliferative

Syahadatain Nor Haerani : ANTI-PROLIFERATIVE METABOLITES FROM THE ROOT OF *Calophyllum inophyllum* L.. Advisor: Prof. KHANITHA PUDHOM, Ph.D.

This study aimed to isolate secondary metabolites from the root of *C. inophyllum* L. and to evaluate their anti-proliferative activities against hepatocellular carcinoma and colorectal cancer cells. Chromatographic fractionation of the *n*-hexane and ethyl acetate crude extracts led to the isolation of two new (1 and 2) and twelve known xanthones (3-14). In addition, metabolites 4, 6 and 8 were isolated from the genus *Calophyllum* for the first time. All metabolites were evaluated for their anti-proliferative activity against Hep-G2 and HCT-116 cell lines. Metabolites 5 and 14 showed the most active metabolites against both cancer cells, as well as they displayed strong activities toward HCT-116 with the same IC_{50} value of 3.04 μM. Moreover, both of them exhibited potent activities against Hep-G2 with IC_{50} values of 6.07 and 5.94 μM, respectively. Further, metabolite 14 was subjected to western blot analysis to study its mechanism of action against Hep-G2 cells. The result demonstrated that 14 induced apoptosis in a concentration-dependent manner by the down-regulation of the expression of both Bcl-2 and Bcl-XL proteins.

จุฬาลงกรณ์มหาวิทยาลัย
Chulalongkorn University

Field of Study: Chemistry Student's Signature .....

Academic Year: 2020 Advisor's Signature .....

ACKNOWLEDGEMENTS

First and foremost, praise and thank God, the Almighty Allah, for His showers of blessings throughout my research work to complete the thesis.

I want to express my deep sense of thanks and gratitude to my advisor, Professor Dr. Khanitha Pudhom, Department of Chemistry, Faculty of Science, Chulalongkorn University, for her excellent instruction and valuable guidance, which motivated me to pass through this course successfully.

Moreover, many thanks to the Chairperson: Associate Professor Dr. Vudhichai Parasuk, Department of Chemistry, Faculty of Science, Chulalongkorn University; the thesis examiners: Associate Professor Dr. Nattaya Ngamrojanavanich, Department of Chemistry, Faculty of Science, Chulalongkorn University, and Assistant Professor Dr. Thanesuan Nuanyai, Faculty of Liberal Arts, Rajamangala University of Technology Rattanakosin; for their invaluable discussion and suggestion.

I wish to thank Chulalongkorn University Funding. I am honored to be one of the ASEAN Scholarship awardees. Thanks for the financial support to conduct my two years master's degree.

Special thanks to my fellow lab-mates in KP Lab for all discussions, sharing knowledge and ideas, working overtime together and every memory we have had in the last two years. I am extremely grateful to my parents and my family for their love, prayers and support throughout my life. Last but not least, thanks to everyone for all memories and experiences.

Syahadatain Nor Haerani

จุฬาลงกรณ์มหาวิทยาลัย
Chulalongkorn University

TABLE OF CONTENTS

Page

ABSTRACT (THAI) iii

ABSTRACT (ENGLISH) iv

ACKNOWLEDGEMENTS v

TABLE OF CONTENTS vi

LIST OF FIGURES x

LIST OF SCHEMES xii

LIST OF TABLES xiii

LIST OF ABBREVIATIONS xiv

CHAPTER I INTRODUCTION 1

1.1 General Background 1

1.2 Introduction of *Calophyllum inophyllum* L. 4

1.2.1 Taxonomy of *C. inophyllum* L. 7

1.2.2 Botany of *C. inophyllum* L. 8

1.3 Literature review 9

1.3.1 Phytochemical metabolites from *C. inophyllum* 9

1.3.1.1 Coumarins 9

1.3.1.2 Xanthones 10

1.3.1.3 Flavonoids 10

1.3.1.4 Terpenoids 10

1.3.1.5 Other types of metabolites 10

1.3.2 Biologically active metabolites from *C. inophyllum* 11

จุฬาลงกรณ์มหาวิทยาลัย
Chulalongkorn University

1.3.2.1 Anti-cancer activity 11
1.3.2.2 Anti-inflammatory activity 12
1.3.2.3 Larvicidal activity 12
1.3.2.4 Chemotherapeutic activity 12
1.3.2.5 Anti-bacterial activity 12
1.3.2.6 Wound-healing activity 13
1.3.2.7 Anti-HIV activity 13
1.4 Objectives of the present study 14
CHAPTER II EXPERIMENTS 15
2.1 Plant Materials 15
2.2 General Experimental Procedures 15
2.2.1 Thin-layer chromatography (TLC) 15
2.2.2 Column chromatography 15
2.2.3 Nuclear magnetic resonance spectroscopy (NMR) 16
2.2.4 Mass spectrometry (MS) 16
2.2.5 Fourier transforms infrared spectrophotometry (FT-IR) 16
2.2.6 Optical Rotation 16
2.2.7 Melting Point 16
2.2.8 Ultraviolet-visible spectrophotometry (UV-vis) 16
2.3 Chemicals 16
2.4 Extraction and isolation 17
2.4.1 Extraction of dried sample 17
2.4.2 Isolation of metabolite from *n*-hexane crude extract 17
2.4.3 Isolation of metabolites from EtOAc crude extract 18

จุฬาลงกรณ์มหาวิทยาลัย
Chulalongkorn University

2.5 Biological assay 22
2.5.1 Cell culture 22
2.5.2 Anti-proliferative assay 22
2.5.3 Western blot analysis 23
2.5.4 Statistical analysis 24
CHAPTER III RESULTS AND DISCUSSION 25
3.1 Secondary metabolites from the root of *C. inophyllum* 25
3.2 Structure elucidation of isolated metabolites 27
3.2.1 Structure elucidation of metabolite 1 27
3.2.2 Structure elucidation of metabolite 2 28
3.2.3 Structure elucidation of metabolite 3 30
3.2.4 Structure elucidation of metabolite 4 33
3.2.5 Structure elucidation of metabolite 5 34
3.2.6 Structure elucidation of metabolite 6 35
3.2.7 Structure elucidation of metabolite 7 38
3.2.8 Structure elucidation of metabolite 8 38
3.2.9 Structure elucidation of metabolite 9 39
3.2.10 Structure elucidation of metabolite 10 40
3.2.11 Structure elucidation of metabolite 11 43
3.2.12 Structure elucidation of metabolite 12 43
3.2.13 Structure elucidation of metabolite 13 44
3.2.14 Structure elucidation of metabolite 14 45
3.2.15 Proposed biosynthesis pathway of isolated metabolites 48
3.3 Anti-proliferative activity 50

จุฬาลงกรณ์มหาวิทยาลัย
Chulalongkorn University

3.4 Study on action mechanism of macluraxanthone (14) 52

CHAPTER IV CONCLUSION 57

REFERENCES 58

APPENDIX 69

VITA 99

จุฬาลงกรณ์มหาวิทยาลัย
Chulalongkorn University

LIST OF FIGURES

Figure 1.1 Illustration of cell proliferation in healthy and cancer cell [17].....3

Figure 1.2 Major classes of metabolites of *C. inophyllum* 7

Figure 1.3 *C. inophyllum* L. Alexandrian Laurel 9

Figure 1.4 Representative metabolites from *C. Inophyllum* 11

Figure 1.5 Representative bioactive metabolites from *C. inophyllum* 13

Figure 3.1 Structures of secondary metabolites from the root of *C. inophyllum* 26

Figure 3.2 Structure of metabolite **1**.....27

Figure 3.3 ^{1}H-^{1}H COSY and HMBC correlations of metabolite **1**.....28

Figure 3.4 Structure of metabolite **2**.....28

Figure 3.5 ^{1}H-^{1}H COSY and HMBC correlations of metabolite **2**.....29

Figure 3.6 Structure of metabolite **3**.....30

Figure 3.7 Structure of metabolite **4**.....33

Figure 3.8 ^{1}H-^{1}H COSY and HMBC correlations of metabolite **4**.....33

Figure 3.9 Structure of metabolite **5**.....34

Figure 3.10 ^{1}H-^{1}H COSY and HMBC correlations of metabolite **5** 34

Figure 3.11 Structure of metabolite **6** 35

Figure 3.12 ^{1}H-^{1}H COSY and HMBC correlations of metabolite **6** 35

Figure 3.13 Structure of metabolite **7** 38

Figure 3.14 Structure of metabolite **8** 38

Figure 3.15 ^{1}H-^{1}H COSY and HMBC correlations of metabolite **8** 39

Figure 3.16 Structure of metabolite **9** 39

Figure 3.17 ^{1}H-^{1}H COSY and HMBC correlations of metabolite **9** 40

จุฬาลงกรณ์มหาวิทยาลัย
Chulalongkorn University

Figure 3.18 Structure of metabolite **10**.....40

Figure 3.19 Structure of metabolite **11**.....43

Figure 3.20 Structure of metabolite **12**.....43

Figure 3.21 ^{1}H-^{1}H COSY and HMBC correlations of metabolite **12**.....44

Figure 3.22 Structure of metabolite **13**.....44

Figure 3.23 ^{1}H-^{1}H COSY and HMBC correlations of metabolite **13**.....45

Figure 3.24 Structure of metabolite **14**.....45

Figure 3.25 Proposed biosynthesis pathway of isolated metabolites.....49

Figure 3.26 Summary of SAR of xanthone skeleton for anti-proliferative activity.....51

Figure 3.27 Extrinsic and intrinsic pathways of apoptosis.....53

Figure 3.28 Effects of **14** on the expression level of Bcl-2 and Bcl-XL proteins. Inhibitory effects of **14** on Bcl-2 and Bcl-XL expressions in Hep-G2 cell lines in concentration-dependent manner (**A**). The levels of Bcl-2 and Bcl-XL proteins were examined by western blot analysis. The relative Bcl-2 and Bcl-XL proteins were measured by densitometry analysis (**B**). 56

จุฬาลงกรณ์มหาวิทยาลัย
CHULALONGKORN UNIVERSITY

LIST OF SCHEMES

Scheme 2.1 Extraction of *C. inophyllum* root 17

Scheme 2.2 Isolation procedure of fraction F 18

Scheme 2.3 Isolation procedure of EtOAc crude extract 19

Scheme 2.4 Isolation procedure of fraction P5 19

Scheme 2.5 Isolation of fractions P5.2, P5.6 and P5.9 20

Scheme 2.6 Isolation of fractions P5.12 and P5.13 21

Scheme 2.7 Isolation of fractions Q4 and Q5 22

จุฬาลงกรณ์มหาวิทยาลัย
Chulalongkorn University

LIST OF TABLES

Table 3.1 ^{1}H-NMR data of metabolites **1**-**3** 31

Table 3.2 ^{13}C-NMR data of metabolites **1**-**3** 32

Table 3.3 ^{1}H-NMR data of metabolites **4**-**7** 36

Table 3.4 ^{13}C-NMR data of metabolites **4**-**7** 37

Table 3.5 ^{1}H-NMR data of metabolites **8**-**10** (acetone-d_6, 500 MHz) 41

Table 3.6 ^{13}C-NMR data of metabolites **8** and **9** (acetone-d_6, 125 MHz) 42

Table 3.7 ^{1}H-NMR data of metabolites **11**-**14** 46

Table 3.8 ^{13}C-NMR data of metabolites **11**-**14** 47

จุฬาลงกรณ์มหาวิทยาลัย
Chulalongkorn University

LIST OF ABBREVIATIONS

J	Coupling constant
δ	Chemical shift
δ_H	Chemical shift proton
δ_C	Chemical shift carbon
s	Singlet (for NMR spectra)
d	Doublet (for NMR spectra)
dd	Doublet of doublet (for NMR spectra)
t	Tripet (for NMR spectra)
m	Multiplet (for NMR spectra)
q	Quartet (for NMR spectra)
brs	Broad singlet (for NMR spectra)
qC	Quaternary carbon
calcd.	Calculated
^{1}H NMR	Proton nuclear magnetic resonance
^{13}C NMR	Carbon-13 nuclear magnetic resonance
2D NMR	Two-dimensional nuclear magnetic resonance
^{1}H-^{1}H COSY	Homonuclear (proton-proton) correlation spectroscopy
HSQC	Heteronuclear single quantum coherence
HMBC	Heteronuclear multiple bond correlation
HRESIMS	High-resolution electrospray ionization mass spectrometry
CC	Column chromatography
RP-18	Reversed-phase C-18
TLC	Thin-layer chromatography
IC_{50}	Half maximal inhibitory concentration

$CDCl_3$	Deuterated chloroform
Acetone-d_6	Deuterated acetone
MeOH	Methanol
EtOH	Ethanol
CH_2Cl_2	Dichloromethane
EtOAc	Ethyl acetate
DMSO	Dimethylsulfoxide
$(NH_4)_6Mo_7O_{24}$	Ammonium molybdate
H_2SO_4	Sulfuric acid
SiO_2	Silicon dioxide
g	Gram (s)
mg	Milligram (s)
mL	Milliliter (s)
µg	Microgram (s)
µL	Microliter (s)
µM	Micromolar
mM	Millimolar
L	Liter (s)
M	Molar
min	Minute
H	Hour
m	Meter (s)
mm	Millimeter (s)
cm	Centimeter (s)
nm	Nanometer
Hz	Hertz
MHz	Megahertz

จุฬาลงกรณ์มหาวิทยาลัย
Chulalongkorn University

cm^{-1}	Reciprocal centimeter (unit of wavenumber)
ppm	Part per million
NMR	Nuclear magnetic resonance
MS	Mass spectrometry
IR	Infrared
UV	Ultraviolet
$[M+H]^+$	Protonated molecule
$[M+Na]^+$	Pseudomolecular ion
m.p.	Melting Point
α	Alpha
β	Beta
γ	Gamma
$[\alpha]^{24}_{D}$	Specific rotation at 24 °C and sodium D line (589 nm)
λ_{max}	The wavelength of maximum absorption
c	Concentration
ε	Molar extinction coefficient
°C	Degree Celcius
deg.	Degree
spp.	Species
No.	Number

จุฬาลงกรณ์มหาวิทยาลัย
Chulalongkorn University

CHAPTER I
INTRODUCTION

1.1 General Background

Cancer is one of the top health problems worldwide. Based on the World Health Organization (WHO) data, cancer is the second leading cause of death globally. In 2018, there was 9.6 million death caused by cancer [1]. The top five most common causes of cancer death are lung, colorectal, stomach, liver and breast cancer [2]. In Thailand, four of those cancers were the top five new cases in 2018 [3]. In this research we will focus on colon and liver cancer cell lines.

One of the crucial factors in the development of colon cancer is inflammatory bowel disease (IBD). IBD patients with a family history of colorectal cancer (CRC) have more than twice the higher risk for colon cancer development. However, environmental and food-borne mutagens are the most causes of CRC than genetic changes [4]. Besides, dietary factors may account for up to 90% of colon cancer [5]. Two hypotheses, overconsumption of food in general and a sedentary lifestyle, may increase colon cancer development risk. Intake of meat, protein and alcohol may increase the risk. Meanwhile, anti-oxidant, folate, calcium and vitamin D may be protective [6].

จุฬาลงกรณ์มหาวิทยาลัย
Chulalongkorn University

Hepatocellular carcinoma (HCC) is the most familiar form of liver cancer, approximately 70-85% of cases worldwide, and more than 80% of those occur in developing countries [7, 8]. The relative survival rates are less than 11% within five years, even in developed countries [8]. People with hepatitis B virus (HBV) and hepatitis C virus (HCV) are at risk of developing liver cirrhosis and liver cancer. A blood infection most likely transmits HBV and HCV. High-risk behaviors of new infections are related to drug injection, tattooing and piercing [9]. The infection of HBV affects cellular signaling and growth control. Meanwhile, HCV leads to chronic

inflammation, cell death and proliferation [8]. Besides, obesity, type 2 diabetes and nonalcoholic fatty liver disease might be other pathogenic promoters for the liver disease [7].

The hallmarks of cancer provides a useful principle for studying various mechanisms of cancer progression [10]. There are six hallmarks of cancer [11]:

1. Sustaining proliferative signaling
2. Evading growth suppressors
3. Activating invasion and metastasis
4. Enabling replicative immortality
5. Inducing angiogenesis
6. Resisting cell death

In this study, we will focus on the first hallmarks of cancer.

The most fundamental properties of the living cell are cell proliferation, cell replication's leading proses. A single cell can replicate up to 10^{13} cells in the replication process [12]. Cell proliferation will eventually stop due to the balance of cell death and cell growth. Meanwhile, proliferation of cancer cell will be uncontrolled cellular growth (**Figure 1.1**). Thus, anti-proliferative metabolites are needed to suppress cancer cells' replication by inhibiting or stopping cell growth.

Metastasis is the spread of cancer cells into the surrounding tissue. It is a multistep process that includes cell migration. One of the earliest development methods to study cell migration in vitro is the wound-healing assay. This method focuses on monitoring migration cells toward a wound that is scratched on a cell monolayer. This method imitates cell migration through cell migration in vivo, even if it is not an exact copy [13].

Doxorubicin is most frequently used for cancer therapy, for example, breast, stomach, lung, ovaries, thyroid and lymphoma. Nevertheless, doxorubicin's

cumulative dose manifests adverse effect such as cardio toxicity, a chronic complication of cardiomyopathy [14]. Sorafenib is a potential therapeutic drug for renal carcinoma and hepatocellular carcinoma. However, some adverse events, including diarrhea, weight loss, hypertension and abdominal pain, have been reported. Some patients also undergo resistance to sorafenib due to genetic heterogeneity of hepatocellular carcinoma [15]. Consequently, the finding of novel anti-cancer candidates carries on essential issues. Along with that, natural products have been a potential source of lead metabolites for drug discovery and development [16].

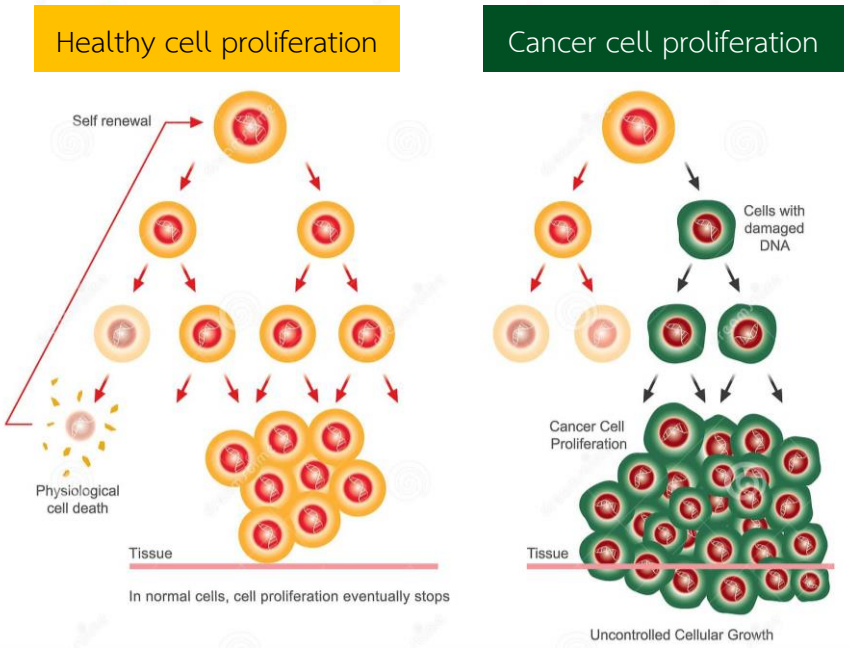

Figure 1.1 Illustration of cell proliferation in healthy and cancer cell [17]

Some plant-derived natural products showed good activity against cancer cell lines. Antrovirisidone B was isolated from the roots of *Garcinia antroviridis*. It showed cytotoxic activity against MCF-7 (human breast), DU-145 (human prostate) and H-460 (human lung) cancer cells with IC_{50} values of 22.93, 9.34 and 16.47 μM, respectively [18]. Cowanin, 3,6-dimethyl-γ-mangostin, norcowanin and cowaxanthone were isolated from the twigs of *G. cowa*. These metabolites exhibited cytotoxic activity

toward NCI-H187 (human, small cell lung cancer) with IC_{50} values of 7.03, 8.58, 5.92 and 3.87 μg/mL, respectively. Besides, these metabolites also displayed cytotoxic activity against KB (oral human epidermal carcinoma) with IC_{50} values of 7.36, 6.64, 6.43 and 15.43 μg/mL, respectively [19]. 30-Epicambogin and guttiferone K were isolated from the twigs of *G. cowa*. The isolated metabolites demonstrated their selective cytotoxicity against HT-29 (human colon cancer) with IC_{50} values of 5.51 and 5.54 μM, respectively [20]. 1,6-Dihydroxy-5-methoxyxanthone was isolated from *G. cowa.* This metabolite was highly active against HT-29 and P-388 (mouse lymphocytic leukemia) cells with an IC_{50} values of 0.84 and 0.27 μg/mL, respectively [21]. 1,7-Dihydroxyxanthone was isolated from *G. linii.* It exhibited anti-proliferative activity against both HT-29 and P-388 cells with an IC_{50} value of 3.94 μg/mL [22]. 8-Methoxysmyrindiol from *Gerbera anandria* showed cytotoxicity against Hep-G2 (liver cancer) with IC_{50} value of 5.3 μg/mL [23]. 1,5-Dihydroxyxanthone was isolated from *Allanblackia floribunda.* This metabolite significantly inhibited HT-29, P-388 and KB cell lines with an IC_{50} values of 5.01, 4.71 and 3.30 μg/mL, respectively [24]. 3',4'-Deoxy-4'-chloropsoroxanthin-3',5'-diol and psoroxanthin were isolated from *Psorospermum molluscum*, displayed significant cytotoxic effects against A2780 (human ovary cancer) (IC_{50}: 0.0042 and 0.33 μM, respectively) and HCT-116 (IC_{50}: 0.0068 and 0.10 μM, respectively). 3',4'-Deoxy-4'-chloropsoroxanthin-3',5'-diol also showed cytotoxicity toward SKBR3 (human breast cancer) with IC_{50} value of 2.0 μM) [25]. Those studies lead us to isolate metabolites from the plant species *Calophyllum inophyllum* and evaluate their anti-proliferative activity toward colon and liver cancer cell lines.

จุฬาลงกรณ์มหาวิทยาลัย
CHULALONGKORN UNIVERSITY

1.2 Introduction of *Calophyllum inophyllum* L.

The genus *Calophyllum* belongs to the Calophyllaceae family, has approximately 186 species, 14 of which occur in Thailand. Secondary metabolites

produced from the genus *Calophyllum* have been a global interest for its pharmacological actions, including anti-cancer activity. Calotetrapterins A-C were isolated from the stem barks of *C. tetrapterum.* Those metabolites showed good activity against P-388 cell lines with IC_{50} values of 5.4, 1.0 and 4.1 μM, respectively [26]. Ananixanthone was obtained from the stem bark of *C. teysmannii*. It was inhibiting SNU-1 (stomach), LS174T (colon) and K562 (leukemia) cancer cell lines with IC_{50} values of 8.97, 7.48 and 2.96 μM, respectively [27]. Calaxanthone C was isolated from the root of *C. calaba*. It was tested against five cancer cell lines such as KB, HeLa S-3 (cervical adenocarcinoma), HT-29, MCF-7 and Hep-G2. Calaxanthone C displayed promising activity with IC_{50} values of 1.72, 0.82, 1.17, 5.04 and 1.65 μM, respectively [28]. Inophynnin and pyranojacareubin were afforded from *C. inophyllum*. Inophinnin showed good activity toward HeLa cancer cell line with IC_{50} value of 9.51 μM, while pyranojacareubin displayed IC_{50} value of 8.62 μM against K562 cancer cell line. Besides, *C. soulattri* gave soulattrin, phyllattrin, caloxanthone C and trapezifolixanthone. Soulattrin inhibited SNU-1, HeLa, NCI-H23 and K562 cancer cell lines with IC_{50} values of 1.98, 2.77, 2.64 and 2.23 μM, respectively. Phylattrin showed IC_{50} values of 9.79 and 9.20 μM against SNU-1 and HeLa, respectively. Trapezifolixanthone displayed good activity against HeLa cancer cell lines with IC_{50} value of 7.57 μM [29]. For these reasons, this current research focuses on the isolation of chemical constituents from the root of *C. inophyllum* L.

จุฬาลงกรณ์มหาวิทยาลัย
CHULALONGKORN UNIVERSITY

C. inophyllum is one species of the genus *Calophyllum*. The distribution of this genus is worldwide in tropical areas, including Africa, North and South America, Tropical and Temperate Asia, Australasia and the Pacific. *C. inophyllum* is used in many countries for different purposes. In Java (Indonesia), the seed oil and latex are used to dye batik cloth. Durable and robust timber was used as a general-purpose timber for masts, bridgework, boat building and cabinet making. The oil produced

from the fruits is used to treat ulcers, rheumatism and skin diseases. A decoction of the bark and latex are used internally and externally to remedy many infections, skin and eye diseases and rheumatism. The flowers, leaves and seeds are also used for local medicine. Although this tree grows slowly, it is also used for reforestation and afforestation projects and it placed at shorelines to protect the coast [30].

Seventeen species of the genus *Calophyllum* were found naturally in Thailand, namely: *C. calaba, C. canum*, C*. dryobalanoides*, *C. depressinervosum*, C*. inophyllum*, *C. macrocarpum*, *C. molle*, *C. pisiferum*, *C. polyathum, C. rupicola*, *C. sclerophyllum*, *C. soulattri*, *C. symingtonianum*, *C. tetrapterum*, *C. teysmannii*, *C. thorelii* and *C. touranense. C. inophyllum* is usually found in beach forest or coastal area and commonly plated for ornamental trees. *C. inophyllum* is locally known as Kra thing (กระทิง) (Central), saaraphee thale (สารภีทะเล) (Prachuap Khiri Khan) and thing (ทิง) (Krabi). *C. inophyllum* is also known as "Alexandrian Laurel" [31]. A numbers of metabolites have been isolated from the genus *Calophyllum*. Those metabolites showed potential sources for a wide range of drug discovery and development. A phytochemical study of *C. inophyllum* reported that coumarins, xanthones, flavonoids and triterpenoids are the major metabolites (**Figure 1.2**). Those chemical constituents were obtained from their bark, root, seed, fruit and leaves. Coumarins are phenolic metabolites, mostly found in the leaves and classified as simple coumarins, furanocoumarins, pyranocoumarins and furo-puranocoumarins [16]. The previous report showed their anti-hyperglycemic and neuroprotective activity. Xanthones are heterocyclic metabolites containing oxygen. Xanthones can be classified into simple xanthones, xanthone glycosides, prenylated xanthones, bisxanthones and xanthonolignoids [32]. Xanthones have well-known medicinal chemistry roles due to broad-spectrum as pharmacological agents, such as anti-microbial, anti-cancer, anti-oxidant, anti-inflammatory and anti-viral activity.

จุฬาลงกรณ์มหาวิทยาลัย
Chulalongkorn University

Flavonoids such as amentoflavone and carpachromene showed promising α-glucosidase activity [33]. Triterpenoids are metabolites that contain six isoprene units and exhibited a wide spectrum of bioactivities, including bactericidal, cardiovascular, analgesic and anti-allergic properties [34].

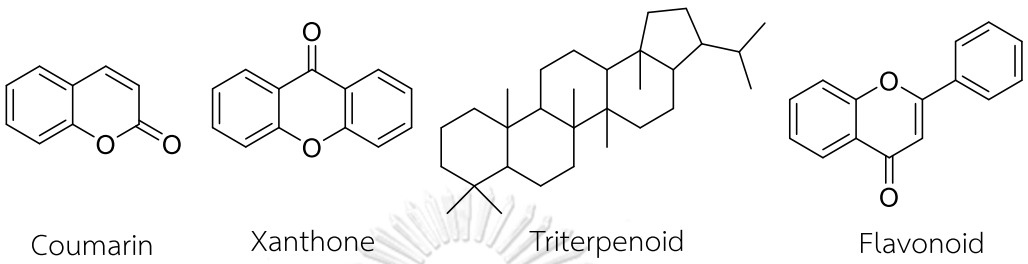

Figure 1.2 Major classes of metabolites of *C. inophyllum*

1.2.1 Taxonomy of *C. inophyllum* L.

The genus *Calophyllum* was previously included in the Clusiacease, also known as Guttiferae family before APG III (Angiosperm Phylogeny Group 2009). Based on the APG III system of flowering plant classification, this genus is now placed in the Calophyllaceae family [16]. Based on the Integrated Taxonomical Information System (ITIS), taxonomy of *C. inophyllum* L. is classified as:

จุฬาลงกรณ์มหาวิทยาลัย
Chulalongkorn University

Kingdom: Plantae

Division: Tracheophyta

Class: Magnoliopsida

Order: Malpighiales

Family: Calophyllaceae

Genus: *Calophyllum* L.

Species: *Calophyllum inophyllum* L.

1.2.2 Botany of *C. inophyllum* L.

C. inophyllum is a tree up to 7-30 m tall without buttresses. The diameter of breast height is 11-12 cm. Outer bark slightly fissured, rough, grey to brown; exudate the color of clear honey. The branchlets are striate, slightly brown pubescent or glabrous, with yellow-greenish sap in the center of branchlets. It has an internode 2-3 cm long. The leaves are petioled for 1.5-3 cm long; blade 8-15 × 4-8 cm, elliptic-obovate, sometimes oblong, obtuse, rounded, coriaceous, dark green and concave adaxially, dull green and convex adaxially, rarely glaucous, base cuneate to attenuate, apex retuse to round, rarely acute or emarginate; midrib depressed on the upper surface in the channel about ¾ of lamina length, underside raised, secondary veins present, dense and distinct on both surfaces, 6-8 veins per 0.5 cm. The inflorescence is axillary panicles 5-10 cm long, pubescent or glabrous, up to 12 flowers per inflorescence, pedicels 0.6-4 cm long. The floral parts are tepals 8, reflexed when the flower is fully open, the outer pain oval to suborbicular, glabrous, imbricate the next pair elliptic and the inner pairs elliptic to obovate. The stamens in fascicles but not distinct fascicles, 40-250 stamens per flower; filaments 4-5 mm long, white to yellow-green; anthers 1-1.5 mm long, bright yellow/orange. Ovary is subglobose, 1.5-3.5 mm long; style 5-7 mm long with flat stigma, almost white, 8-9 mm long, has one ovule, red. Fruit globose, apex round, 2.5-3.2 × 3 cm. Ecology and phenology: evergreen and deciduous forests, marshy ground, sandy and rocky shorelines, from near sea level to 300 m. It's flowering around October-December. It's fruiting for all year. Visited by bees [30]. The picture of *C. inophyllum* L. and its various parts are shown in **Figure 1.3** [35]. (1) Growing as a street tree; (2) leaves; (3) bark; (4) flower; (5) fruit; (6) seed.

จุฬาลงกรณ์มหาวิทยาลัย
Chulalongkorn University

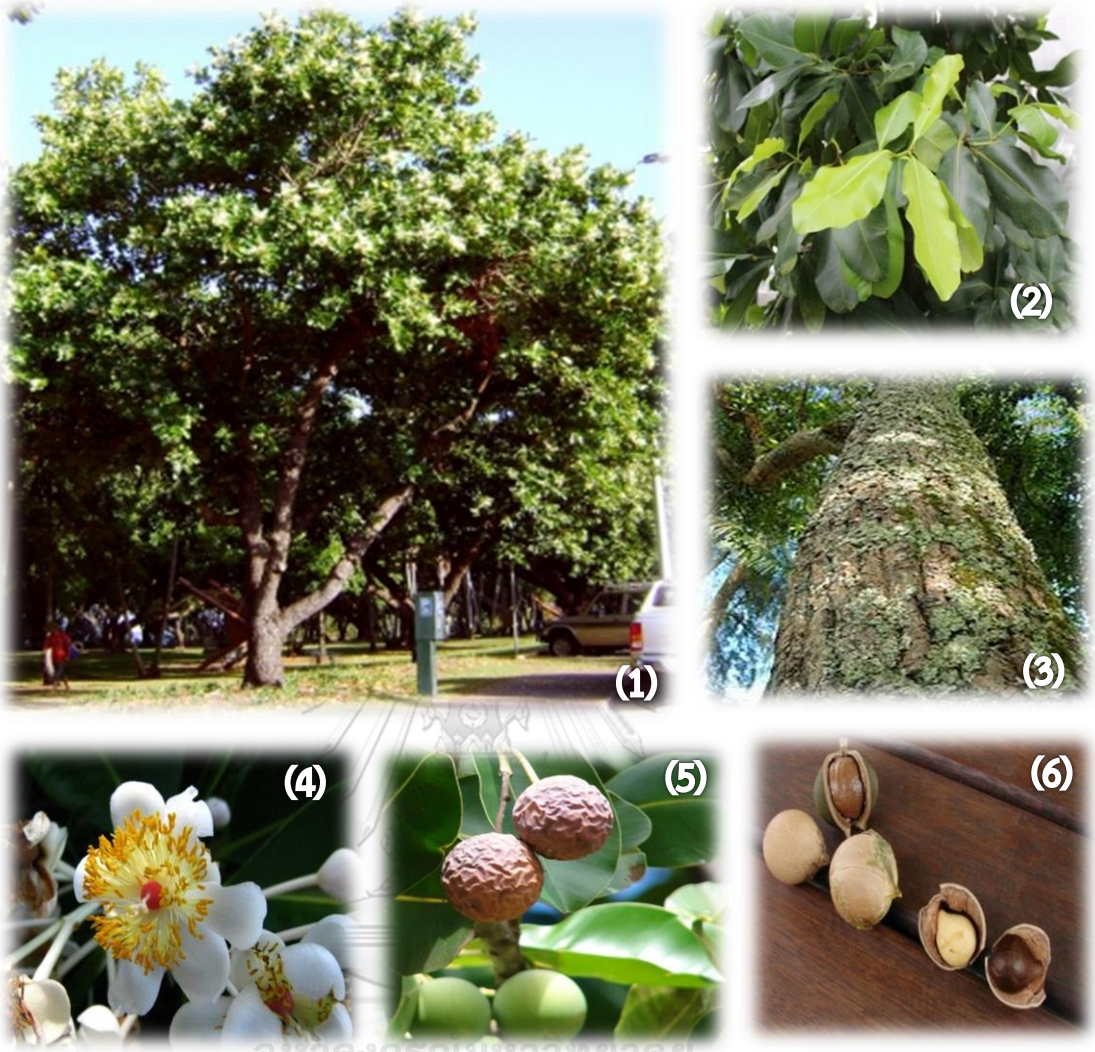

จุฬาลงกรณ์มหาวิทยาลัย
Chulalongkorn University

Figure 1.3 *C. inophyllum* L. Alexandrian Laurel

1.3 Literature review

1.3.1 Phytochemical metabolites from *C. inophyllum*

1.3.1.1 Coumarins

Four coumarins, namely 12-*O*-butylinophyllum D, 12-*O*-ethylinophyllum D, inophyllums H and I, were isolated from the leaves of *C. inophyllum* collected from China [36]. Moreover, nine 4-phenylcoumarins were isolated from aerial parts of plant sample collected from Singapore. Those metabolites were inophyllums A and C-E, calocoumarins A-C, apetatolide and calophyllolide [37]. In addition, (-)-12-

methoxyinophyllum A, (+)-12-methoxyinophyllum H-1, (-)-12-methoxyinophyllum H-2 and inophyllum J were obtained from the leaves collected from China [38].

1.3.1.2 Xanthones

Caloxanthones A-E were isolated from the root bark and heartwood root of *C. inophyllum* collected from Japan, Cameroon, Malaysia and Thailand [39-43]. In addition, other xanthone derivatives such as macluraxanthone, pyranojacareubin, *6*-deoxyjacareubin and inophyllin B were also isolated from the same parts of the plant [40, 42, 44, 45]. Caloxanthone Q, together with 2-deprenylrheediaxanthone B and jacareubin were isolated from the branches [46], while caloxanthone N and gerontoxanthone C were isolated from the twigs of *C. inophyllum* collected from China [47].

1.3.1.3 Flavonoids

Some flavonoid derivatives such as nobiletin, pentamethylquercetin, 3,5,7,4'-tetramethoxyflavone, 5,7,4'-trimethoxyflavone and (-)-epicatechin were isolated from the root part [39, 41]. Amentoflavone was a biflavonoid obtained from the leaves collected from India [48] and isoinophynone was isolated from the leaves collected from China [38].

จุฬาลงกรณ์มหาวิทยาลัย
Chulalongkorn University

1.3.1.4 Terpenoids

Canophyllic acid was isolated from the leaves collected from India [48]. Friedelane-type triterpene, namely 3β,23-epoxy-friedelan-28-oic acid, along with six known triterpenoids, including friedelin, epofriedelanol, canophyllal, canophyllol, 3-oxo-friedelan-28-oic acid and oleanolic acid, were obtained from the stems and leaves from China [49].

1.3.1.5 Other types of metabolites

Two new chromanone derivatives, caloinophyllins A and B were isolated from the root of *C. inophyllum* collected from Mahasarakham Province, Thailand [39, 50].

Moreover, other type of metabolite, brasiliensic acid and inophylloidic acid were isolated from the root of *C. inophyllum* collected from Cameroon [44].

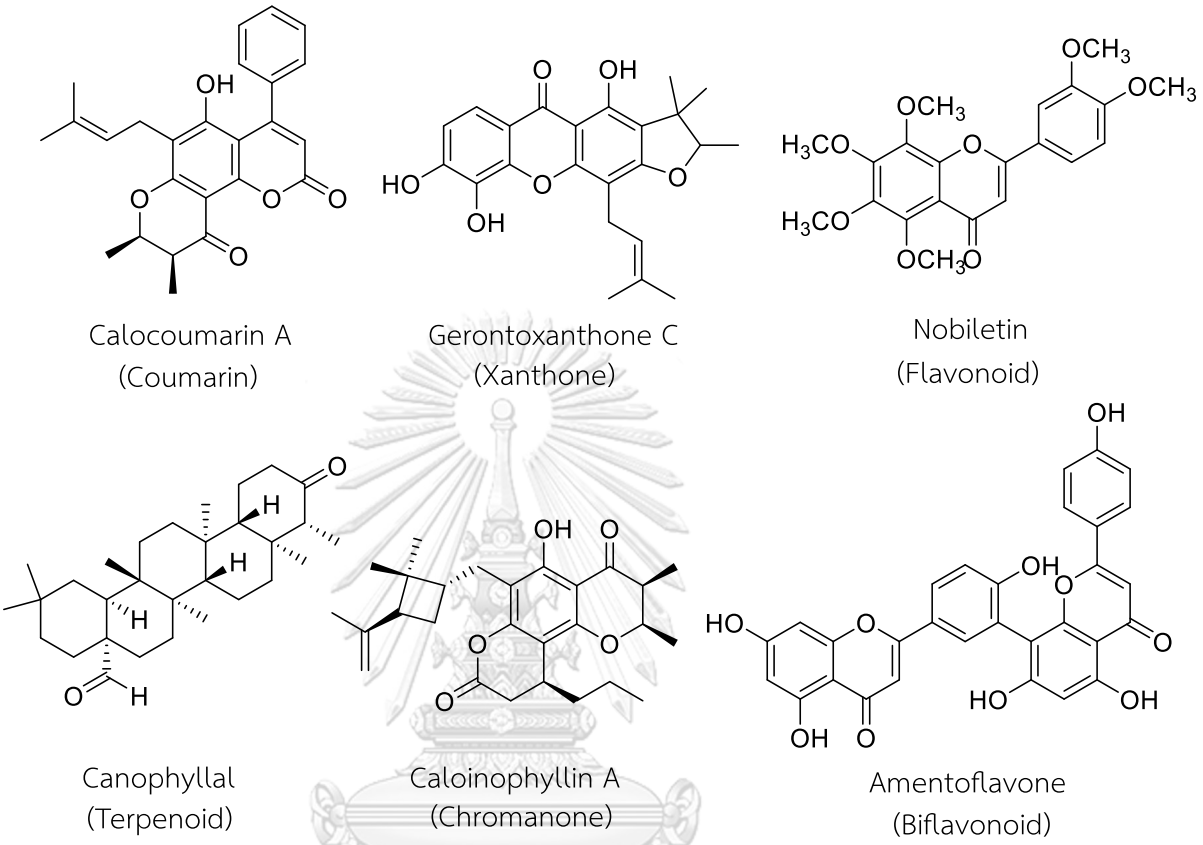

Figure 1.4 Representative metabolites from *C. Inophyllum*

จุฬาลงกรณ์มหาวิทยาลัย
Chulalongkorn University

1.3.2 Biologically active metabolites from *C. inophyllum*

1.3.2.1 Anti-cancer activity

Macluraxanthone showed broad activity as an anti-cancer with IC_{50} values of 4.95, 6.95, 4.62 and 5.28 μM against SNU-1 (stomach), HeLa (cervical), NCI-H23 (lung) and K562 (leukemia), respectively [29]. Moreover, calophyllolide, caloxanthone A and inophylloidic acid displayed good activity against KB (nasopharynx cancer) with IC_{50} values of 3.50, 7.40 and 9.70 μg/mL, respectively [44], whereas 3-oxo-friedelan-28-oic acid and canophyllic acid from the stems and leaves were active against HL-60 (leukemia) with IG_{50} values of 2.67 and 4.64 μM, respectively [49].

1.3.2.2 Anti-inflammatory activity

Two new triterpenoids, (*E*)- and (*Z*)-27-[*p*-coumaroyloxy]canophyllic acids from the leaves part could inhibit the production of nitric oxide (NO) in macrophage cells induced by LPS (lipopolysaccharide) with IC_{50} values of 2.44 μM and 7.00 μM, respectively [51]. The stem bark extracts of *C. inophyllum* furnished one new furanoxanthone, inophinnin. This metabolite exhibited anti-inflammatory activity in nitric oxide assay with concentration-dependent manner [52].

1.3.2.3 Larvicidal activity

Inophyllin A, a xanthone from roots part, showed moderate activity with LC_{50} value of 75–100 μg/mL, indicating that the metabolite was moderately toxic to the larvae of *Aedes aegypti* and might be considered to be a potential larvicide against the Dengue Fever mosquito larvae [53].

1.3.2.4 Chemotherapeutic activity

Apart from larvicidal activity, inophyllin A also represents a new xanthone with potential chemotherapeutic activity. It induced Jurkat cell apoptosis in a concentration-dependent manner based on the externalization of phosphatidylserine, and treatment with 50 and 100 μM of inophyllin A resulted in a significant increase of 47.9% and 83.8% of apoptotic cells, respectively. Thus, it could be concluded inophyllin A induced oxidative stress in Jurkat cells leading to DNA damage-mediated intrinsic apoptosis [54].

1.3.2.5 Anti-bacterial activity

Caloxanthone A, inophylloidic acid, calophynic acid and brasiliensic acid from the root bark displayed significant anti-bacterial activity against *Staphylococcus aureus* at the dose of 20 μg per dish with a diameter of inhibition 9.0, 9.0, 10.0 and 11.0 mm, respectively. From the nut part, isolated metabolites including inophyllums

จุฬาลงกรณ์มหาวิทยาลัย
Chulalongkorn University

C and E, calaustralin and calophyllolide also exhibited inhibition with diameter 10.0, 13.0, 11.0 and 16.0 mm, respectively [44].

1.3.2.6 Wound-healing activity

Calophyllolide, a coumarin from fresh seed, effectively promoted the wound closure by approximately 78% and 97% at day 7 and day 14 post-treatment, which was faster than PBS (phosphate-buffer saline) and povidone-iodine (PI) [55].

1.3.2.7 Anti-HIV activity

Inophyllums B and P were isolated from the leaves and twigs part, these reported inhibiting HIV-1 in cell culture with IC_{50} values of 1.4 and 1.6 μM, respectively. Both metabolites were inhibited HIV reverse transcriptase with IC_{50} values of 38 and 130 nM, respectively [56].

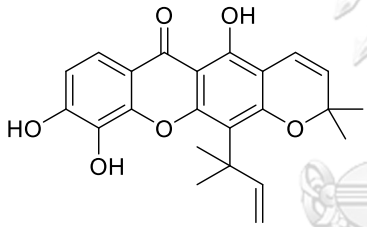

Macluraxanthone
(Anti-cancer)

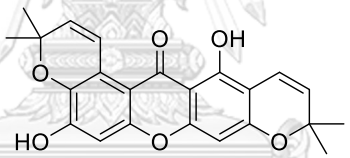

Caloxanthone A
(Anti-bacteria)

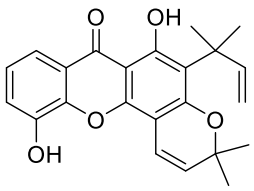

Inophyllin A
(Larvicidal and chemotherapeutic)

จุฬาลงกรณ์มหาวิทยาลัย
Chulalongkorn University

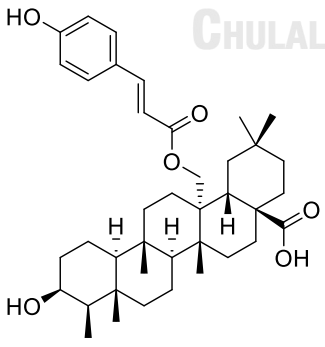

27-[(*E*)-*p*-coumaroyloxy]canophyllic acid
(Anti-inflammatory)

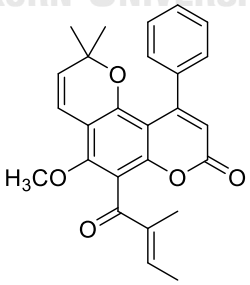

Calophyllolide
(Wound-healing)

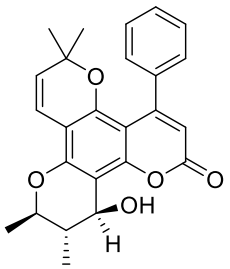

Inophyllum B
(Anti-HIV)

Figure 1.5 Representative bioactive metabolites from *C. inophyllum*

1.4 Objectives of the present study

Although many metabolites of *C. inophyllum* and their biological activities have been published, there were only two reports from the root of which the plant samples were collected from Thailand's northeastern region, Mahasarakham Province. Metabolites in the root part are mainly affected by the variation of nutrient factors from different geographical features. In this present study, the plant sample was collected from Nakhon Si Thammarat province, the southern part of Thailand.

Hence, the objectives of this study are summarized as follows;

1. To isolate secondary metabolites from the root of *C. inophyllum* L.
2. To determine the structures of the isolated metabolites by spectroscopy techniques
3. To evaluate the potential of isolated metabolites on anti-proliferative activity against liver cancer Hep-G2 and colon cancer HCT-116

จุฬาลงกรณ์มหาวิทยาลัย
Chulalongkorn University

CHAPTER II

EXPERIMENTS

2.1 Plant Materials

The root of *C. inophyllum* was collected from Nakhon Si Thammarat, Thailand (March 2019), and was identified by a Royal Forest Department staff, Nakhon Si Thammarat Province. A voucher specimen was assigned with the code CUCHEM2019-002 and is deposited at the Department of Chemistry, Faculty of Science, Chulalongkorn University.

2.2 General Experimental Procedures

2.2.1 Thin-layer chromatography (TLC)

TLC analysis was performed on Silicycle's aluminum sheet coated with silica gel F-254, 20 × 20 cm, layer thickness 200 µm. The TLC reverse phase analysis was performed on Merck's aluminum sheets coated with silica gel 60 RP-18 F_{245}s. The spot of metabolites was observed with UV light at 256 nm wavelength and dipped with ammonium molybdate ($(NH_4)_6MO_7O_{24}$) in 5% H_2SO_4/EtOH then heating for 1-2 mins at 105-120°C on a hot plate.

จุฬาลงกรณ์มหาวิทยาลัย
Chulalongkorn University

2.2.2 Column chromatography

Column chromatography (CC) was performed using Silica gel 60H (Merck code No. 7734 and No. 9385) as packing materials. Reverse-phase C-18 (RP-18) chromatography was performed using Silica gel C-18 (Wako code No. 237-01555) as packing materials. Size exclusion chromatography was performed by Sephadex LH-20 (Pharmacia Code No. 17-0090-01) to separate metabolites according to their molecular weight.

2.2.3 Nuclear magnetic resonance spectroscopy (NMR)

The NMR spectra were recorded on a Bruker AV400 (400 MHz for ^{1}H-NMR, 100 MHz for ^{13}C-NMR) and JEOL (500 MHz for ^{1}H-NMR, 125 MHz for ^{13}C-NMR) using tetramethylsilane (TMS) as an internal standard.

2.2.4 Mass spectrometry (MS)

High-resolution electrospray ionization mass spectrometry (HRESIMS) spectra were obtained with a Bruker micrOTOF-Q II.

2.2.5 Fourier transforms infrared spectrophotometry (FT-IR)

FT-IR spectra were recorded on a Perkin-Elmer Model 1760X Fourier Transform Infrared Spectrophotometer. Solid samples were formally examined by incorporating the sample with potassium bromide (KBr) to form a pellet.

2.2.6 Optical Rotation

Optical rotation was measured on a Perkin-Elmer 341 polarimeter at 589 nm.

2.2.7 Melting Point

Melting points were recorded on a Fisher-Johns melting point apparatus.

2.2.8 Ultraviolet-visible spectrophotometry (UV-vis)

UV data were recorded on a CARY 50 Probe UV-visible spectrophotometer.

2.3 Chemicals

All commercial-grade solvents used in the present study, such as methanol (MeOH), acetone, ethyl acetate (EtOAc), dichloromethane (DCM) and *n*-hexane, were purified by distillation before use. The deuterated solvent for NMR experiments was chloroform-*d* ($CDCl_3$) and acetone-d_6.

2.4 Extraction and isolation

2.4.1 Extraction of dried sample

The root of *C. inophyllum* (2.39 kg) was dried, powdered and extracted with MeOH (2 × 5L, 3 days, each) at room temperature. The combined MeOH extract was concentrated under reduced pressure. The extract was suspended in H_2O (1:1 v/v) and then partitioned with *n*-hexane and EtOAc, respectively. The extraction procedure is shown in **Scheme 2.1**.

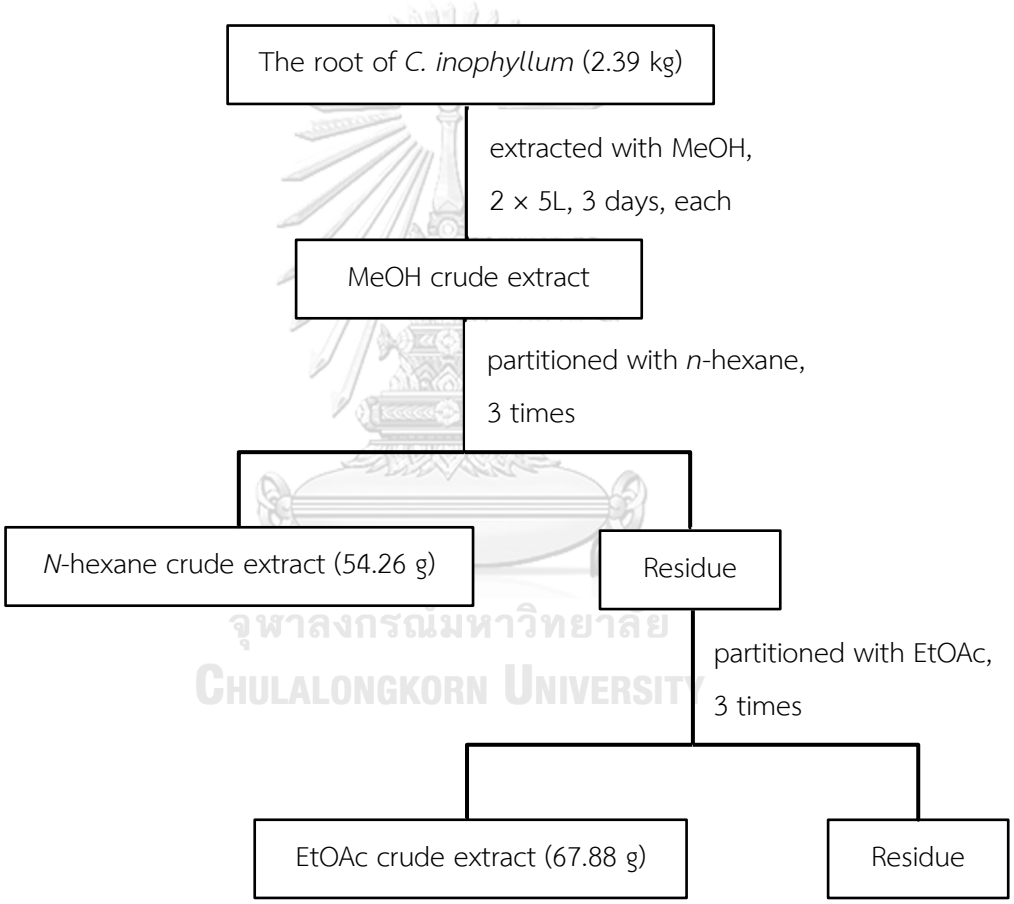

Scheme 2.1 Extraction of *C. inophyllum* root

2.4.2 Isolation of metabolite from *n*-hexane crude extract

The *n*-hexane crude extract of *C. inophyllum* (54.26 g) was chromatographed over a SiO_2 column chromatography (CC) with gradient EtOAc : *n*-hexane (1:9 to 1:1),

to give thirteen fractions, A-M. Fraction F (1.60 g) was diluted in acetone and formed a solid and liquid phases. The solid phase was washed with *n*-hexane to afford compound **13** (5.3 mg). The isolation procedure is shown in **Scheme 2.2**.

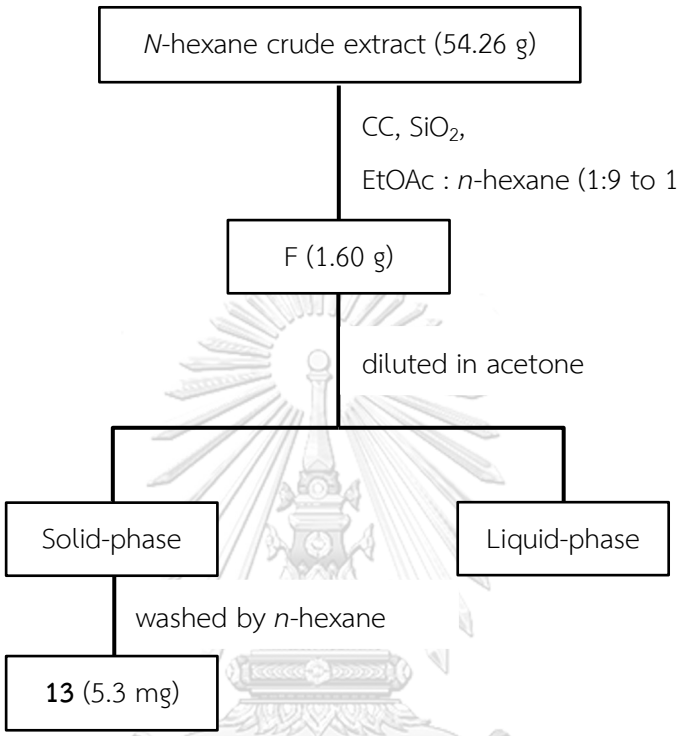

Scheme 2.2 Isolation procedure of fraction F

จุฬาลงกรณ์มหาวิทยาลัย
Chulalongkorn University

2.4.3 Isolation of metabolites from EtOAc crude extract

The EtOAc crude extract of *C. inophyllum* (67.88 g) was fractionated over a SiO_2 CC with gradient EtOAc : *n*-hexane (1:1 to 1:0) then MeOH : EtOAc (1:9 to 1:1) to afford seven fractions, N-T. Fraction P (3.56 g) was separated by SiO_2 CC with EtOAc : DCM (1:9) to obtain six subfractions, P1-P6. The isolation procedure is shown in **Scheme 2.3.**

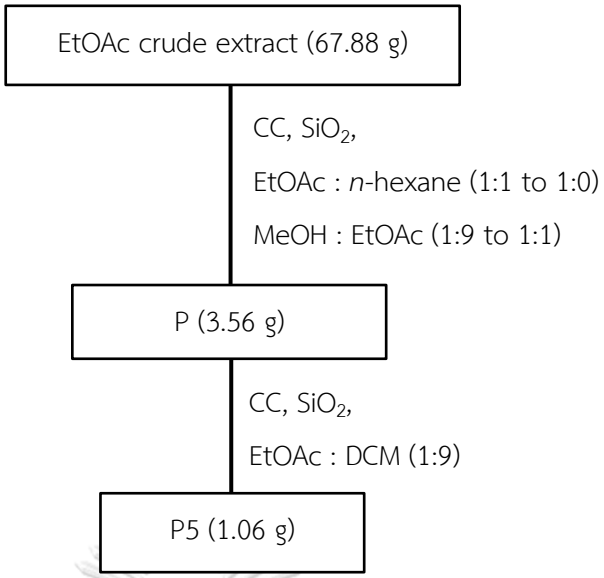

Scheme 2.3 Isolation procedure of EtOAc crude extract

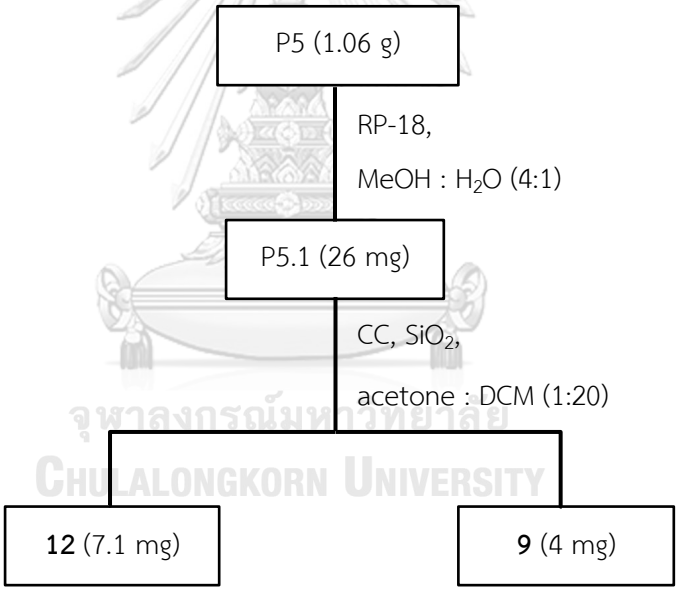

จุฬาลงกรณ์มหาวิทยาลัย
Chulalongkorn University

Scheme 2.4 Isolation procedure of fraction P5

Fraction P5 (1.06 g) was subjected to passage over a reverse phase C-18 (RP-18) with MeOH : H_2O (4:1) to give fifteen subfractions, P5.1-P5.15. Fraction P5.1 (26 mg) was purified by SiO_2 CC with acetone : DCM (1:20) to obtain metabolites **12** (7.1 mg) and **9** (4 mg). The isolation procedure is shown in **Scheme 2.4.**

Fraction P5.2 (26.2 mg) was filtrated with MeOH to separate the solid and liquid phases. Metabolite **11** (4.2 mg) was obtained from the solid phase by filtration with MeOH. Fraction P5.6 (33.7 mg) was chromatographed over RP-18 with MeOH : H_2O (4:1 to 1:0) to collect metabolite **1** (10.1 mg). Moreover, fraction P5.9 was purified by SiO_2 CC with EtOAc : *n*-hexane (1:4 to 3:7) to yield metabolites **6** (6.5 mg) and **2** (17.5 mg). The isolation of fractions P5.2, P5.6 and P5.6 are shown in **Scheme 2.5.**

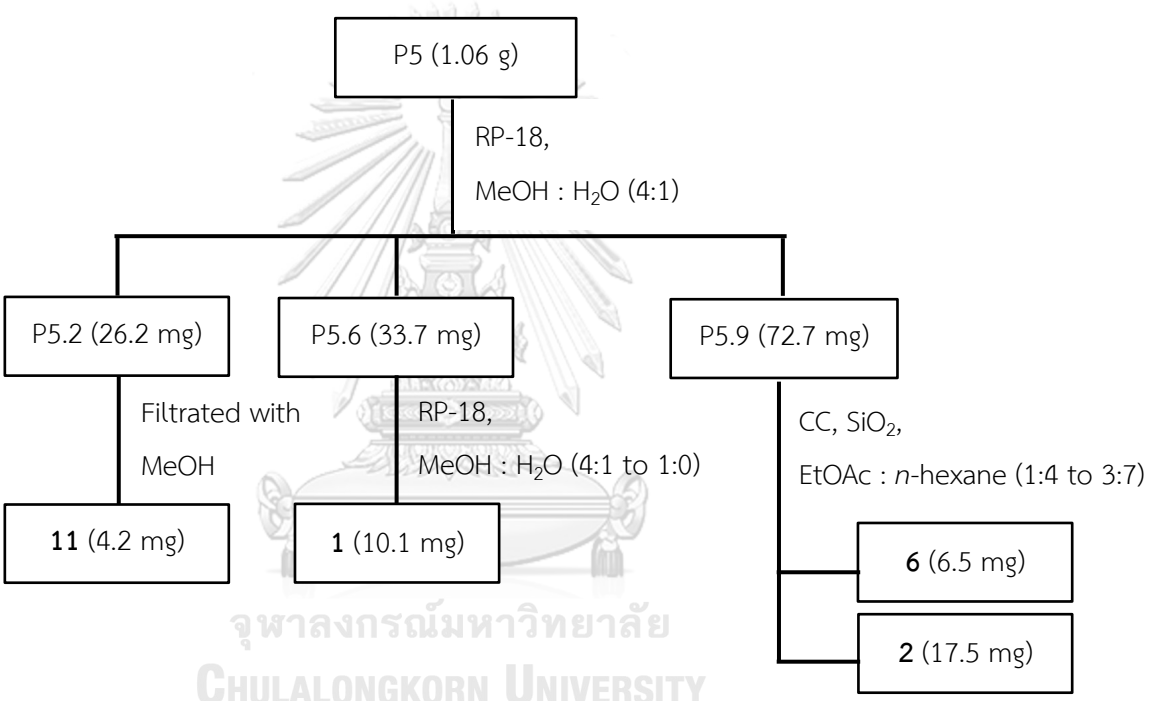

จุฬาลงกรณ์มหาวิทยาลัย
CHULALONGKORN UNIVERSITY

Scheme 2.5 Isolation of fractions P5.2, P5.6 and P5.9

The liquid phase of fraction P5.12 (160.1 mg) was chromatographed over SiO_2 CC with EtOAc : *n*-hexane (1:4) to obtain metabolites **7** (10.5 mg), **14** (25.4 mg) and **4** (12.6 mg)**.** Besides, the liquid phase of fraction P5.13 (160.1 mg) was chromatographed by SiO_2 CC with EtOAc : *n*-hexane (1:4) to give metabolite **3** (5.2 mg), whereas the solid phase afforded metabolite **5** (28.2 mg). The isolation of fractions P5.12 and P5.13 are shown in **Scheme 2.6.**

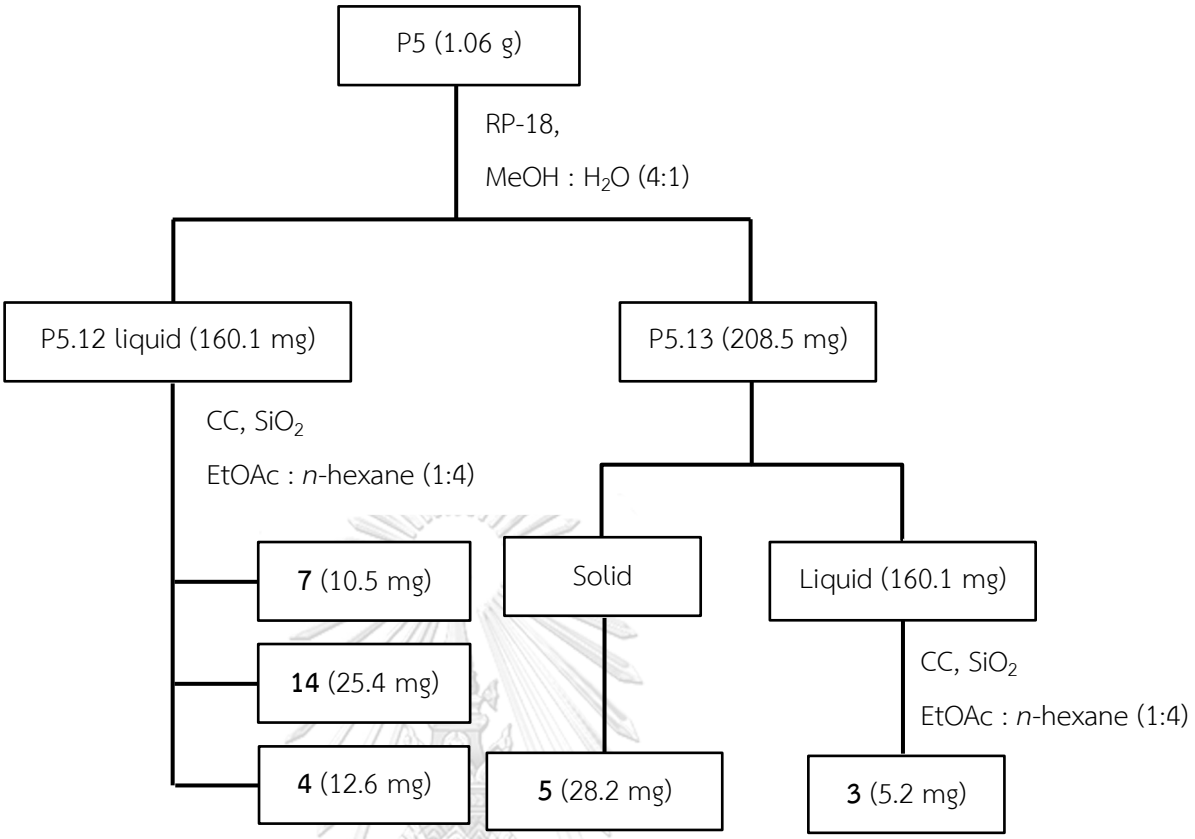

Scheme 2.6 Isolation of fractions P5.12 and P5.13

Fraction Q (3.64 g) was chromatographed over Sephadex LH-20 with MeOH to yield nine subfractions, Q1-Q9. Fraction Q4 (401.8 mg) was performed on Sephadex LH-20 with MeOH to give five subfractions, Q4.1-Q4.5. Fraction Q4.5 was purified using Sephadex LH-20 with MeOH to obtain metabolite **8** (18.8 mg). Additionally, metabolite **10** (2.2 mg) was afforded from fraction Q5.4-5 (52.6 mg) by RP-18 with MeOH : H_2O (1:1). The isolation procedure of fractions Q4 and Q5 are shown in **Scheme 2.7**.

จุฬาลงกรณ์มหาวิทยาลัย
CHULALONGKORN UNIVERSITY

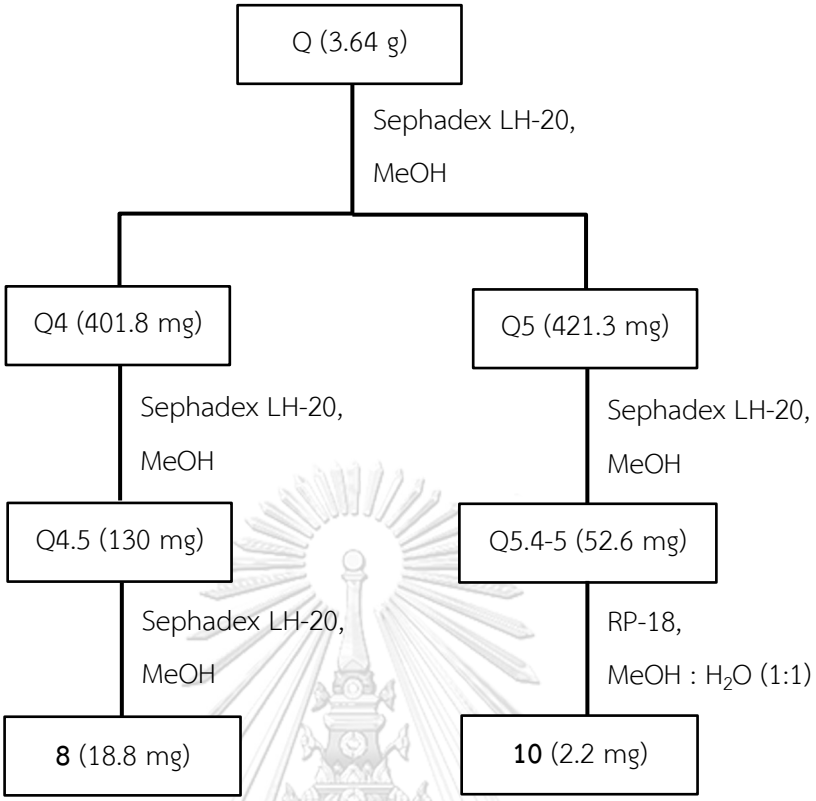

Scheme 2.7 Isolation of fractions Q4 and Q5

2.5 Biological assay

2.5.1 Cell culture

Colon cancer (HCT-116) and liver cancer (Hep-G2) cells were cultured in Dulbecco's Modified Eagle's Medium (DMEM) at 37 °C in a 5% CO_2 humidified incubator. Both media were supplemented with 10% Fetal Bovine Serum (FBS), 2 mM L-glutamine, 100 U/mL of penicillin and 100 mg/mL of streptomycin.

จุฬาลงกรณ์มหาวิทยาลัย
Chulalongkorn University

2.5.2 Anti-proliferative assay

Bioassay of anti-proliferative activity was performed *in vitro* by a colorimetric method that measures the reduction of MTT (3-(4,5-dimethylthiazol-2-yl)-2,5-diphenyltetrazolium bromide) by mitochondrial succinate dehydrogenase. The MTT entered cells and passed into the mitochondria, it reduced to dark purple (formazan), followed by solubilization and measurement by spectrophotometry. Generally, the

reduction of MTT occurs in metabolically active cells. The level of activity was thus measured from viability of the cell, which was proportional.

The cells were cultured from tissue culture dishes, counted and seeded cells in a 96-wells plate at a density of 1 x 10^4 cells/well in 100 µL. Cells were incubated in a 5% CO_2 atmosphere at 37 $^{\circ}C$ for 24 h. The samples were added to the cells and the cells were incubated for 72 h. MTT solution (5 mg/mL PBS, 10 µL/well) was added and the cells were incubated for 3-4 hours until the purple precipitate appears. After removing the medium, DMSO 100 µL/well was added to dissolve formazan crystal. The absorbance was measured at 570 nm using a Microplate Reader BioTek™ ELx800™ with sorafenib and doxorubicin as positive controls. The results were presented as the percentage of inhibition and the half-maximal inhibitory concentration (IC_{50}).

2.5.3 Western blot analysis

According to the manufacturer's instructions, cells treated as indicated in the text were washed with cold PBS and lysed with cell lysis buffer. Cell lysates were centrifuged at 5000 rpm for 5 min and supernatants were collected as samples. Equal amounts (30 µg) of total protein in each cell lysate were separated in 10% SDS-PAGE and transferred to the PVDF membrane. The membranes were blocked with 3% skim milk in PBS containing 0.05% Tween-20 and incubated overnight at 4 ºC with corresponding primary antibodies in 3% skim milk in PBS containing 0.05% Tween-20 followed by incubation with horseradish peroxidase-conjugated secondary antibodies for 1 h at room temperature. The signals were detected using the chemiluminescence method.

2.5.4 Statistical analysis

Data are expressed as mean values and standard deviation. Significance was analyzed by one-way analysis of variance and Dunnett's multiple comparison tests by GraphPad Prism 8. A p-value of <0.05 was considered statistically significant.

จุฬาลงกรณ์มหาวิทยาลัย
Chulalongkorn University

CHAPTER III

RESULTS AND DISCUSSION

3.1 Secondary metabolites from the root of *C. inophyllum*

The *n*-hexane crude extract of *C. inophyllum* was purified by chromatography technique to afford one metabolite, namely caloxanthone C (**13**)**.** Moreover, purification of EtOAc crude extract by column chromatography brought out two new prenylated xanthones, namely 1,3,6,7-tetrahydroxy-5-methoxy-4-(1',1'-dimethyl-2'-propenyl)-8-(3",3"-dimethyl-2"-propenyl)-xanthone (**1**) and 7-hydroxycaloxanthone B (**2**), along with eleven known metabolites. The eleven known metabolites were identified as caloxanthone B (**3**), 7-*O*-demethylmangostanin (**4**), caloxanthone A (**5**), 7-prenyljacaerubin (**6**), pyranojacareubin (**7**), daphnifolin (**8**)**,** tovopyrifolin C (**9**), 1,3,5-trihydroxyxanthone (**10**), 2-hydroxyxanthone (**11**), 4-hydroxyxanthone (**12**) and macluraxanthone (**14**). Their structures (**Figure 3.1**) were established by 1D and 2D NMR analysis and then by comparing the NMR data with some references. HR-ESI-MS were used to complete their structural characterization. Besides, metabolites **4, 6** and **8** were firstly reported from the genus *Calophyllum*.

จุฬาลงกรณ์มหาวิทยาลัย
Chulalongkorn University

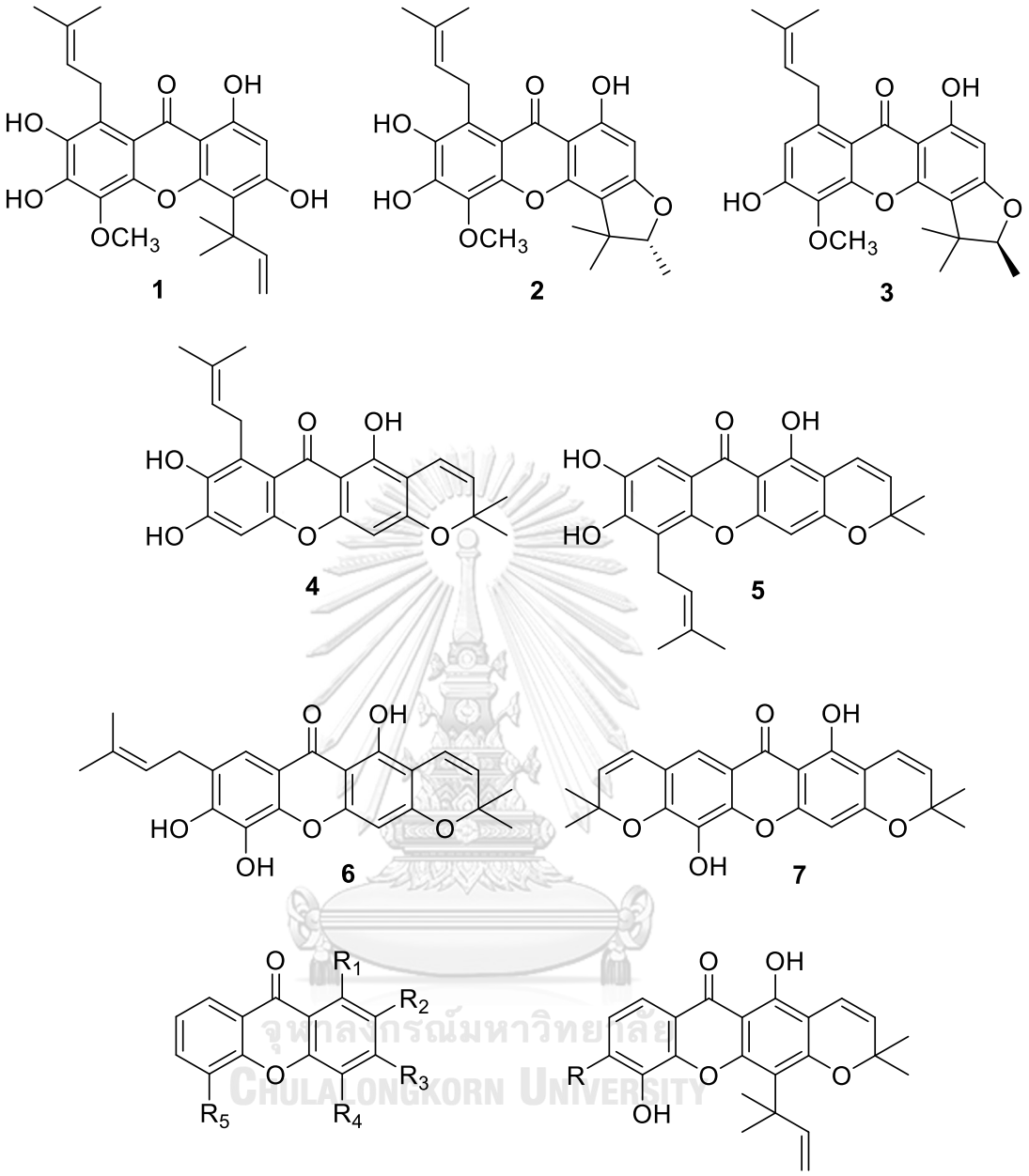

จุฬาลงกรณ์มหาวิทยาลัย
Chulalongkorn University

Figure 3.1 Structures of secondary metabolites from the root of *C. inophyllum*

3.2 Structure elucidation of isolated metabolites

3.2.1 Structure elucidation of metabolite **1**

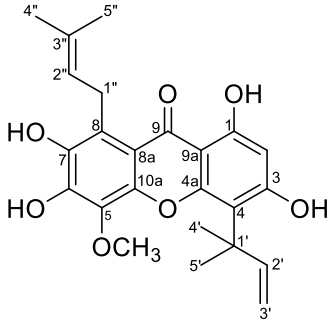

Figure 3.2 Structure of metabolite **1**

Metabolite **1** was obtained as a yellow amorphous solid with melting point 132-133 ºC and UV (MeOH) λ_{max} 269 and 330 nm. The IR spectrum gave absorptions of free hydroxyl (3370 cm^{-1}), conjugated carbonyl (1647 cm^{-1}) and an aromatic ring (1570 cm^{-1}), which reflected similarity to typical IR bands for xanthone [45, 57, 58]. The HR-ESI-MS showed molecular ion peak at *m/z* 449.1564 $[M+Na]^+$ (Calcd. for $C_{24}H_{26}O_7Na$, 449.1579), corresponding to the molecular formula $C_{24}H_{26}O_7$ and determined by analysis of 1D and 2D NMR as shown in **Tables 3.1** and **3.2**.

The characterization of chemical shifts for proton at δ_H 1.74 (s, 6H, H-4' and H-5'), 5.39 (d, *J* = 10.6 Hz, 1H, H-3'a), 5.49 (d, *J* = 17.8 Hz, 1H, H-3'b) and 6.51 (dd, *J* = 10.6, 17.8 Hz, 1H, H-2') suggested the presence of a 1,1-dimethyl-2-propenyl moiety in the molecule. This was further confirmed by the HMBC correlations (**Figure 3.3**) of the two methyl proton singlets at δ_H 1.74 (H-4' and H-5') with their neighboring carbon at δ_C 40.9 (C-1'). Placement of 1,1-dimethyl-2-propenyl moiety at C-4 was achieved by HMBC correlations between δ_H 1.74 (H-4' and H-5') with δ_C 109.5 (C-4) as shown in **Figure 3.3**.

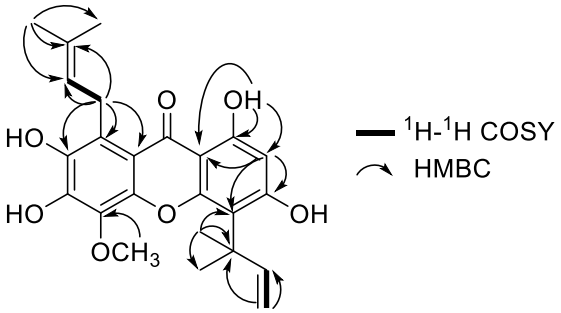

Figure 3.3 ^{1}H-^{1}H COSY and HMBC correlations of metabolite **1**

An isoprenyl group with its characteristic chemical shifts was also seen in the ^{1}H-NMR spectrum of **1**. The ^{1}H resonances occurred at δ_H 1.73 (s, 3H, H-4"), 1.86 (s, 3H, H-5"), 4.20 (d, *J* = 6.6 Hz, 2H, H-1") and 5.29 (t, *J* = 5.9 Hz, 1H, H-2"). Proton at δ_H 4.20 (H-1") showed HMBC correlations with δ_C 111.5 (C-8a), 123.2 (C-8) and 139.8 (C-7), suggested that the isoprenyl group bonded with C-8 as shown in **Figure 3.3**. The NMR spectra of metabolite **1** were very similar to those of cudraxanthone C [59], except for the existence of methoxy group at C-5 and hydroxyl group at C-7. Therefore, metabolite **1** was elucidated as a new xanthone, named 1,3,6,7-tetrahydroxy-5-methoxy-4-(1',1'-dimethyl-2'-propenyl)-8-(3",3"-dimethyl-2"-propenyl)-xanthone and given the trivial name, calinoxanthone.

จุฬาลงกรณ์มหาวิทยาลัย
CHULALONGKORN UNIVERSITY

3.2.2 Structure elucidation of metabolite **2**

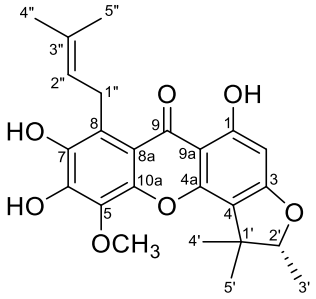

Figure 3.4 Structure of metabolite **2**

Metabolite **2** was obtained as a yellow amorphous solid with negative optical rotation $[\alpha]^{24}_{D}$ −22.9 (c 0.1, MeOH), melting point 116-118 °C and UV (MeOH) λ_{max}

263 and 326 nm. The IR spectrum showed absorptions of free hydroxyl (3379 cm^{-1}), conjugated carbonyl (1647 cm^{-1}) and an aromatic ring (1578 cm^{-1}) [45, 57, 58]. The 1D and 2D NMR established the molecular formula $C_{24}H_{26}O_7$. The HR-ESI-MS confirmed molecular ion peak at *m/z* 427.1743 $[M+H]^+$ (Calcd. for $C_{24}H_{27}O_7$, 427.1757) and *m/z* 449.1572 $[M+Na]^+$ (Calcd. for $C_{24}H_{26}O_7Na$, 449.1576).

The NMR spectra of metabolite **2** (**Tables 3.1** and **3.2**) were very similar to those of metabolite **1**, except for the existence of 2,3,3-trimethyldihydrofuran ring. Protons at δ_H 1.40 (d, *J* = 6.6 Hz, 3H, H-3'), 1.32 (s, 3H, H-4'), 1.62 (s, 3H, H-5') and 4.55 (d, *J* = 6.6 Hz, 1H, H-2') confirmed the presence of 2,3,3-trimethyldihydrofuran ring (**Figure 3.4**). The appearance of a prenyl moiety implied by protons at δ_H 1.63 (s, 3H, H-4"), 1.82 (d, *J* = 1.0 Hz, 3H, H-5"), 5.29 (t, *J* = 6.9 Hz, 1H, H-2") and 4.14 (d, *J* = 6.9 Hz, 2H, H-1"). Proton at δ_H 4.14 (H-1") showed HMBC correlations with δ_C 124.6 (C-8) and 141.7 (C-7), further confirming the prenyl moiety at C-8 (**Figure 3.5**). The NMR spectra of metabolite **2** were very similar to those of metabolite **3**, except the appearance of hydroxyl group at C-7. The absolute configuration at C-2' was postulated as *R* on the basis of the opposite sign of optical rotation for metabolite **2** ($[\alpha]_D$ −22.9) and the known xanthone, caloxanthone B ($[\alpha]_D$ +43.7) [41]. Therefore, metabolite **2** was elucidated as a new xanthone, named 7-hydroxycaloxanthone B.

จุฬาลงกรณ์มหาวิทยาลัย
Chulalongkorn University

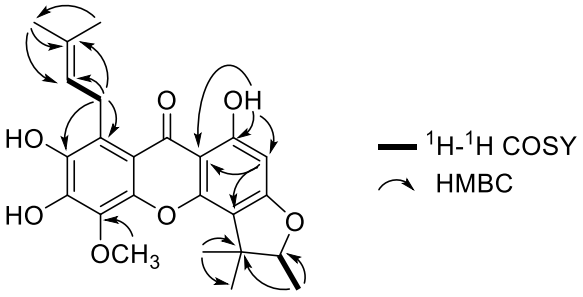

Figure 3.5 ^{1}H-^{1}H COSY and HMBC correlations of metabolite **2**

3.2.3 Structure elucidation of metabolite **3**

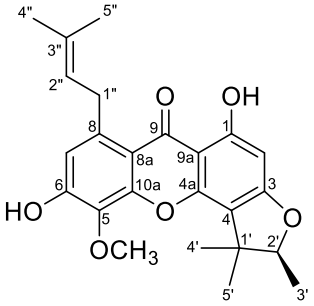

Figure 3.6 Structure of metabolite **3**

Metabolite **3** was obtained as a yellow amorphous solid with positive optical rotation $[\alpha]^{24}_{D}$ +22.2 (c 0.1, MeOH) and had a molecular formula $C_{24}H_{26}O_6$ established by ^{1}H- and ^{13}C-NMR data (**Tables 3.1** and **3.2**). The existence of 2,3,3-trimethyldihydrofuran ring could be seen at δ_H 1.31 (s, 3H, H-4'), 1.59 (s, 3H, H-5'), 1.42 (d, *J* = 6.5 Hz, 3H, H-3') and 4.52 (d, *J* = 6.5 Hz, 1H, H-2'). Two vinylic methyl doublets at δ_H 1.74 (*J* = 11.7 Hz, H-4" and H-5"), a methylene singlet at δ_H 4.01 (H-1") and an olefinic singlet 5.36 (H-2") revealed the presence of a prenyl moeity. Hence, metabolite **3** was confirmed as caloxanthone B by comparing its NMR data to those previously reported [41].

จุฬาลงกรณ์มหาวิทยาลัย
Chulalongkorn University

Table 3.1 ^{1}H-NMR data of metabolites **1-3**

Position	δ_H (ppm), mult, *J* in Hz		
	1[a]	**2**[b]	**3**[a]
1	13.66, s	13.88, s	13.72, s
2	6.24, s	6.12, s	6.19, s
3			
4			
4a			
5			
6			6.24, s
7			6.82, s
8			
8a			
9			
9a			
10a			
1'			
2'	6.51, dd, 8.0, 10.6	4.55, d, 6.6	4.52, d, 6.5
3'	5.49, d, 17.8	1.40, d, 6.6	1.42, d, 6.5
	5.39, d, 10.6		
4'	1.74, s	1.32, s	1.31, s
5'	1.74, s	1.62, s	1.59, s
1"	4.20, d, 6.6	4.14, d, 6.9	4.01, s
2"	5.29, t, 5.9	5.29, t, 6.9	5.36, s
3"			
4"	1.73, s	1.63, s	1.74, d, 11.7
5"	1.86, s	1.82, d, 1.0	1.74, d, 11.7
5-OCH_3	3.95, s	3.98, s	4.01, s

a: $CDCl_3$, 400 MHz; b: acetone-d_6, 500 MHz

จุฬาลงกรณ์มหาวิทยาลัย
Chulalongkorn University

Table 3.2 ^{13}C-NMR data of metabolites **1**-**3**

Position	δ_C (ppm)		
	1[a]	**2**[b]	**3**[c]
1	162.2	165.4	164.7
2	100.4	93.8	94.2
3	162.0	166.3	165.7
4	109.5	112.7	112.9
4a	155.2	152.8	151.8
5	133.2	134.1	133.6
6	143.4	145.7	153.4
7	139.8	141.7	113.4
8	123.2	124.6	142.2
8a	111.5	111.7	112.2
9	183.0	183.3	182.3
9a	104.9	104.5	104.1
10a	146.3	146.9	151.1
1'	40.9	44.4	43.8
2'	149.7	91.5	90.8
3'	113.5	14.4	14.3
4'	27.7	21.7	21.8
5'	27.7	26.0	25.7
1"	25.6	25.9	33.8
2"	122.2	124.4	122.4
3"	134.2	131.2	132.3
4"	26.0	26.0	26.1
5"	18.2	18.3	18.1
5-OCH_3	61.9	62.2	62.1

a: $CDCl_3$, 100 MHz; b: acetone-d_6, 125 MHz; c: $CDCl_3$, 125 MHz

จุฬาลงกรณ์มหาวิทยาลัย
Chulalongkorn University

3.2.4 Structure elucidation of metabolite **4**

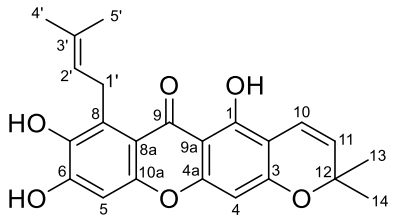

Figure 3.7 Structure of metabolite **4**

Metabolite **4** was obtained as a yellow amorphous solid and had a molecular formula $C_{23}H_{22}O_6$ established by ^{1}H- and ^{13}C-NMR data (**Tables 3.3** and **3.4**). The ^{1}H-NMR displayed the appearance of prenyl moeity at δ_H 4.31 (d, *J* = 5.6 Hz, 2H, H-1'), 5.29 (m, 1H, H-2'), 1.77 (d, *J* = 1.0 Hz, 3H, H-4') and 1.87 (s, 3H, H-5'). NMR spectra of metabolite **4** exhibited signals for pyran ring at δ_H 5.55 (d, *J* = 10 Hz, 1H, H-11) and 6.71 (d, *J* = 10 Hz, 1H, H-10). Proton at δ_H 6.71 (H-10) showed HMBC correlations with δ_C 78.1 (C-12) and 160.0 (C-3). Meanwhile, proton at δ_H 5.55 (H-10) displayed HMBC correlations with δ_C 78.1 (C-12) and 104.0 (C-2). Those HMBC correlations confirmed the pyran ring fused at C-2 and C-3 (**Figure 3.8**). The structure of metabolite **4** was established as shown in **Figure 3.7** and it was identified as 7-*O*-demethylmangostanin by comparing its NMR data to the previous report [60]. To the best of our knowledge, this metabolite was found from the genus *Calophyllum* for the first time.

จุฬาลงกรณ์มหาวิทยาลัย
CHULALONGKORN UNIVERSITY

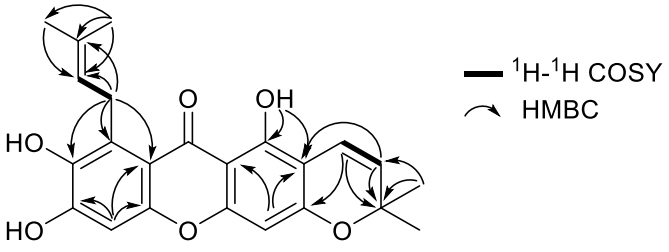

Figure 3.8 ^{1}H-^{1}H COSY and HMBC correlations of metabolite **4**

3.2.5 Structure elucidation of metabolite **5**

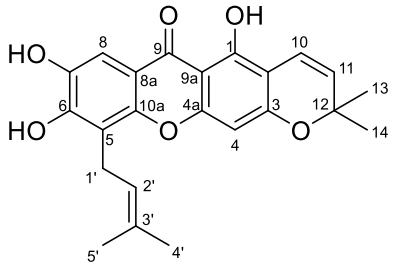

Figure 3.9 Structure of metabolite **5**

Metabolite **5** was obtained as a yellow solid. The molecular formula $C_{23}H_{22}O_6$ was determined according to 1D and 2D NMR data (**Tables 3.3** and **3.4**). NMR spectra of metabolite **5** were very similar to those of metabolite **4**. The ^{1}H-NMR displayed the presence of 2,2-dimethylchromene ring at δ_H 6.67 (d, *J* = 10.0 Hz, H-10), 5.72 (d, *J* = 10.0 Hz, H-10) and 1.47 (s, 6H, H-13 and H-14). The characteristic signals of prenyl moiety appeared at δ_H 1.67 (d, *J* = 1.4 Hz, 3H, H-4'), 1.90 (d, *J* = 1.7 Hz, 3H, H-5'), 3.62 (d, *J* = 7.4 Hz, 2H, H-1') and 5.32 (t, *J* = 7.4 Hz, 1H, H-2'). The HMBC correlations (**Figure 3.10**) showed that the prenyl moiety connected with C-5. Therefore, the complete structure of metabolite **5** was confirmed by 2D NMR (**Figure 3.10**) and its comparison with previous report [43, 61], then it was assigned as caloxanthone A.

จุฬาลงกรณ์มหาวิทยาลัย
Chulalongkorn University

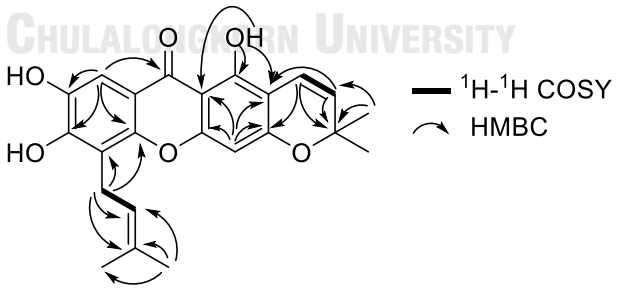

Figure 3.10 ^{1}H-^{1}H COSY and HMBC correlations of metabolite **5**

3.2.6 Structure elucidation of metabolite **6**

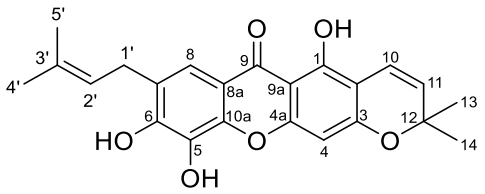

Figure 3.11 Structure of metabolite **6**

Metabolite **6** was obtained as a yellow amorphous solid. 1D and 2D NMR established the molecular formula $C_{23}H_{22}O_6$. The ^{1}H- and ^{13}C-NMR spectrum (**Tables 3.3** and **3.4**) indicated the appearance of prenyl moeity at δ_H 1.75 (dd, *J* = 1.3, 6.7 Hz, 6H, H-4' and H-5'), 3.43 (d, *J* = 7.4 Hz, 2H, H-1') and 5.40 (t, *J* = 7.4 Hz, 1H, H-2'). The HMBC spectrum (**Figure 3.12**) showed the prenyl moiety was connected at C-7. Protons at δ_H 6.67 (d, *J* = 10.0 Hz, 1H, H-10), 5.73 (d, *J* = 10.0 Hz, 1H, H-11) and 1.46 (s, 6H, H-13 and H-14) were observed as characteristic of 2,2-dimethylchromene ring. A proton at δ_H 6.67 (H-10) showed HMBC correlations with δ_C 160.8 (C-1) and 78.9 (C-12), whereas, a proton at 5.73 (H-11) displayed HMBC correlations with δ_C 105.1 (C-2) and 78.9 (C-12). These data confirmed that the 2,2-dimethylchromene ring was linked with C-2 and C-3 (**Figure 3.12**). Therefore, the complete structure of metabolite **6** was confirmed by 2D NMR (**Figure 3.12**) and its comparison with the previous report [62], then it was elucidated as 7-prenyljacaerubin. To the best of our knowledge, this metabolite was firstly reported from the genus *Calophyllum*.

จุฬาลงกรณ์มหาวิทยาลัย
Chulalongkorn University

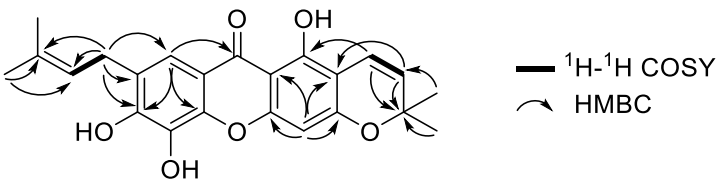

Figure 3.12 ^{1}H-^{1}H COSY and HMBC correlations of metabolite **6**

Table 3.3 ^{1}H-NMR data of metabolites **4**-**7**

Position	δ_H (ppm), mult, *J* in Hz			
	4[c]	**5**[b]	**6**[b]	**7**[a]
1	13.69, s	13.62, s	13.62, s	13.30, s
2				
3				
4	6.22, s	6.35, s	6.31, s	6.43, s
4a				
5	6.81, s			5.55, s
6				
7				
8		7.46, s	7.52, s	7.47, s
8a				
9				
9a				
10a				
10	6.71, d, 10.0	6.67, d, 10.0	6.67, d, 10.0	6.72, d, 10.2
11	5.55, d, 10.0	5.72, d, 10.0	5.73, d, 10.0	5.59, d, 10.0
12				
13	1.44, s	1.47, s	1.46, s	1.47, s
14	1.44, s	1.47, s	1.46, s	1.47, s
15				6.44, d, 9.4
16				5.73, d, 9.8
17				
18				1.54, s
19				1.54, s
1'	4.31, d, 5.6	3.62, d, 7.4	3.43, d, 7.4	
2'	5.29, m	5.32, t, 7.4	5.40, t, 7.4	
3'				
4'	1.77, d, 1.0	1.67, d, 1.4	1.75, dd, 6.7, 1.3	
5'	1.87, s	1.90, d, 1.7	1.75, dd, 6.7, 1.3	

a: $CDCl_3$, 400 MHz; b: acetone-d_6, 500 MHz; c: $CDCl_3$, 500 MHz

จุฬาลงกรณ์มหาวิทยาลัย
Chulalongkorn University

Table 3.4 ^{13}C-NMR data of metabolites **4**-**7**

Position	δ_C (ppm)			
	4[b]	**5**[a]	**6**[a]	**7**[b]
1	158.1	158.4	160.8	157.9
2	104.0	105.0	105.1	104.9
3	160.0	160.8	158.6	160.6
4	94.3	95.4	95.4	95.5
4a	156.5	158.0	157.8	157.0
5	101.5	116.7	132.3	132.2
6	153.8	150.8	150.8	144.9
7	139.9	143.3	126.9	117.9
8	127.5	106.3	116.6	113.6
8a	111.7	113.4	113.6	114.8
9	182.9	180.9	181.2	180.4
9a	104.6	103.6	103.6	103.7
10a	151.0	152.0	145.4	145.2
10	116.0	115.9	115.8	115.6
11	127.3	128.6	128.6	127.7
12	78.1	78.9	78.9	78.3
13	28.5	28.5	28.5	28.5
14	28.5	28.5	28.5	28.5
15				127.4
16				131.2
17				79.1
18				28.6
19				28.6
1'	26.1	23.1	28.7	
2'	121.6	122.4	122.7	
3'	135.9	132.6	133.6	
4'	26.2	25.9	25.9	
5'	18.3	18.2	17.9	

a: acetone-d_6, 125 MHz; b: $CDCl_3$, 125 MHz

จุฬาลงกรณ์มหาวิทยาลัย
Chulalongkorn University

3.2.7 Structure elucidation of metabolite **7**

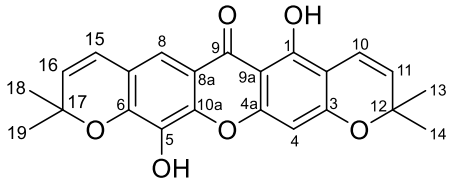

Figure 3.13 Structure of metabolite **7**

Metabolite **7** was obtained as a yellow amorphous solid and had the molecular formula $C_{22}H_{20}O_6$ determined by the ^{1}H- and ^{13}C-NMR data (**Tables 3.3** and **3.4**). The NMR spectra of metabolite **7** were very similar to those of metabolite **6**, except for the existence of pyranyl rings. Two pairs of doublets at δ_H 5.59 (*J* = 10.0 Hz, 1H, H-11) and 6.72 (*J* = 10.2 Hz, 1H, H-10), as well as at δ_H 5.73 (*J* = 9.8 Hz, 1H, H-16) and 6.44 (*J* = 9.4 Hz, 1H, H-15) indicated the presence of two pyranyl rings in the structure. This metabolite was identified as the known chromenoxanthone, pyranojacareubin (**7**), by comparing its NMR data with published data [63].

3.2.8 Structure elucidation of metabolite **8**

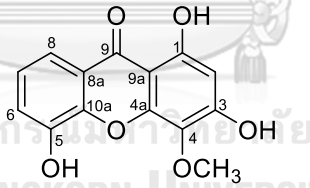

จุฬาลงกรณ์มหาวิทยาลัย
CHULALONGKORN UNIVERSITY

Figure 3.14 Structure of metabolite **8**

Metabolite **8** was isolated as a yellow gum. 1D and 2D NMR established the molecular formula $C_{14}H_{10}O_6$. The ^{1}H-NMR spectrum (**Table 3.5**) exhibited aromatic protons at δ_H 6.47 (s, 1H, H-2), 7.18 (t, *J* = 7.9 Hz, 1H, H-7), 7.28 (d, *J* = 7.7 Hz, 1H, H-6) and 7.59 (d, *J* = 8.0 Hz, 1H, H-8), and the remaining singlet at δ_H 3.87 (3H, 4-OCH_3) was attributed to the methoxy protons. The ^{13}C-NMR spectrum (**Table 3.6**) confirmed the presence of methoxy group at δ_C 60.4 (4-OCH_3). From the HMBC spectrum (**Figure 3.15**), proton at δ_H 6.47 (H-2) displayed correlations with δ_C 102.1 (C-9a), 132.8 (C-4),

154.5 (C-1) and 165.2 (C-3). Therefore, metabolite **8** was assigned to be 1,3,5-trihydroxy-4-methoxyxanthone as known as daphnifolin. Daphnifolin was firstly isolated from *Mesua daphnifolia* [64], and here is the first report from the genus *Calophyllum*.

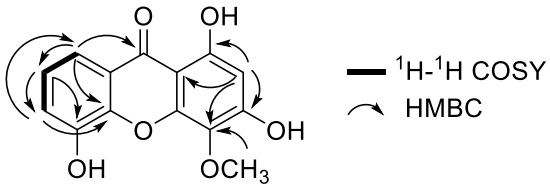

Figure 3.15 ^{1}H-^{1}H COSY and HMBC correlations of metabolite **8**

3.2.9 Structure elucidation of metabolite **9**

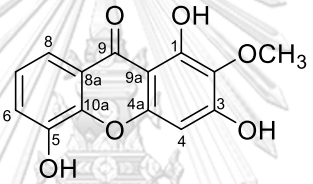

Figure 3.16 Structure of metabolite **9**

Metabolite **9** was obtained as a yellow amorphous solid. 1D and 2D NMR established the molecular formula $C_{14}H_{10}O_6$. NMR spectra of metabolite **9** were very similar with those of metabolite **8**. Its ^{1}H- and ^{13}C-NMR spectrum (**Tables 3.5** and **3.6**) presented signals of proton at δ_H 3.88 (s, 3H) and carbon at δ_C 60.8 (2-OCH_3), proposed the appearance of methoxy group. Proton at δ_H 6.53 (s, 1H, H-4) showed HMBC correlations with δ_C 104.0 (C-9a), 131.5 (C-2), 153.8 (C-4a) and 159.2 (C-3) (**Figure 3.17**). The structure of metabolite **9** was confirmed by ^{1}H-^{1}H COSY and HMBC correlations (**Figure 3.17**). By comparing its NMR data with those reported in the literature [65], metabolite **9** was elucidated as 1,3,5-trihydroxy-2-methoxyxanthone.

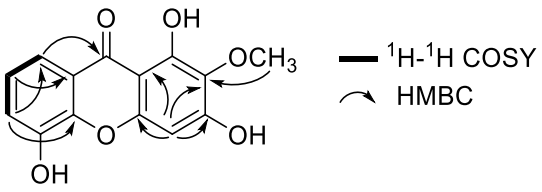

Figure 3.17 ^{1}H-^{1}H COSY and HMBC correlations of metabolite **9**

3.2.10 Structure elucidation of metabolite **10**

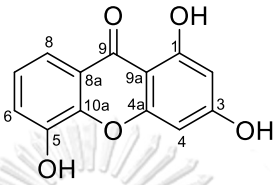

Figure 3.18 Structure of metabolite **10**

Metabolite **10** was isolated as a yellow gum and the molecular formula $C_{13}H_8O_5$ was determined according to ^{1}H-NMR data (**Table 3.5**). NMR data of metabolite **10** were very similar with those of metabolite **8**, except for the absence of methoxy group. The ^{1}H-NMR spectrum showed aromatic protons at δ_H 6.11 (d, *J* = 1.9 Hz, 1H, H-2), 6.28 (d, *J* = 2.3 Hz, 1H, H-4), 7.16 (t, *J* = 7.8 Hz, 1H, H-7), 7.24 (dd, *J* = 1.6, 7.8 Hz, 1H, H-6) and 7.55 (dd, *J* = 1.6, 7.8 Hz, 1H, H-8). Therefore, metabolite **10** was assigned as 1,3,5-trihydroxyxanthone. The NMR data was matched with the literature [66].

จุฬาลงกรณ์มหาวิทยาลัย
Chulalongkorn University

Table 3.5 ^{1}H-NMR data of metabolites **8**-**10** (acetone-d_6, 500 MHz)

Position	δ_H (ppm), mult, *J* in Hz		
	8	**9**	**10**
1		13.13, s	
2	6.47, s		6.11, d, 1.9
3			
4		6.53, s	6.38, d, 2.3
4a			
5			
6	7.28, d, 7.7	7.35, dd, 1.6, 7.8	7.24, dd, 1.6, 7.8
7	7.18, t, 7.9	7.28, t, 7.9	7.16, t, 7.8
8	7.59, d, 8.0	7.67, dd, 1.6, 7.9	7.55, dd, 1.6, 7.8
8a			
9			
9a			
10a			
2-OCH_3		3.88, s	
4-OCH_3	3.87, s		

จุฬาลงกรณ์มหาวิทยาลัย
CHULALONGKORN UNIVERSITY

Table 3.6 ^{13}C-NMR data of metabolites **8** and **9** (acetone-d_6, 125 MHz)

Position	δ_C (ppm)	
	8	**9**
1	154.5	155.4
2	96.0	131.5
3	165.2	159.2
4	132.8	94.7
4a	155.0	153.8
5	147.5	146.9
6	120.8	121.7
7	124.2	124.8
8	115.4	116.2
8a	122.0	121.3
9	180.9	182.1
9a	102.1	104.0
10a	146.1	146.1
2-OCH_3		60.8
4-OCH_3	60.4	

จุฬาลงกรณ์มหาวิทยาลัย
CHULALONGKORN UNIVERSITY

3.2.11 Structure elucidation of metabolite **11**

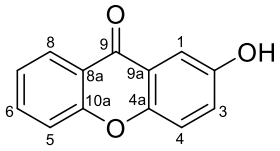

Figure 3.19 Structure of metabolite **11**

Metabolite **11** was obtained as a yellow amorphous solid and the molecular formula $C_{13}H_8O_3$ was determined according to ^{1}H- and ^{13}C-NMR data (**Tables 3.7** and **3.8**). The ^{1}H-NMR displayed one hydroxyl group at δ_H 8.89 (s, OH-2) and seven aromatic protons at δ_H 7.38 (dd, *J* = 3.1, 8.9 Hz, 1H, H-3), 7.52 (d, *J* = 9.0 Hz, 1H, H-4), 7.63 (d, *J* = 3.1 Hz, 1H, H-1), 7.44 (m, 1H, H-5), 7.58 (m, 1H, H-7), 7.83 (ddd, *J* = 1.7, 7.1, 8.6 Hz, 1H, H-6) and 8.24 (dd, *J* = 1.6, 8.0 Hz, 1H, H-8). Its ^{13}C-NMR showed conjugated carbonyl carbon at δ_C 176.9 (C-9) and one oxygenated quaternary carbon at δ_C 154.8 (C-2). Moreover, the complete structure of metabolite **11** was confirmed by comparing its NMR data with previously reported, and it was identified as 2-hydroxyxanthone [67].

3.2.12 Structure elucidation of metabolite **12**

จุฬาลงกรณ์มหาวิทยาลัย
CHULALONGKORN UNIVERSITY

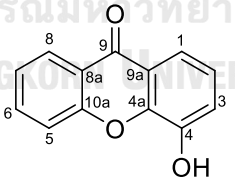

Figure 3.20 Structure of metabolite **12**

Metabolite **12** was obtained as a light yellow powder and the molecular formula $C_{13}H_8O_3$ was determined according to 1D and 2D-NMR data. NMR data (**Tables 3.7** and **3.8**) of metabolite **12** were very similar to those of metabolite **11**, except for the appearance of a hydroxyl group at δ_H 9.24 (s, OH-4) attached with oxygenated quaternary carbon at δ_C 147.3 (C-4) in metabolite **12**. Proton at δ_H 7.73 (dd, *J* = 1.6, 7.9 Hz, 1H, H-1) and 8.26 (dd, *J* = 1.7, 7.9 Hz, 1H, H-1) showed HMBC

correlations with conjugated carbonyl carbon at δ_C 177.1 (C-9) (**Figure 3.21**). Hence, metabolite **12** was assigned as 4-hydroxyxanthone, further confirmed by comparing its NMR data to those previously reported [67].

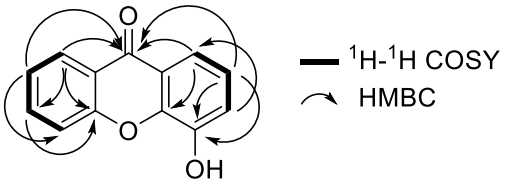

Figure 3.21 ^{1}H-^{1}H COSY and HMBC correlations of metabolite **12**

3.2.13 Structure elucidation of metabolite **13**

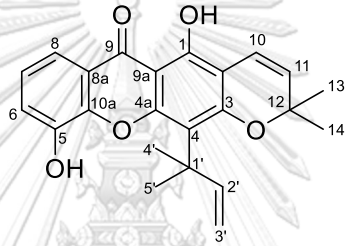

Figure 3.22 Structure of metabolite **13**

Metabolite **13** was obtained as yellow needles with molecular formula $C_{23}H_{22}O_5$ deduced from its NMR data. Analysis of ^{1}H- and ^{13}C-NMR (**Tables 3.7** and **3.8**) data of **13** was similar to those of metabolite **6**, except for the absence of hydroxyl group at C-6 and prenyl group at C-7. The ^{1}H-NMR spectrum of **13** showed the existence of pyran ring by a pair of ortho-coupled protons at δ_H 5.64 (d, *J* = 10.0 Hz, 1H, H-11) and 6.79 (d, *J* = 10.0 Hz, 1H, H-10) and a pair of overlapping methyls gave a signal at δ_H 1.53 (s, H-13 and H-14). The doublet signals at δ_H 5.64 (H-11) and 6.79 (H-10) showed HMBC correlations to the carbon signal at δ_C 105.7 (C-2). Consequently, the pyran ring was assigned at C-2 and C-3 (**Figure 3.22**).

A 1,1-dimethylallyl group with its characteristic chemical shift was appeared at δ_H 1.66 (s, 6H, H-4' and H-5'), 5.08 (d, *J* = 10.6 Hz, 1H, H-3'b), 5.24 (d, *J* = 17.7 Hz, 1H, H-3'a) and 6.72 (dd, *J* = 17.7 and 10.6 Hz, 1H, H-2'). Placement of the 1,1-

dimethylallyl group at C-4 was achieved via observed HMBC correlations between δ_H 1.66 (H-4' and H-5') and δ_C 113.4 (C-4) (**Figure 3.22**). The structure of **13** was confirmed by comparing its NMR data to those previously reported and elucidated as caloxanthone C [63].

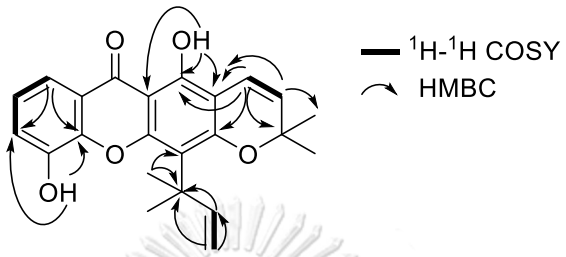

Figure 3.23 ^{1}H-^{1}H COSY and HMBC correlations of metabolite **13**

3.2.14 Structure elucidation of metabolite **14**

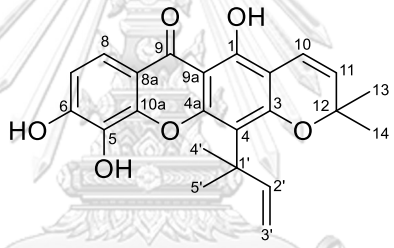

Figure 3.24 Structure of metabolite **14**

Metabolite **14** was obtained as a yellow amorphous solid with molecular formula $C_{23}H_{22}O_6$ determined by analysis of ^{1}H- and ^{13}C-NMR data, as shown in **Tables 3.7** and **3.8**. NMR data of metabolite **14** were very similar with those of metabolite **13**, except the presence of hydroxyl group at C-6. A pair of doublets at δ_H 5.61 (J = 10.0 Hz, 1H, H-11) and 6.76 (J =9.9 Hz, 1H, H-10) pointed to the existence of a pyran ring in the structure. The structure of metabolite **14** was confirmed by comparing its NMR data with previously reported and metabolite **14** was confirmed as macluraxanthone [60].

Table 3.7 ^{1}H-NMR data of metabolites **11-14**

Position	δ_H (ppm), mult, *J* in Hz			
	11[b]	**12**[b]	**13**[a]	**14**[a]
1	7.63, d, 3.1	7.73, dd, 1.6, 7.9	13.45, s	13.53, s
2	8.89, s	7.29, t, 7.9		
3	7.38, dd, 3.1, 8.9	7.36, dd, 1.6, 7.8		
4	7.52, d, 9.0	9.24, s		
4a				
5	7.44, m	7.63, m	6.41, s	5.96, s
6	7.83, ddd, 1.7, 7.1, 8.6	7.85, ddd, 1.7, 7.1, 8.6	7.25, d, 7.4	6.27, s
7	7.58, m	7.47, m	7.27, t, 2.9	6.94, d, 8.1
8	8.24, dd, 1.6, 8.0	8.26, dd, 1.7, 7.9	7.71, dd, 7.2, 1.2	7.68, d, 8.7
8a				
9				
9a				
10a				
10			6.79, d, 10.0	6.76, d, 9.9
11			5.64, d, 10.0	5.61, d, 10.0
12				
13			1.53, s	1.51, s
14			1.53, s	1.51, s
1'				
2'			6.72, dd, 17.7, 10.6	6.72, d, 10.3
3'			5.24, d, 17.7	5.22, d, 17.7
			5.08, d, 10.6	5.05, d, 10.4
4'			1.66, s	1.64, s
5'			1.66, s	1.64, s

a: $CDCl_3$, 400 MHz; b: acetone-d_6, 500 MHz

จุฬาลงกรณ์มหาวิทยาลัย
Chulalongkorn University

Table 3.8 ^{13}C-NMR data of metabolites **11**-**14**

Position	δ_C (ppm)			
	11[b]	**12**[b]	**13**[a]	**14**[c]
1	109.9	117.0	156.9	156.9
2	154.8	124.9	105.7	105.7
3	125.1	121.0	159.6	159.1
4	120.3	147.3	113.4	113.2
4a	150.9	146.3	155.5	154.2
5	118.9	119.0	145.5	131.2
6	135.7	135.9	119.8	149.1
7	124.6	125.1	124.3	112.9
8	127.0	127.0	116.2	117.6
8a	122.0	122.4	120.1	113.8
9	176.9	177.1	181.5	180.9
9a	123.2	123.6	103.7	103.2
10a	157.0	156.7	144.3	144.7
10			116.2	116.2
11			127.4	127.3
12			78.6	78.5
13			28.5	28.1
14			28.5	28.1
1'			41.5	41.6
2'			155.9	157.0
3'			104.3	103.4
4'			28.1	28.3
5'			28.1	28.3

a: $CDCl_3$, 100 MHz; b: acetone-d_6, 125 MHz; c: $CDCl_3$, 125 MHz

จุฬาลงกรณ์มหาวิทยาลัย
Chulalongkorn University

3.2.15 Proposed biosynthesis pathway of isolated metabolites

Finnegan, Patel and Bachman [68] suggested **11** and **12** would be derived from 2,3'-dihydroxybenzophenone. **Figure 3.25** shows a proposed biosynthetic pathway to the xanthones **1-10** and **13-14**. The 1,3,5-trihydroxyxanthone (**10**) and 1,3,7-trihydroxyxanthone (**10.1**) would be produced from 2,3',4,6-tetrahydroxy-benzophenone; they are likely the precursors of all plant xanthones [69]. Further oxidation and *O*-methylation at C-4 and C-2 of **10** would give metabolites **8** and **9**, respectively. The intermediate **10.7** would be generated from **10** via prenylation and cyclization at C-2. Metabolite **6** would be obtained from intermediate **10.7** via oxidation at C-6, followed by prenylation at C-7. The further cyclization of **6** would give metabolite **7**. Prenylation at C-4 of **10**, followed by Claisen rearrangement of the isoprenyl group at C-4, would give intermediate **10.4**. Metabolite **13** would be obtained from intermediate **10.4** via prenylation and cyclization at C-2. Metabolite **14** would be obtained from the oxidation at C-6 of **13.** Prenylation at C-8 and oxidation at C-6 of intermediate **10.4** would give intermediate **10.5**. Intermediate **10.6** would be produced from the methylation at C-5 of **10.5**. Cyclization of **10.6** would generate compound **3**. Besides, oxidation at C-7 of **10.6** would generate metabolite **1**. Moreover, metabolite **2** could be obtained via cyclization of **1**. On the other hand, intermediate **10.1** (not isolated in this study) would generate intermediate **10.2** by oxidation at C-6. Further prenylation and cyclization at C-2 of **10.2** would produce intermediate **10.3**. Finally, prenylation at C-5 and C-8 would give metabolites **5** and **4**, respectively.

จุฬาลงกรณ์มหาวิทยาลัย
CHULALONGKORN UNIVERSITY

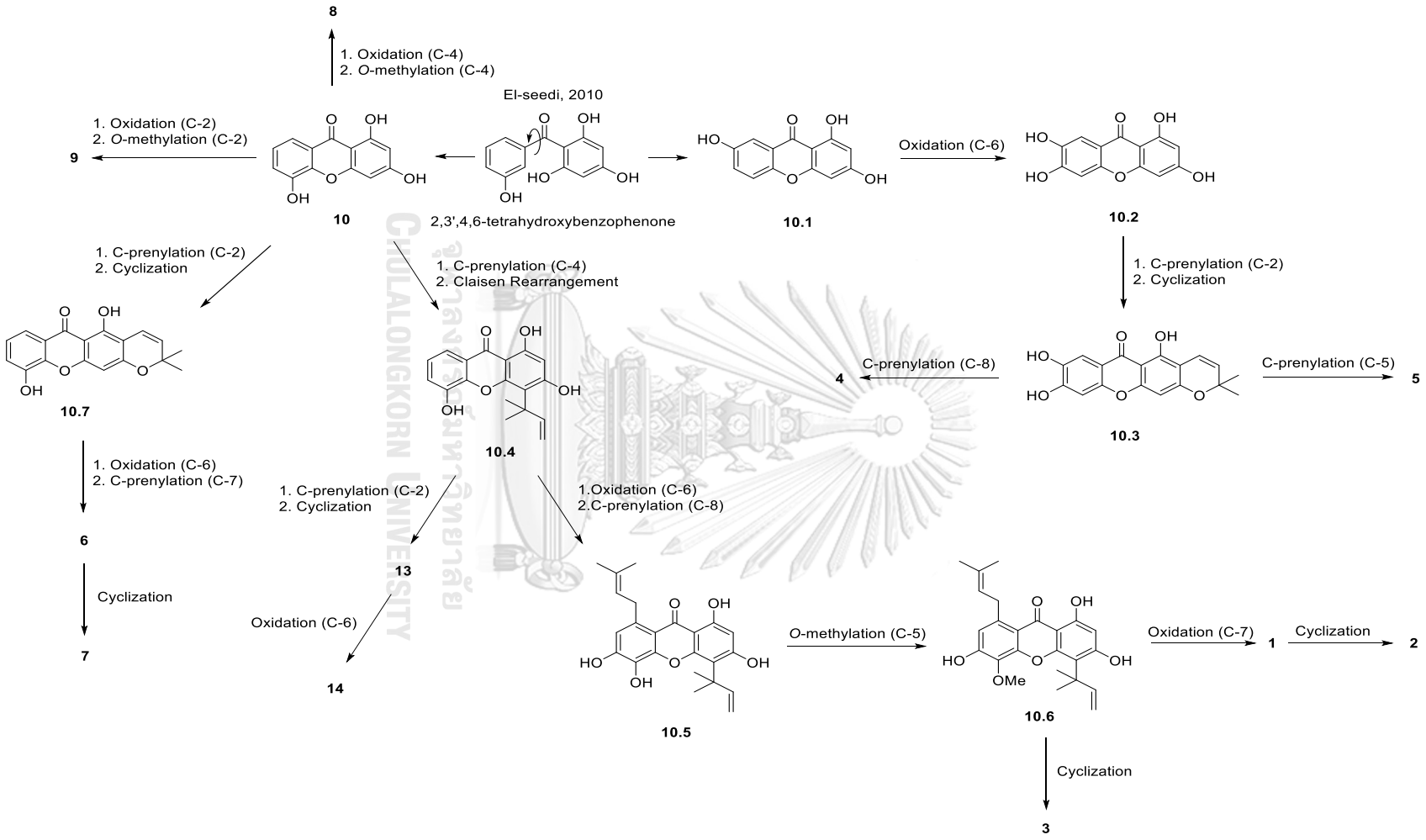

Figure 3.25 Proposed biosynthesis pathway of isolated metabolites

3.3 Anti-proliferative activity

All isolated metabolites (**1**-**14**) were evaluated for their anti-proliferative activity against liver cancer (Hep-G2) and colon cancer (HCT-116) cell lines. The MTT assay examined cell viability to determine the effect of the metabolites on cancer cells. Doxorubicin and sorafenib were used as positive controls. The results are summarized in **Table 3.9**. Twelve metabolites, **1-6**, **8**-**12** and **14** showed anti-proliferative activity toward Hep-G2 and HCT-116 cancer cell lines. The activity of metabolites **7** and **13** did not determine due to the solubility problem, as well as metabolites **8** and **10** did not determine due to the contamination of Hep-G2 cell line.

Table 3.9 Anti-proliferative activity of isolated metabolites on cancer cell lines

Metabolites	IC_{50}[a] (μM)	
	Hep-G2	HCT-116
1	24.50 ± 0.15	9.78 ± 0.14
2	12.37 ± 0.24	12.11 ± 0.08
3	17.95 ± 0.33	11.01 ± 0.07
4	11.40 ± 0.06	10.24 ± 0.04
5	6.07 ± 0.11	3.04 ± 0.12
6	11.00 ± 0.18	4.98 ± 0.21
7	-[b]	-[b]
8	-[b]	>100
9	>100	>100
10	-[b]	>100
11	>100	>100
12	>100	>100
13	-[b]	-[b]
14	5.94 ± 0.13	3.04 ± 0.20
Doxorubicin	3.02 ± 0.39	3.15 ± 0.11
Sorafenib	1.83 ± 0.13	-[b]

a: IC_{50} = 50% inhibition concentration; b: Did not determine;

HCT-116 = colon cancer; Hep-G2 = liver cancer

จุฬาลงกรณ์มหาวิทยาลัย
Chulalongkorn University

Metabolites **1-6** and **14** were more sensitive against HCT-116 than Hep-G2 cells. The proliferation rate of HCT-116 cells was strongly inhibited at IC_{50} values of 3.04 μM by metabolites **5** and **14** comparable to doxorubicin, a standard drug. These xanthones have a prenyl moiety attached at different carbon and a pyrano ring fused at C-2 and C-3. Metabolites **1**-**4** and **6** resulted in decreased activity with IC_{50} values of 9.78, 12.11, 11.01, 10.24 and 4.98 μM, respectively. It is probably caused by prenyl moiety at C-7 and C-8 that increases the steric effect [29]. This is because hydroxy at C-1 or C-8, which ortho to the carbonyl, plays an essential role in increasing the activity due to their capability as hydrogen bond donor and acceptor to enhance the binding affinity of the potential biomolecular targets [70]. When the prenyl moiety is attached at C-7 or C-8, it may prevent the hydrogen bond interactions from occurring and caused a reduction in activity.

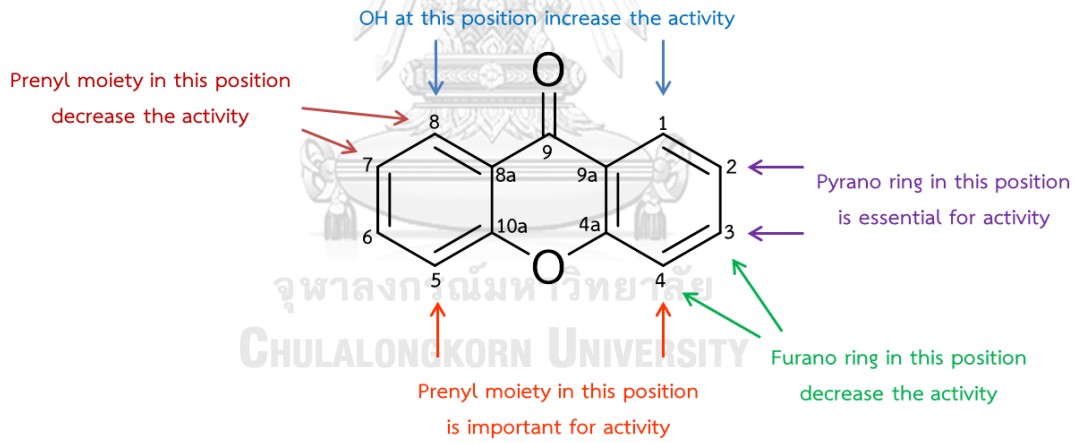

จุฬาลงกรณ์มหาวิทยาลัย
Chulalongkorn University

Figure 3.26 Summary of SAR of xanthone skeleton for anti-proliferative activity

Metabolites **5** and **14** were also found to have good activities toward Hep-G2 cells with IC_{50} values of 6.07 and 5.94 μM, respectively. Meanwhile, the activity of xanthones **1**-**6** were decreased probably due to the prenyl moiety in the xanthone nucleus, C-7 and C-8 [29]. Those metabolites exhibited IC_{50} values of 24.50, 12.37, 17.95, 11.40 and 11.00 μM, respectively. The activity of **4** and **6** were 2-fold increased compare to **1.** It may occur due to the presence of pyrano ring fused at C-2 and C-3.

Therefore, metabolites **5** and **14** were the most active metabolites against both HCT-116 and Hep-G2 cancer cell lines.

Metabolites **1** and **2** have similar structure. Fusion of 1,1-dimethylallyl to 2,3,3-trimethyldihydrofuran ring at C-3 and C-4 showed that it did not significantly decrease the activity for both metabolites toward HCT-116 cell lines. On the other hand, it displayed a two-fold increase in activity against Hep-G2 for metabolite **2** (IC_{50} 12.37 μM), compare with metabolite **1** (IC_{50} 24.50 μM). The furan ring fused at C-3 and C-4 of **2** and **3** might cause a decrease in activity toward HCT-116 cells; however, their activity increased against Hep-G2 cells [29]. The summary of structure activity relationship (SAR) is shown in **Figure 3.26**.

The results indicated that prenyl group and heterocycles (such as furano and pyrano rings) play an important role in the anti-proliferative activity. Prenylation at C-4 could increase their binding affinity [71]. Prenyl moiety might lead to higher membrane permeability by their lipophilic nature [72]. However, heterocycles play a much more significant role in medicinal chemistry. It has some drug properties, including potency and selectivity through bioisosteric replacements, lipophilicity, polarity and aqueous solubility [73]. Heterocycles could engage in a wide variety of intermolecular interactions. Their abilities include hydrogen bond donor/acceptor, pi stacking interactions, hydrophobic forces, metal co-ordination and van der Waals bonds [74].

จุฬาลงกรณ์มหาวิทยาลัย
Chulalongkorn University

3.4 Study on action mechanism of macluraxanthone (14)

Apoptosis is a natural mechanism for programmed cell death. One of the main functions of apoptosis is cancer prevention. Apoptosis plays a critical role to eliminating any unnecessary or unwanted cells. Two different pathways lead to apoptosis: the intrinsic pathway activated by intracellular signal and the extrinsic pathway activated by extracellular signals [75]. The intracellular signals include DNA

damage, growth factor deprivation and cytokine deprivation. The extracellular signals are commonly produced by cytotoxic T cells from the immune system in response to damaged or infected [76]. The illustration of the apoptosis pathway is shown in **Figure 3.27** [77].

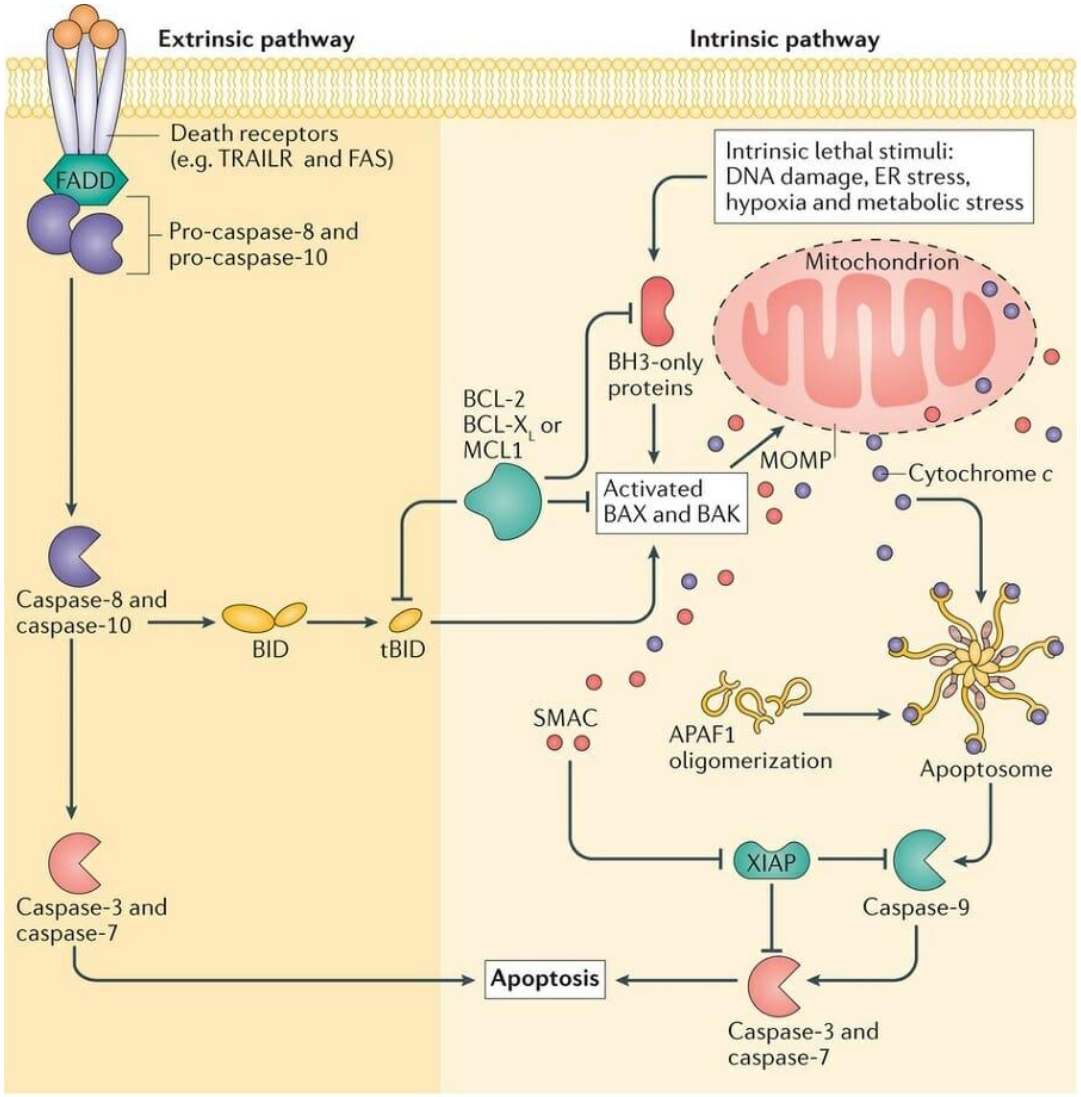

Figure 3.27 Extrinsic and intrinsic pathways of apoptosis

The extrinsic pathway of apoptosis starts with a signal molecule (commonly FAS and TRIAL) binding to a receptor outside the cell membrane. These molecules may be excreted by neighboring cells when they were damaged or no longer needed. The binding process causes FADD activation. The activated FADD interact with pro-

caspase-8 and pro-caspase-10 to form caspase-8 and caspase-10, which play an essential role in starting apoptosis. The activation of caspase-8 and caspase-10 transform BID into tBID, tBID moves to the mitochondria to activate BAX and BAK. After the BAX and BAK are activated, the steps are the same for both the extrinsic and intrinsic pathways [77].

The intrinsic pathway is triggered by cell stress or damage. It then activates BH3-only proteins. BH3-only proteins consist of pro- and anti-apoptosis proteins. Pro-apoptosis BH3-only proteins activates BAX and BAK (the same proteins that are activated by tBID). Activated BAX and BAK cause a condition called mitochondrial outer membrane permeability (MOMP). It plays a key role in apoptosis by allowing the release of cytochrome C into the cytoplasm. Cytochrome C prompts the formation of the apoptosome, which then activates pro-caspase-9 into caspase-9. Caspase-9 activates caspase-3 and caspase-7. Activated caspase-3 and caspase-7 begin the breakdown of cellular materials [77].

B-cell lymphoma-2 (Bcl-2) family of proteins consists of pro- and anti-apoptotic members, which interact to balance newly forming cells and old dying cells [78]. The anti-apoptotic subfamily contains the Bcl-2 and Bcl-XL, whereas the pro-apoptotic proteins including BAX, BAK, BID and BH3-only proteins [79]. When anti-apoptotic Bcl-2 family members are overexpressed, pro- and anti-apoptotic Bcl-2 family members' ratio is disturbed and apoptotic cell death can be prevented. Bcl-2 was found to promote cell survival because it increases the total cell number by preventing cell death. As shown in **Figure 3.27**, the role of Bcl-2-like anti-apoptotic proteins is to inhibit their pro-apoptotic partners by binding with pro-apoptotic proteins or inhibiting the direct activator of pro-apoptotic proteins [80]. High expression of anti-apoptotic members such as Bcl-2 and Bcl-XL are commonly found in a wide variety of human cancers. It mediates cancers' resistance to a broad

จุฬาลงกรณ์มหาวิทยาลัย
Chulalongkorn University

spectrum of chemotherapeutic drugs and gamma-irradiation, which induce apoptosis in tumor cells. By blocking the cell death signals triggered by these drugs, Bcl-2 and Bcl-XL can interfere with many anti-cancer drugs' therapeutic effects. Hence, targeting Bcl-2 and Bcl-XL could either restore the apoptotic process in tumor cells or sensitize these tumors for chemo- and radiotherapies, which necessary for the development of novel anti-cancer treatments [81, 82].

Macluraxanthone (**14**) was tested on western blot analysis to examine whether it can reduce Bcl-2 and Bcl-XL expressions, anti-apoptosis proteins. Herein, Hep-G2 cells were treated with indicated concentrations of **14** to observe the effect on Bcl-2 and Bcl-XL expressions. Treatment of the cells with a different concentration of **14** led to decreased Bcl-2 expression in concentration 5 μM and Bcl-XL expression in concentration 10 μM (**Figure 3.28**). These data indicated that **14** induced apoptosis in a concentration-dependent manner by the down-regulation of the expression of both Bcl-2 and Bcl-XL.

จุฬาลงกรณ์มหาวิทยาลัย
Chulalongkorn University

A

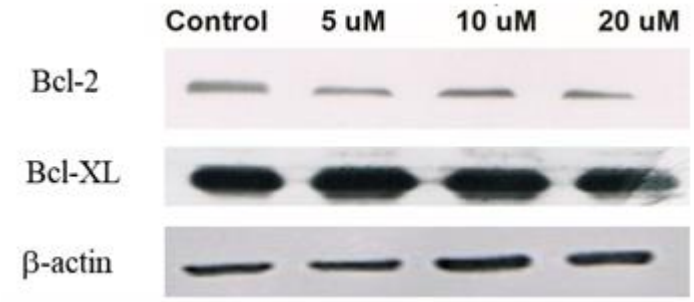

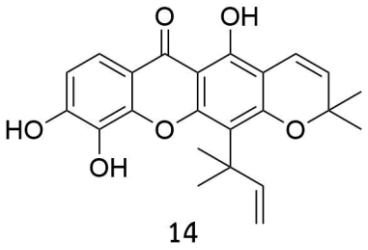

14

B

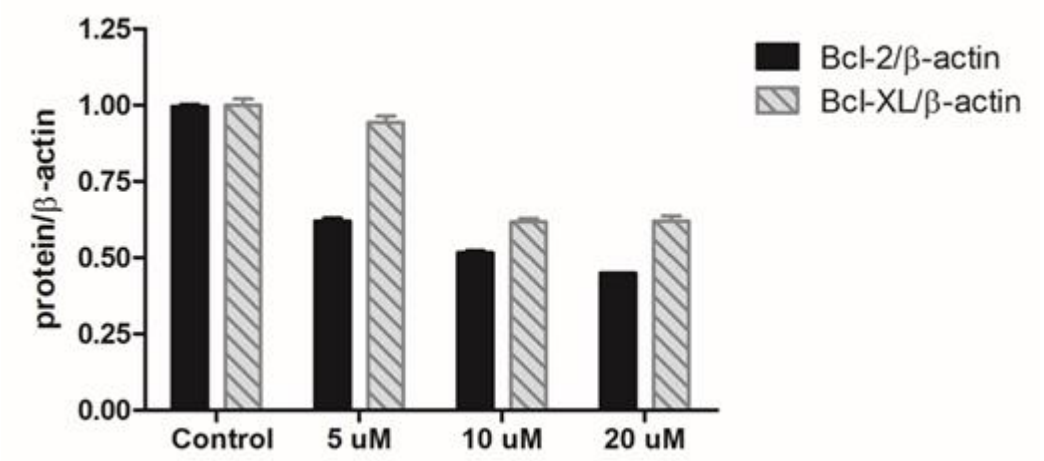

จุฬาลงกรณ์มหาวิทยาลัย
CHULALONGKORN UNIVERSITY

Figure 3.28 Effects of **14** on the expression level of Bcl-2 and Bcl-XL proteins. Inhibitory effects of **14** on Bcl-2 and Bcl-XL expressions in Hep-G2 cell lines in concentration-dependent manner (**A**). The levels of Bcl-2 and Bcl-XL proteins were examined by western blot analysis. The relative Bcl-2 and Bcl-XL proteins were measured by densitometry analysis (**B**).

CHAPTER IV
CONCLUSION

In conclusion, purification of the *n*-hexane and EtOAc crude extracts of *C. inophyllum* root yielded two new prenylated xanthones, namely 1,3,6,7-tetrahydroxy-5-methoxy-4-(1',1'-dimethyl-2'-propenyl)-8-(3",3"-dimethyl-2"-propenyl)-xanthone (**1**) and 7-hydroxycaloxanthone B (**2**), along with twelve known metabolites. These metabolites were identified as caloxanthone B (**3**), 7-*O*-demethylmangostanin (**4**), caloxanthone A (**5**), 7-prenyljacaerubin (**6**), pyranojacareubin (**7**), daphnifolin (**8**), tovopyrifolin C (**9**), 1,3,5-trihydroxyxanthone (**10**), 2-hydroxyxanthone (**11**), 4-hydroxyxanthone (**12**), caloxanthone C (**13**) and macluraxanthone (**14**). In addition, metabolites **4**, **6** and **8** were isolated from the genus *Calophyllum* for the first time. All metabolites were evaluated for their anti-proliferative activity against two cancer cell lines; liver cancer (Hep-G2) and colon cancer (HCT-116). Metabolites **5** and **14** showed the most active metabolites against both Hep-G2 and HCT-116 cancer cell lines, both **5** and **14** displayed strong activities toward HCT-116 with IC_{50} values of 3.04 μM comparable to doxorubicin, a standard drug. Besides, **5** and **14** exhibited potent activities against Hep-G2 with IC_{50} values of 6.07 and 5.94 μM, respectively. Furthermore, metabolite **14** was subjected to western blot analysis to study its mechanism of action. The result demonstrated that **14** induced apoptosis in concentration-dependent manner by the down-regulation of the expression of both Bcl-2 and Bcl-XL proteins.

จุฬาลงกรณ์มหาวิทยาลัย
Chulalongkorn University

REFERENCES

จุฬาลงกรณ์มหาวิทยาลัย
Chulalongkorn University

[1] World Health Organization. Cancer Overview [Online]. 2018. Available from: https://www.who.int/health-topics/cancer#tab=tab_1 [October 26]

[2] Global Cancer Observatory. All cancers fact sheets [Online]. 2018. Available from: https://gco.iarc.fr/today/data/factsheets/cancers/39-All-cancers-fact-sheet.pdf [October 26]

[3] Global Cancer Observatory. Thailand fact sheets [Online]. 2018. Available from: https://gco.iarc.fr/today/data/factsheets/populations/764-thailand-fact-sheets.pdf [October 26]

[4] Terzić, J., Grivennikov, S., Karin, E., and Karin, M. Inflammation and colon cancer. Gastroenterology 138(6) (2010): 2101-2114. e5.

[5] Doll, R. and Peto, R. The causes of cancer: quantitative estimates of avoidable risks of cancer in the United States today. Journal of the National Cancer Institute 66(6) (1981): 1192-1308.

[6] Giovannucci, E. and Willett, W.C. Dietary factors and risk of colon cancer. Annals of Medicine 26(6) (1994): 443-452.

[7] Marengo, A., Rosso, C., and Bugianesi, E. Liver cancer: connections with obesity, fatty liver, and cirrhosis. Annual Review of Medicine 67 (2016): 103-117.

[8] Castello, G., Scala, S., Palmieri, G., Curley, S.A., and Izzo, F. HCV-related hepatocellular carcinoma: From chronic inflammation to cancer. Clinical Immunology 134(3) (2010): 237-250.

[9] Tresó, B., Barcsay, E., Tarján, A., Horváth, G., Dencs, Á., Hettmann, A., Csépai, M.M. Győri, Z., Rusvai, E., and Takács, M. Prevalence and correlates of HCV, HVB, and HIV infection among prison inmates and staff, Hungary. Journal of Urban Health 89(1) (2012): 108-116.

จุฬาลงกรณ์มหาวิทยาลัย
Chulalongkorn University

[10] MacCarthy-Morrogh, L. and Martin, P. The hallmarks of cancer are also the hallmarks of wound healing. Science Signaling 13(648) (2020): eaay8690.

[11] Hanahan, D. and Weinberg, R.A. Hallmarks of cancer: the next generation. Cell 144(5) (2011): 646-674.

[12] López-Sáez, J.F., De la Torre, C., Pincheira, J., and Martín, G.G. Cell proliferation and cancer. Histology and Histopathology 13(4) (1998): 1197-1214.

[13] Guan, J.-L. Cell migration: developmental methods and protocols. Vol. 294: Springer Science & Business Media, 2005.

[14] Rivankar, S. An overview of doxorubicin formulations in cancer therapy. Journal of Cancer Research and Therapeutics 10(4) (2014): 853.

[15] Zhu, Y.-j., Zheng, B., Wang, H.-y., and Chen, L. New knowledge of the mechanisms of sorafenib resistance in liver cancer. Acta Pharmacologica Sinica 38(5) (2017): 614-622.

[16] Gupta, S. and Gupta, P. The Genus *Calophyllum*: Review of Ethnomedicinal Uses, Phytochemistry and Pharmacology. in Bioactive Natural Products in Drug Discovery, pp. 215-242: Springer, 2020.

[17] Chompipat, P. Proliferation of Healthy Cells and Cancer Cells. Comparison illustration of normal cell proliferation and Cancer cell. [Online]. 2020. Available from: https://www.dreamstime.com/proliferation-healthy-cells-cancer-comparison-illustration-normal-cell-body-image167464732 [February 26]

[18] Permana, D., Abas, F., Maulidiani, Shaari, K., Stanslas, J., Ali, A.M., and Lajis, N.Hj. Atrovirisidone B, a new prenylated depsidone with cytotoxic property from the roots of *Garcinia atroviridis*. Zeitschrift für Naturforschung C 60(7-8) (2005): 523-526.

จุฬาลงกรณ์มหาวิทยาลัย
Chulalongkorn University

[19] Cheenpracha, S., Phakhodee, W., Ritthiwigrom, T., Prawat, U., and Laphookhieo, S. A new depsidone from the twigs of *Garcinia cowa.* Heterocycles 83(5) (2011): 1139.

[20] Xu, G., Kan, W.L.T., Zhou, Y., Song, J.-Z., Han, Q.-B., Qiao, C.-F., Cho, C.-H., Rudd, J.A., Lin, G., and Xu. H.-X. Cytotoxic acylphloroglucinol derivatives from the twigs of *Garcinia cowa.* Journal of Natural Products 73(2) (2010): 104-108.

[21] Shen, J., Tian, Z., and Yang, J.-S. The constituents from the stems of *Garcinia cowa* Roxb. and their cytotoxic activities. Die Pharmazie 62(7) (2007): 549.

[22] Chen, J.-J., Chen, I.-S., and Duh, C.-Y. Cytotoxic xanthones and biphenyls from the root of *Garcinia linii.* Planta Medica 70(12) (2004): 1195-1200.

[23] He, F., Wang, M., Gao, M., Zhao, M., Bai, Y., and Zhao, C. Chemical composition and biological activities of *Gerbera anandria.* Molecules 19(4) (2014): 4046-4057.

[24] Nkengfack, A.E., Azebaze, G.A., Vardamides, J.C., Fomum, Z.T., and van Heerden, F.R. A prenylated xanthone from *Allanblackia floribunda.* Phytochemistry 60(4) (2002): 381-384.

[25] Leet, J.E., Liu, X., Drexler, D.M., Cantone, J.L., Huang, S., Mamber, S.W. Fairchild, C.R., Hussain, R., Newman, D.J., and Kingston, D.G.I. Cytotoxic xanthones from *Psorospermum molluscum* from the Madagascar rain forest. Journal of Natural Products 71(3) (2008): 460-463.

[26] Tanjung, M., Tjahjandarie, T.S., Saputri, R.D., Kurnia, B.D., Rachman, M.F., and Syah, Y.M. Calotetrapterins A-C, three new pyranoxanthones and their cytotoxicity from the stem bark of *Calophyllum tetrapterum* Miq. Natural Product Research (2019): 1-6.

[27] Kar Wei, L., Zamakshshari, N.H., Ee, G.C.L., Mah, S.H., and Mohd Nor, S.M. Isolation and structural modifications of ananixanthone from *Calophyllum*

teysmannii and their cytotoxic activities. Natural Product Research 32(18) (2018): 2147-2151.

[28] Laopian, F., Kaennakam, S., Rassamee, K., Siripong, P., and Tip-pyang, S. Calaxanthones A-C, three new xanthones from the roots of *Calophyllum calaba* and the cytotoxicity. Natural Product Research 33(11) (2019): 1584-1590.

[29] Mah, S.H., Ee, G.C.L., Teh, S.S., and Sukari, M.A. *Calophyllum inophyllum* and *Calophyllum soulattri* source of anti-proliferative xanthones and their structure–activity relationships. Natural Product Research 29(1) (2015): 98-101.

[30] Byrne, C., Parnell, J.A.N., and Chayamarit, K.J.T.F.B. Systematics of the Thai *Calophyllaceae* and *Hypericaceae* with comments on the *Kielmeyeroidae* (Clusiaceae). 46(2) (2018): 162-216.

[31] Sungkaew, S., Pongumpai, S., Sookchaloen, D., and Santisuk, T. The Genus *Calophyllum* (Guttiferae) in Thailand. Journal of Forest Management 3 (2009): 2552-2575.

[32] Kainuma, M., Baba, S., Chan, H.T., Inoue, T., Tangah, J., and Chan, E.W.C. Medicinal plants of sandy shores: A short review on *Calophyllum inophyllum* and *Thespesia populnea.* International Journal of Pharmacognosy and Phytochemical Research 8 (2016): 2056-2062.

[33] Aminudin, N.I., Ahmad, F., Taher, M., and Zulkifli, R.M. α-Glucosidase and 15-lipoxygenase inhibitory activities of phytochemicals from *Calophyllum symingtonianum.* Natural Product Communications 10(9) (2015): 1934578X1501000925.

[34] Sundur, S., Shrivastava, B., Sharma, P., Raj, S.S., and Jayasekhar, V. A review article of pharmacological activities and biological importance of *Calophyllum inophyllum.* International Journal of Advanced Research 2(12) (2014): 599-603.

จุฬาลงกรณ์มหาวิทยาลัย
Chulalongkorn University

[35] Fern, K. *Calophyllum inophyllum* [Online]. Available from: http://tropical.theferns.info/viewtropical.php?id=Calophyllum+inophyllum [November 14]

[36] Zou, J., Wu, J., Liu, S.Z., and Zhao, W.M. New coumarins and triterpenes from *Calophyllum inophyllum.* Helvetica Chimica Acta 93(9) (2010): 1812-1821.

[37] Itoigawa, M., Ito, C., Tan, H.T-W., Kuchide, M., Tokuda, H., Nishino, H., and Furukawa, H. Cancer chemopreventive agents, 4-phenylcoumarins from *Calophyllum inophyllum.* Cancer letters 169(1) (2001): 15-19.

[38] Li, Z.-l., Li, Y., Qin, N-b., Li, D-h., Liu, Z-g., Liu, Q., and Hua, H-m. Four new coumarins from the leaves of *Calophyllum inophyllum.* Phytochemistry Letters 16 (2016): 203-206.

[39] Ponguschariyagul, S., Sichaem, J., Khumkratok, S., Siripong, P., Lugsanangarm, K., and Tip-Pyang, S. Caloinophyllin A, a new chromanone derivative from *Calophyllum inophyllum* roots. Natural Product Research 32(21) (2018): 2535-2541.

[40] Ee, G., Jong, V., Sukari, M., Rahmani, M., and Kua, A. Xanthones from *Calophyllum inophyllum.* Pertanika Journal of Science and Technology 17(2) (2009): 307-312.

[41] Iinuma, M., Tosa, H., Tanaka, T., and Yonemori, S. Two xanthones from root bark of *Calophyllum inophyllum.* Phytochemistry 35(2) (1994): 527-532.

[42] Iinuma, M., Tosa, H., Tanaka, T., and Yonemori, S. Two new xanthones in the underground part of *Calophyllum inophyllum.* Heterocycles 37(2) (1994): 833-838.

[43] Iinuma, M., Tosa, H., Tanaka, T., and Yonemori, S. Two xanthones from roots of *Calophyllum inophyllum.* Phytochemistry 38(3) (1995): 725-728.

จุฬาลงกรณ์มหาวิทยาลัย
Chulalongkorn University

[44] Yimdjo, M.C., Azebaze, A.G., Nkengfack, A.E., Meyer, A.M., Bodo, B., and Fomum, Z.T. Antimicrobial and cytotoxic agents from *Calophyllum inophyllum.* Phytochemistry 65(20) (2004): 2789-2795.

[45] Ee, G., Kua, A., Cheow, Y., Lim, C., Jong, V., and Rahmani, M. A new pyranoxanthone inophyllin B from *Calophyllum inophyllum.* Natural Product Sciences 10 (2004): 220-222.

[46] Wei, D.-J., Mei, W.-L., Zhong, H.-M., Zeng, Y.-B., Wu, X.-D., and Dai, H.-F. A new prenylated xanthone from the branches of *Calophyllum inophyllum.* Journal of Asian Natural Products Research 13(03) (2011): 265-269.

[47] Xiao, Q., Zeng, Y.-B., Mei, W.-L., Zhao, Y.-X., Deng, Y.-Y., and Dai, H.-F. Cytotoxic prenylated xanthones from *Calophyllum inophyllum.* Journal of Asian Natural Products Research 10(10) (2008): 993-997.

[48] Prasad, J., Shrivastava, A., Khanna, A., Bhatia, G., Awasthi, S., and Narender, T. Antidyslipidemic and antioxidant activity of the constituents isolated from the leaves of *Calophyllum inophyllum*. Phytomedicine 19(14) (2012): 1245-1249.

[49] Li, Y.-Z., Li, Z-L., Yin, S-L., Shi, G., Liu, M-S., Jing, Y-K., and Hua, H-M. Triterpenoids from *Calophyllum inophyllum* and their growth inhibitory effects on human leukemia HL-60 cells. Fitoterapia 81(6) (2010): 586-589.

[50] Sichaem, J., Tip-Pyang, S., and Siripong, P. Chemical Constituents from the Root Bark of *Calophyllum inophyllum.* Natural Product Communications 13(6) (2018): 1934578X1801300618.

[51] Van Thanh, N., Jang, H-J., Vinh, L.B., Linh, K.T.P., Huong, P.T.T., Cuong, N.X., Nam, N.H., Van Minh, C., Kim, Y.H., and Yang, S.Y. Chemical constituents from Vietnamese mangrove *Calophyllum inophyllum* and their anti-inflammatory effects. Bioorganic Chemistry 88 (2019): 102921.

จุฬาลงกรณ์มหาวิทยาลัย
Chulalongkorn University

[52] Ee, G.C.L., Mah, S.H., Rahmani, M., Taufiq-Yap, Y.H., Teh, S.S., and Lim, Y.M. A new furanoxanthone from the stem bark of *Calophyllum inophyllum.* Journal of Asian Natural Products Research 13(10) (2011): 956-960.

[53] Ee, G., Kua, A., Lim, C., Jong, V., and Lee, H. Inophyllin A, a new pyranoxanthone from *Calophyllum inophyllum* (Guttiferae). Natural Product Research 20(05) (2006): 485-491.

[54] Chan, K.M., Hamzah, R., Abd Rahaman, A., Jong, V.Y.M., Khong, H.Y., Rajab, N.F., Ee, G.C.L., and Inayat-Hussain, S.H. The pyranoxanthone inophyllin A induces oxidative stress mediated-apoptosis in Jurkat T lymphoblastic leukemia cells. Food and Chemical Toxicology 50(8) (2012): 2916-2922.

[55] Nguyen, V.-L., Truong, C-T., Nguyen, B.C.Q., Vo, T-N.V., Dao, T-T., Nguyen, V-D., Trinh, D-T.T., Huynh, H.K., and Bui, C-B. Anti-inflammatory and wound healing activities of calophyllolide isolated from *Calophyllum inophyllum* Linn. PloS one 12(10) (2017): e0185674.

[56] Patil, A.D., Freyer, A.J., Eggleston, D.S., Haltiwanger, R.C., Bean, M.F., Taylor, P.B., Caranfa, M.J., Breen, A.L., and Bartus, H.R. The inophyllums, novel inhibitors of HIV-1 reverse transcriptase isolated from the Malaysian tree, *Calophyllum inophyllum* Linn. Journal of Medicinal Chemistry 36(26) (1993): 4131-4138.

จุฬาลงกรณ์มหาวิทยาลัย
CHULALONGKORN UNIVERSITY

[57] Mah, S.H., Ee, G.C.L., Rahmani, M., Taufiq-Yap, Y.H., Sukari, M.A., and Teh, S.S. A new pyranoxanthone from *Calophyllum soulattri.* Molecules 16(5) (2011): 3999-4004.

[58] Cao, S.-G., Lim, T.-B., Sim, K.-Y., and Goh, S. A highly prenylated xanthone from the bark of *Calophyllum gracilipes* (Guttiferae). Natural Product Letters 10(1) (1997): 55-58.

[59] Fujimoto, T., Hano, Y., and Nomura, T. Components of root bark of *Cudrania tricuspidata* l. 1, 2 structures of four new isoprenylated xanthones, cudraxanthones A, B, C and D. Planta Medica 50(03) (1984): 218-221.

[60] Yang, R., Li, P., Li, N., Zhang, Q., Bai, X., Wang, L., Xiao, Y., Sun, L., Yang, Q., and Yan, J. Xanthones from the Pericarp of *Garcinia mangostana.* Molecules 22(5) (2017): 683.

[61] Daud, S.B., Ee, G.C.L., Malek, E.A., Teh, S.S., and See, I. A new coumarin from *Calophyllum hosei.* Natural Product Research 28(19) (2014): 1534-1538.

[62] Fan, Q., Na, Z., Hu, H., Xu, Y., and Tang, T. Chemical constituents from stem barks of *Garcinia paucinervis.* Chinese Traditional and Herbal Drugs 43 (2012): 436-439.

[63] Tee, K.H., Ee, G.C.L., Wong, K.W., Karunakaran, T., Jong, V.Y.M., and Teh, S.S. Natural Products from Stem Bark of *Calophyllum andersonii.* Pertanika Journal of Tropical Agricultural Science 41(2) (2018).

[64] Ee, G., Lim, C., Ong, G., Sukari, M., and Lee, H. Daphnifolin, a new xanthone from *Mesua daphnifolia* (Guttiferae) Note. Journal of Asian Natural Products Research 8(6) (2006): 567-570.

[65] Valentão, P., Areias, F., Amaral, J., Andrade, P., and Seabra, R. Tetraoxygenated xanthones from *Centaurium erythraea.* Natural Product Letters 14(5) (2000): 319-323.

[66] Li, Y.-P. and Huang, S.-T. Xanthones from *Swertia nervosa* and their Inhibitory Effects on Nitric Oxide Production. Chemistry of Natural Compounds 56(4) (2020): 732-735.

[67] Fernandes, E.G., Silva, A.M.S., Cavaleiro, J.A.S., Silva, F.M., Fernanda, M., Borges, M., and Pinto, M.M.M. 1H and 13C NMR Spectroscopy of mono-, di-, tri-and tetrasubstituted xanthones. Magnetic Resonance in Chemistry 36(4) (1998): 305-309.

จุฬาลงกรณ์มหาวิทยาลัย
Chulalongkorn University

[68] Finnegan, R., Patel, J., and Bachman, P. Constituents of *Mammea americana* L., V. Some simple mono-and dihydroxyxanthones. Tetrahedron Letters 7(49) (1966): 6087-6092.

[69] El-Seedi, H.R., Bohlin, L., Borg-Karlson, A-K., Goransson, U., and Verpoorte, R. Recent insights into the biosynthesis and biological activities of natural xanthones. Current Medicinal Chemistry 17(9) (2010): 854-901.

[70] Zhang, X., Li, X., Ye, S., Zhang, Y., Tao, L., Gao, Y., Gong, D., Xi, M., Meng, H., and Zhang, M. Synthesis, SAR and biological evaluation of natural and non-natural hydroxylated and prenylated xanthones as antitumor agents. Medicinal Chemistry 8(6) (2012): 1012-1025.

[71] Pinto, M. and Castanheiro, R. Synthesis of prenylated xanthones: an overview. Current Organic Chemistry 13(12) (2009): 1215-1240.

[72] Klein-Júnior, L.C., Campos, A., Niero, R., Corrêa, R., Vander Heyden, Y., and Filho, V.C. Xanthones and Cancer: from Natural Sources to Mechanisms of Action. Chemistry & Biodiversity 17(2) (2020): e1900499.

[73] Gomtsyan, A. Heterocycles in drugs and drug discovery. Chemistry of Heterocyclic Compounds 48(1) (2012): 7-10.

[74] Pearce, S. The importance of heterocyclic compounds in anti-cancer drug design. Drug Discovery (2017): 67.

[75] Pfeffer, C.M. and Singh, A.T. Apoptosis: a target for anticancer therapy. International Journal of Molecular Sciences 19(2) (2018): 448.

[76] Zaman, S., Wang, R., and Gandhi, V. Targeting the apoptosis pathway in hematologic malignancies. Leukemia & Lymphoma 55(9) (2014): 1980-1992.

[77] Ichim, G. and Tait, S.W. A fate worse than death: apoptosis as an oncogenic process. Nature Reviews Cancer 16(8) (2016): 539.

จุฬาลงกรณ์มหาวิทยาลัย
Chulalongkorn University

[78] Kang, M.H. and Reynolds, C.P. Bcl-2 inhibitors: targeting mitochondrial apoptotic pathways in cancer therapy. Clinical Cancer Research 15(4) (2009): 1126-1132.

[79] Packham, G. and Stevenson, F.K. Bodyguards and assassins: Bcl-2 family proteins and apoptosis control in chronic lymphocytic leukaemia. Immunology 114(4) (2005): 441-449.

[80] Hardwick, J.M. and Soane, L. Multiple functions of BCL-2 family proteins. Cold Spring Harbor Perspectives in Biology 5(2) (2013): a008722.

[81] Huang, Z. Bcl-2 family proteins as targets for anticancer drug design. Oncogene 19(56) (2000): 6627-6631.

[82] Vogler, M. Targeting BCL2-proteins for the treatment of solid tumours. Advances in Medicine 2014 (2014).

จุฬาลงกรณ์มหาวิทยาลัย
Chulalongkorn University

APPENDIX

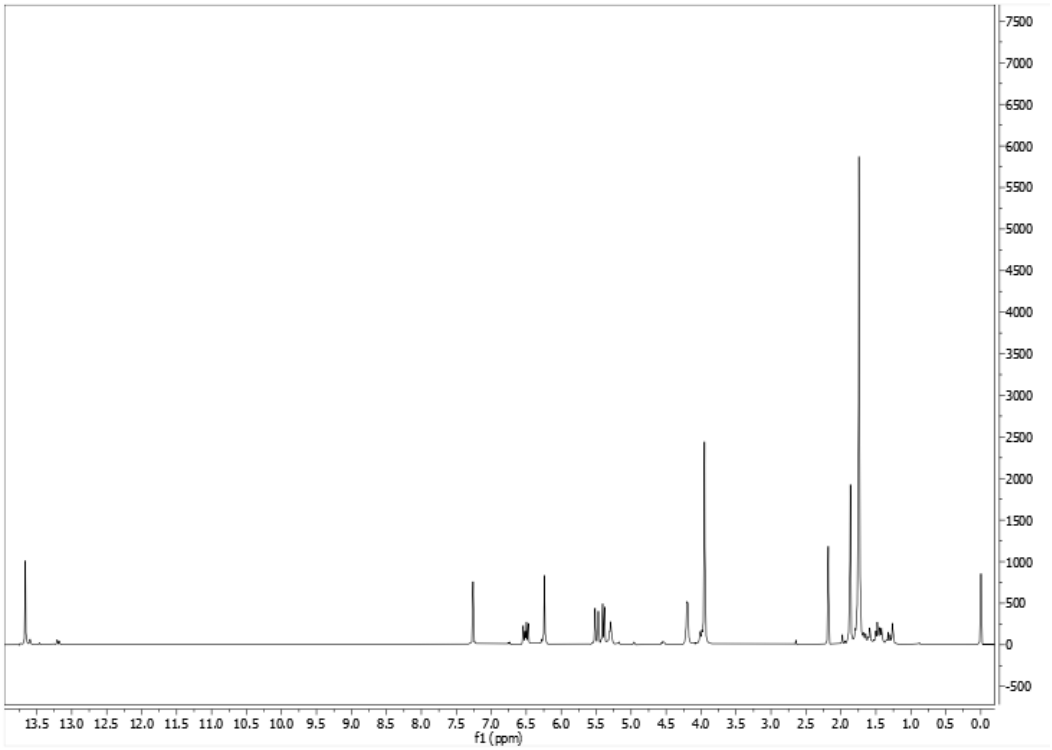

Figure A.1 ^{1}H NMR (400 MHz, $CDCl_3$) spectrum of metabolite **1**

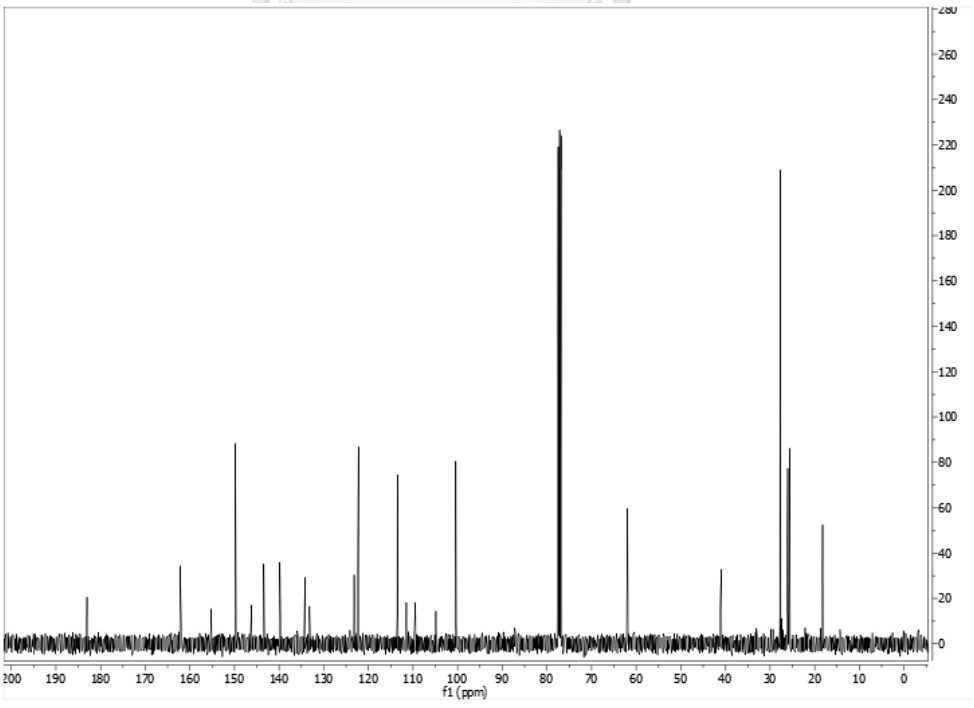

Figure A.2 ^{13}C NMR (100 MHz, $CDCl_3$) spectrum of metabolite **1**

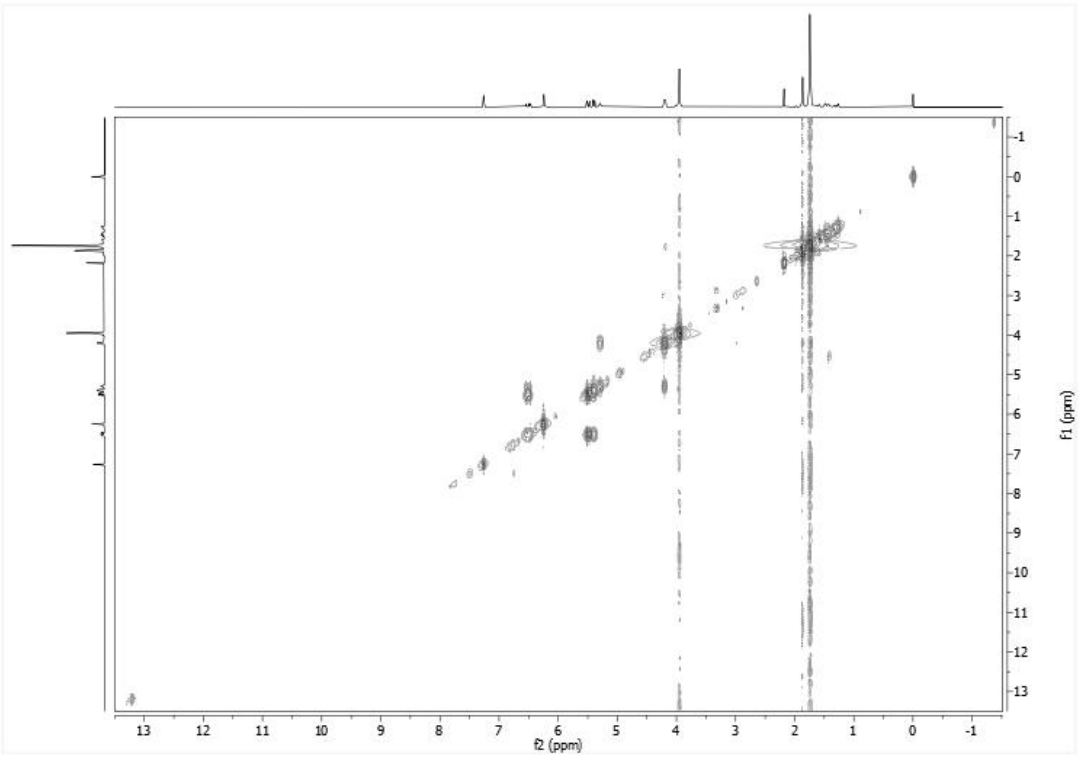

Figure A.3 ^{1}H-^{1}H COSY spectrum ($CDCl_3$) of metabolite **1**

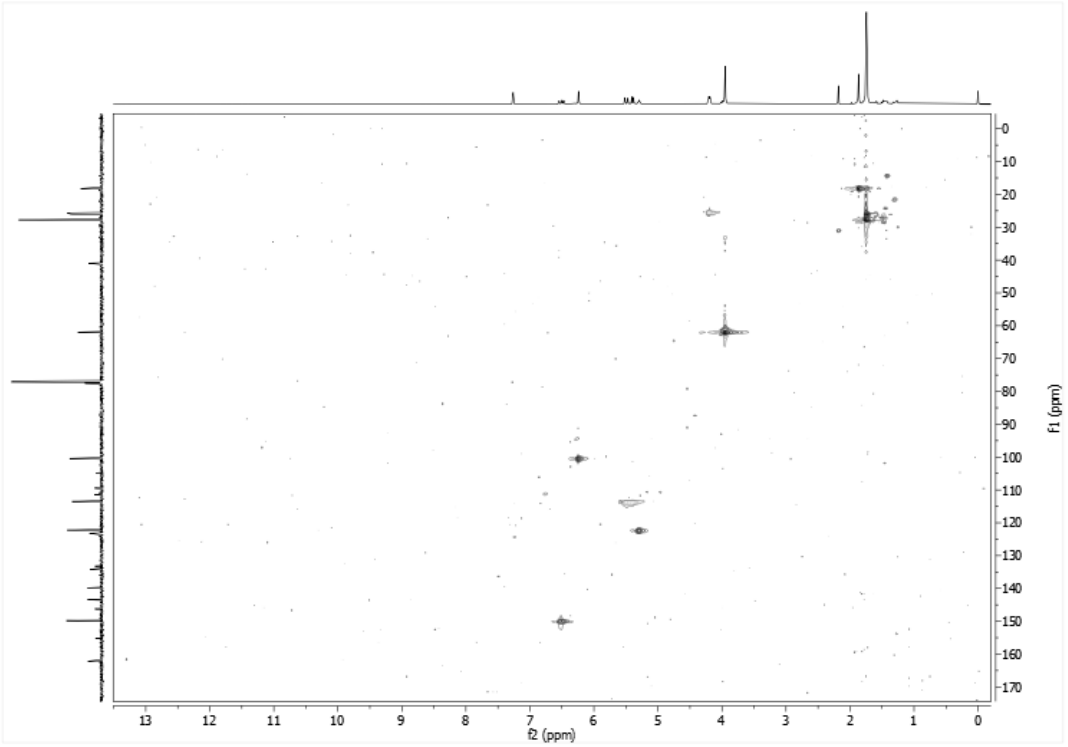

Figure A.4 HSQC spectrum ($CDCl_3$) of metabolite **1**

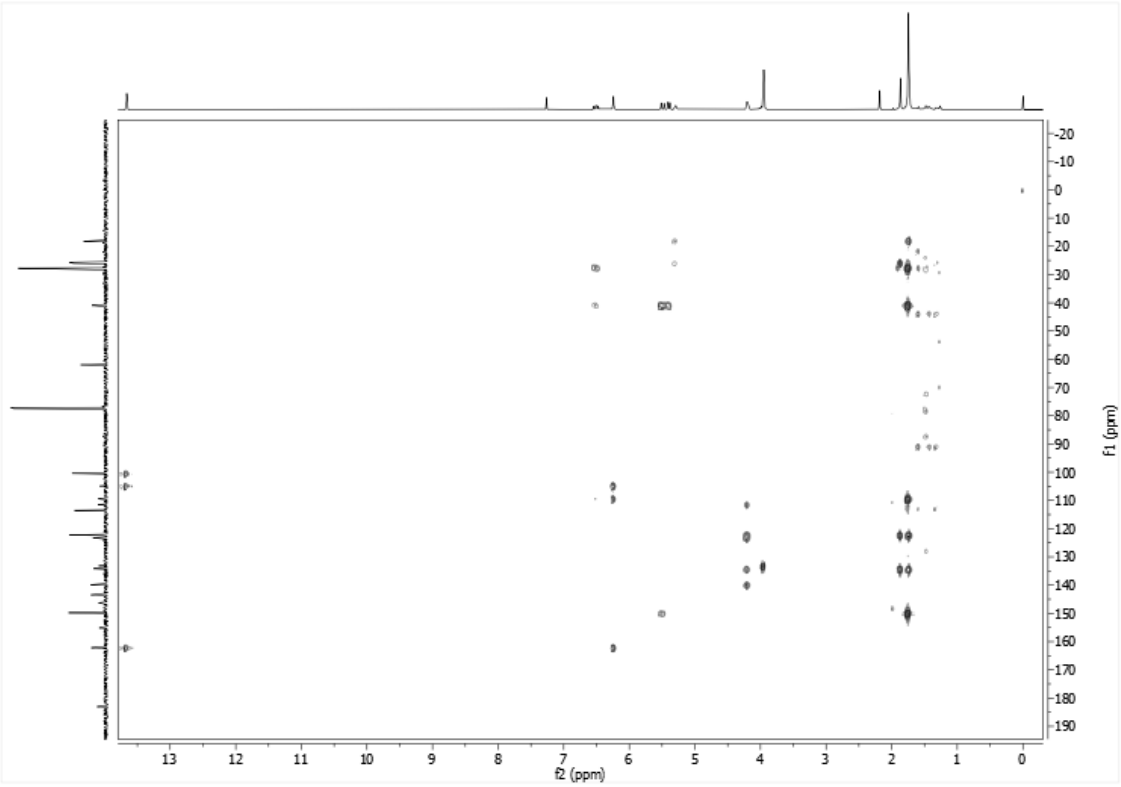

Figure A.5 HMBC spectrum ($CDCl_3$) of metabolite **1**

จุฬาลงกรณ์มหาวิทยาลัย
Chulalongkorn University

Generic Display Report

Analysis Info

Analysis Name	D:\Data\Data Service\191104\KP_SYH_01_RB8_01_3469.d	Acquisition Date	11/4/2019 7:20:37 PM
Method	nv_pos_5min_profile_automsms_190214.m	Operator	CU.
Sample Name	KP_SYH_01	Instrument	micrOTOF-Q II
Comment			

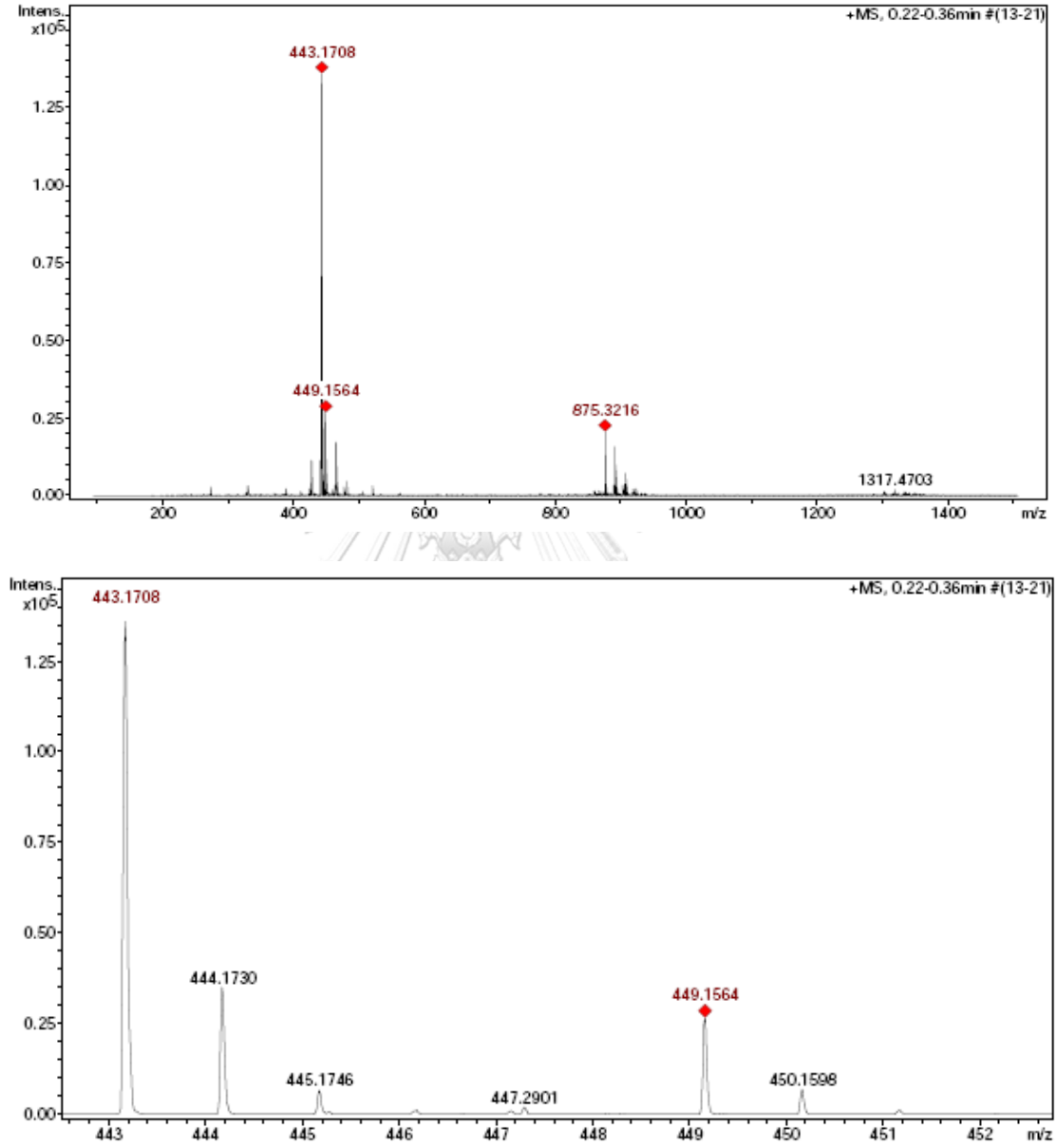

Figure A.6 HR-ESI-MS spectrum of metabolite **1**

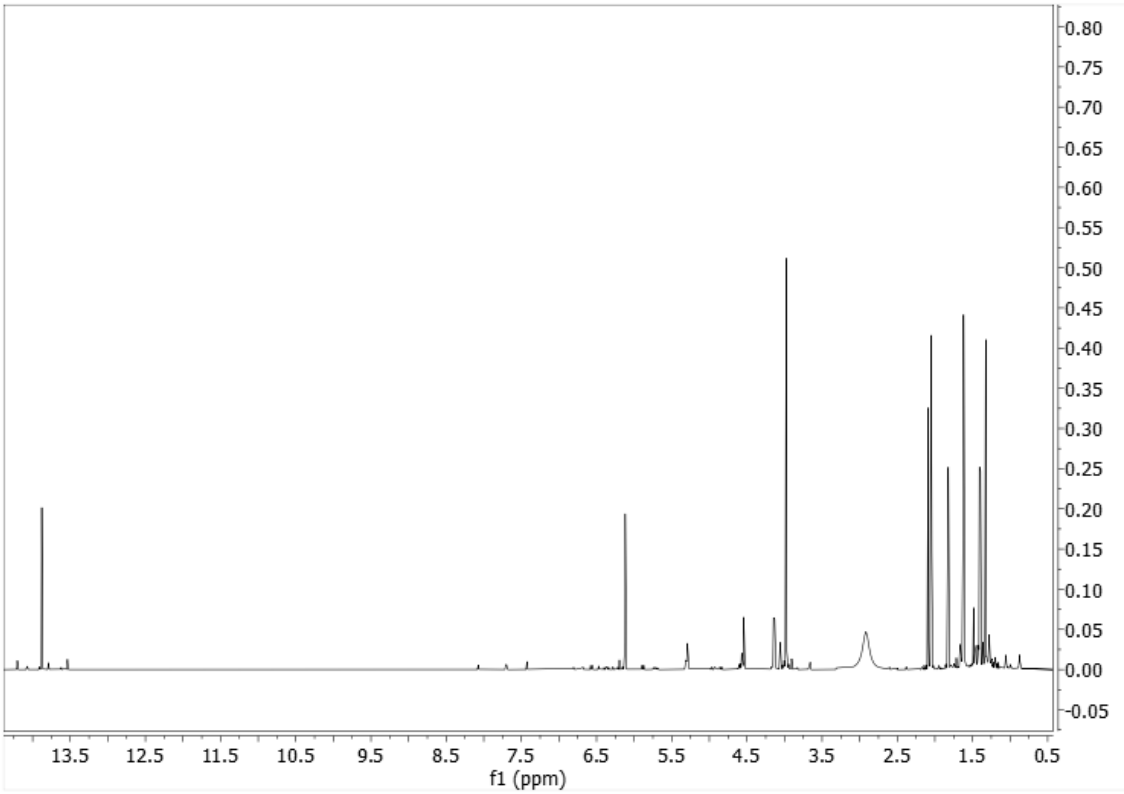

Figure A.7 ^{1}H NMR (500 MHz, acetone-d_6) spectrum of metabolite **2**

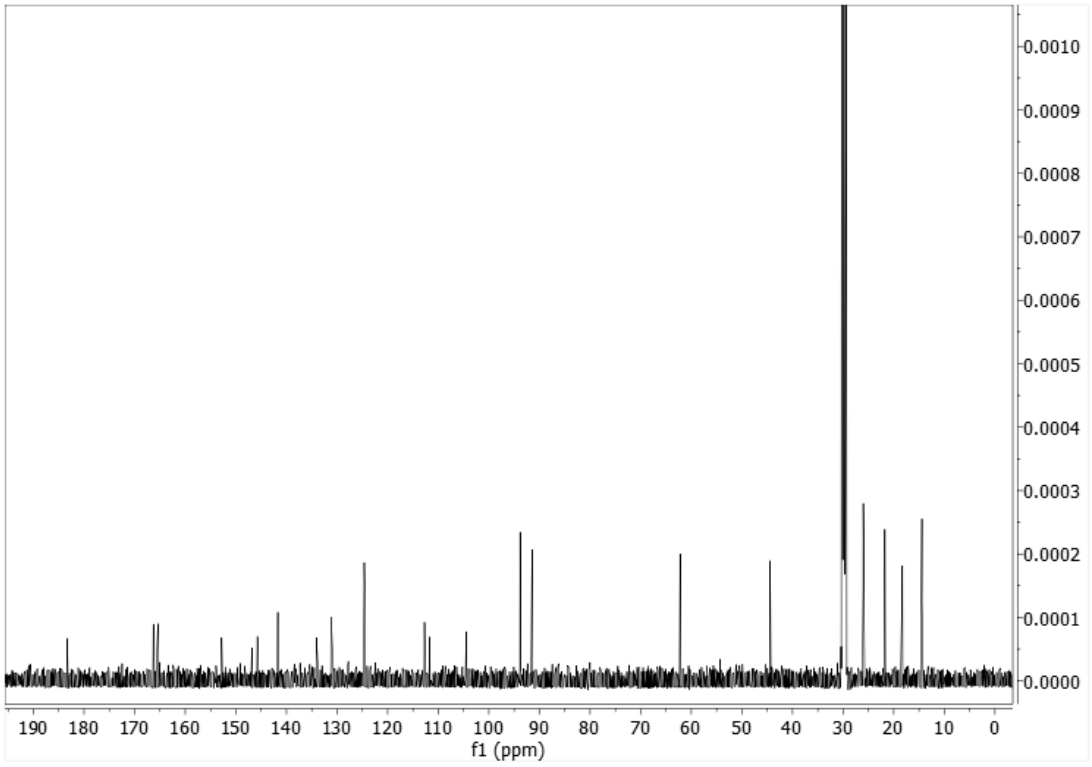

Figure A.8 ^{13}C NMR (125 MHz, acetone-d_6) spectrum of metabolite **2**

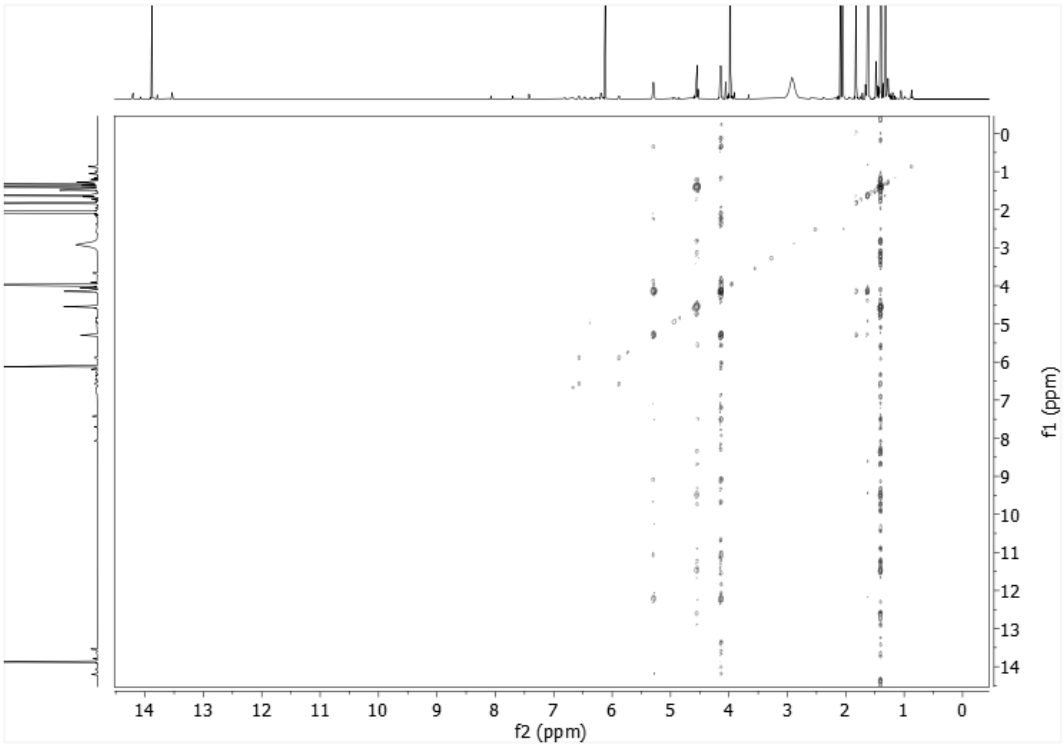

Figure A.9 ^{1}H-^{1}H COSY spectrum ($CDCl_3$) of metabolite **2**

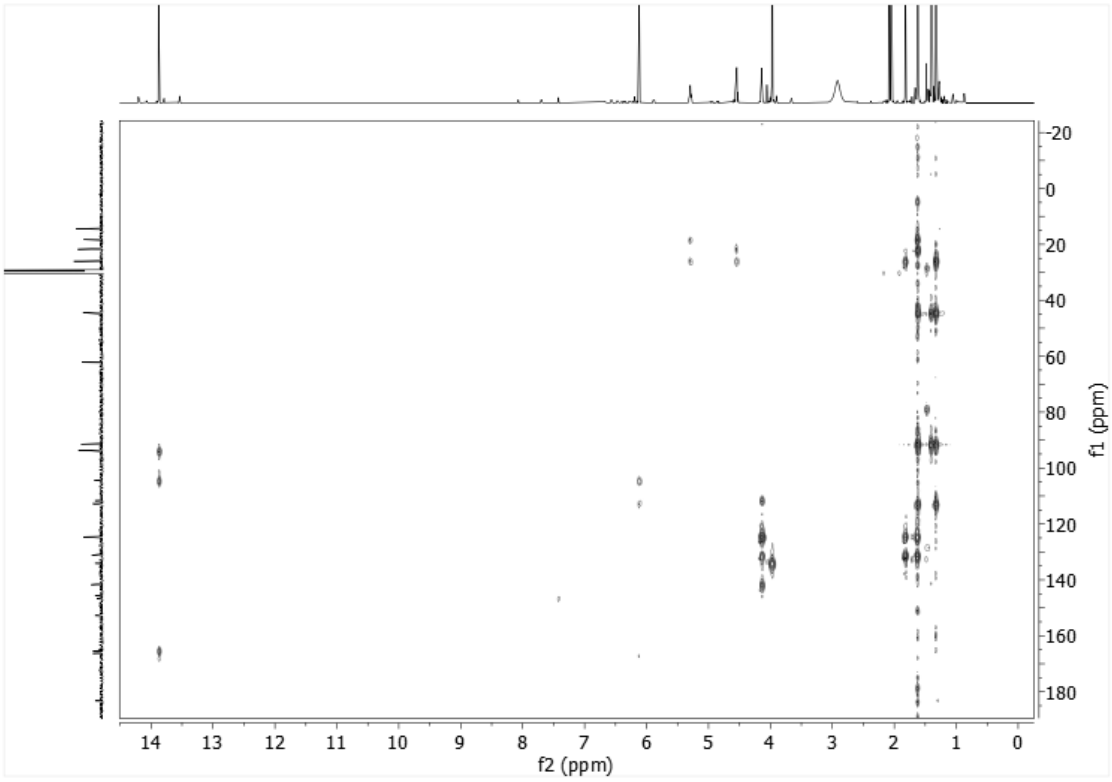

Figure A.10 HSQC spectrum ($CDCl_3$) of metabolite **2**

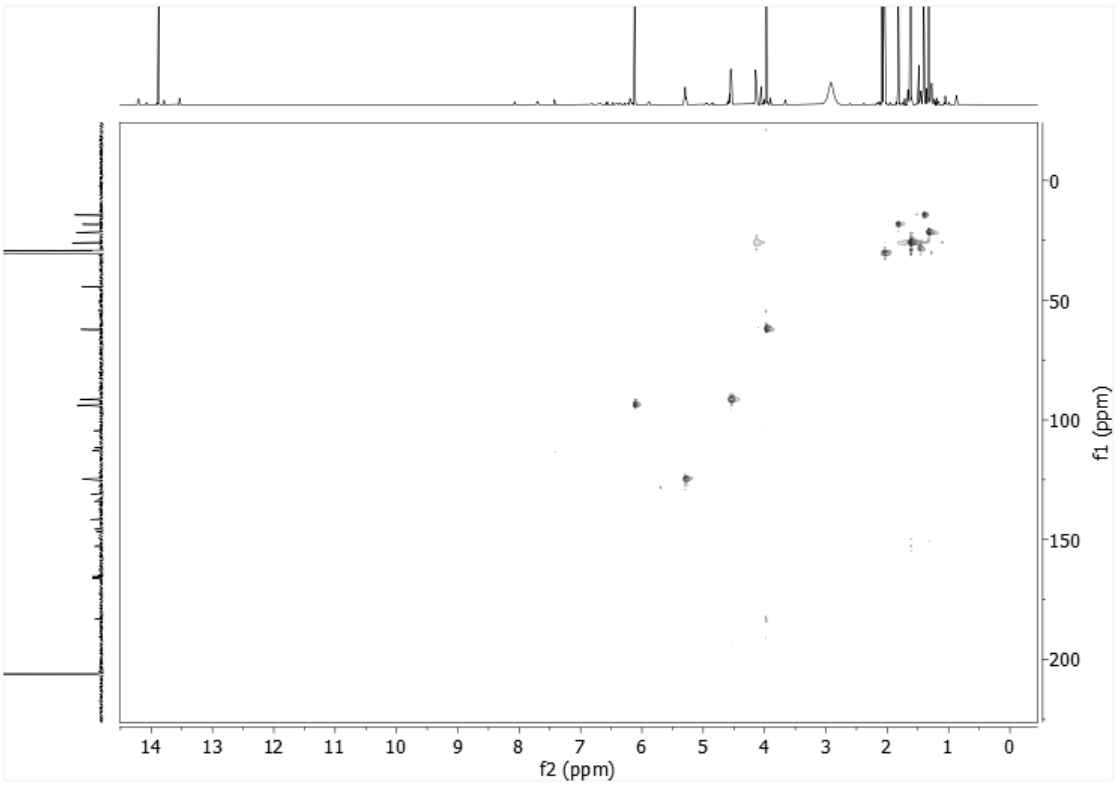

Figure A.11 HMBC spectrum ($CDCl_3$) of metabolite **2**

จุฬาลงกรณ์มหาวิทยาลัย
Chulalongkorn University

Generic Display Report

Analysis Info

Analysis Name	D:\Data\Data Service\200729\Cal 15_RB8_01_4142.d	Acquisition Date	7/29/2020 7:28:31 PM
Method	nv_pos_6min_profile_wguardcol_50-1500_191021.m	Operator	CU.
Sample Name	Cal 15	Instrument	micrOTOF-Q II
Comment			

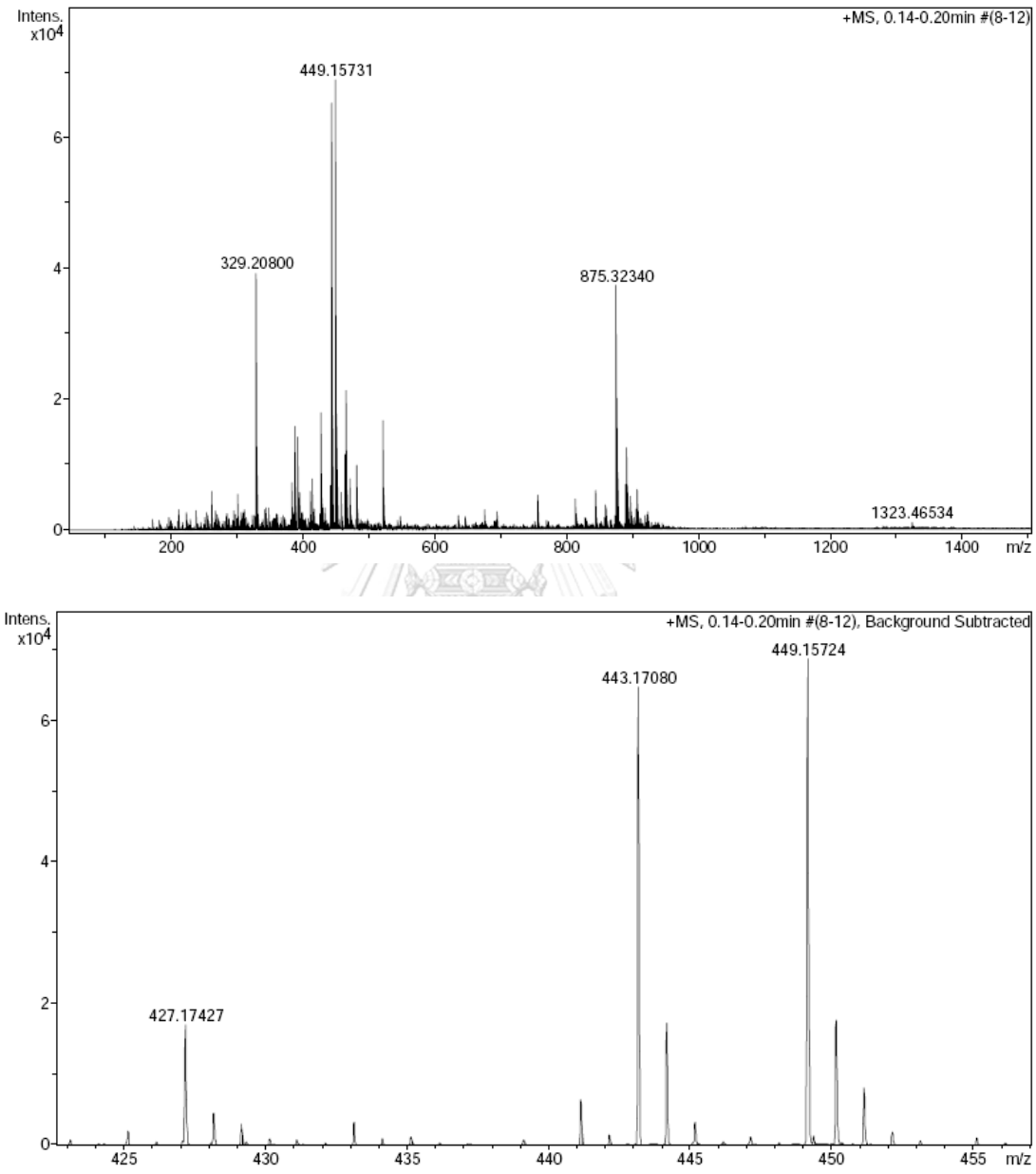

Figure A.12 HR-ESI-MS spectrum of metabolite **2**

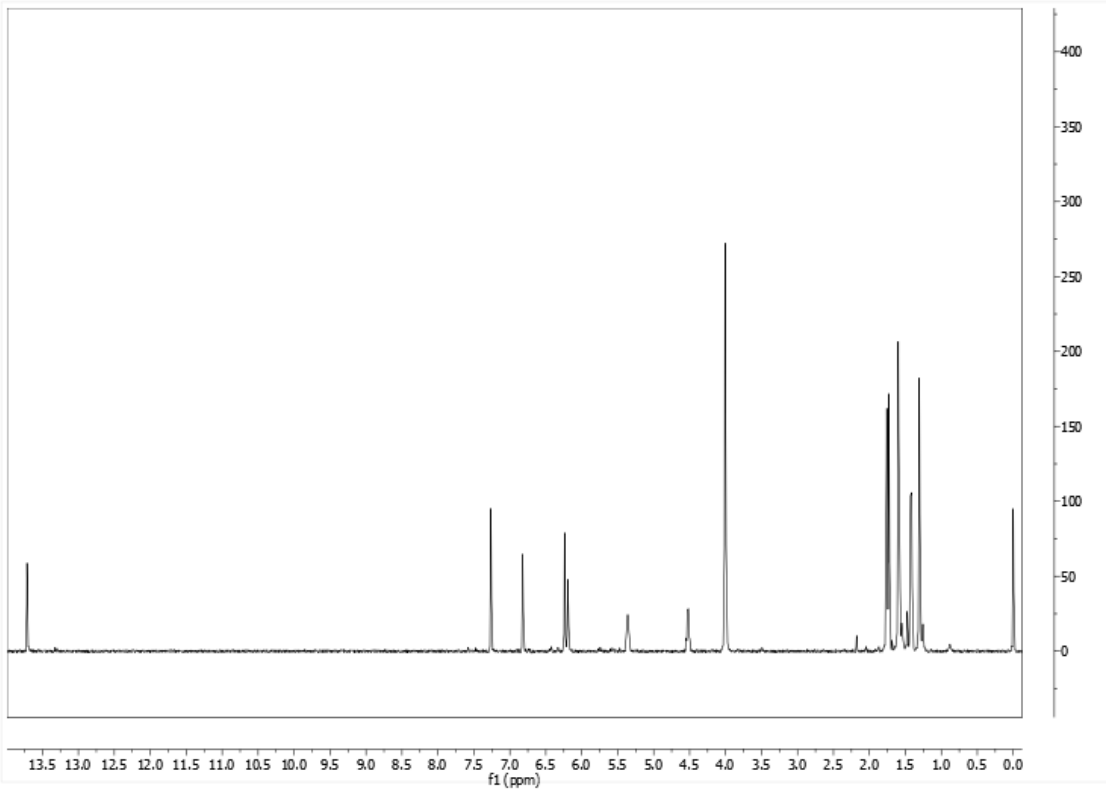

Figure A.13 ^{1}H NMR (400 MHz, $CDCl_3$) spectrum of metabolite **3**

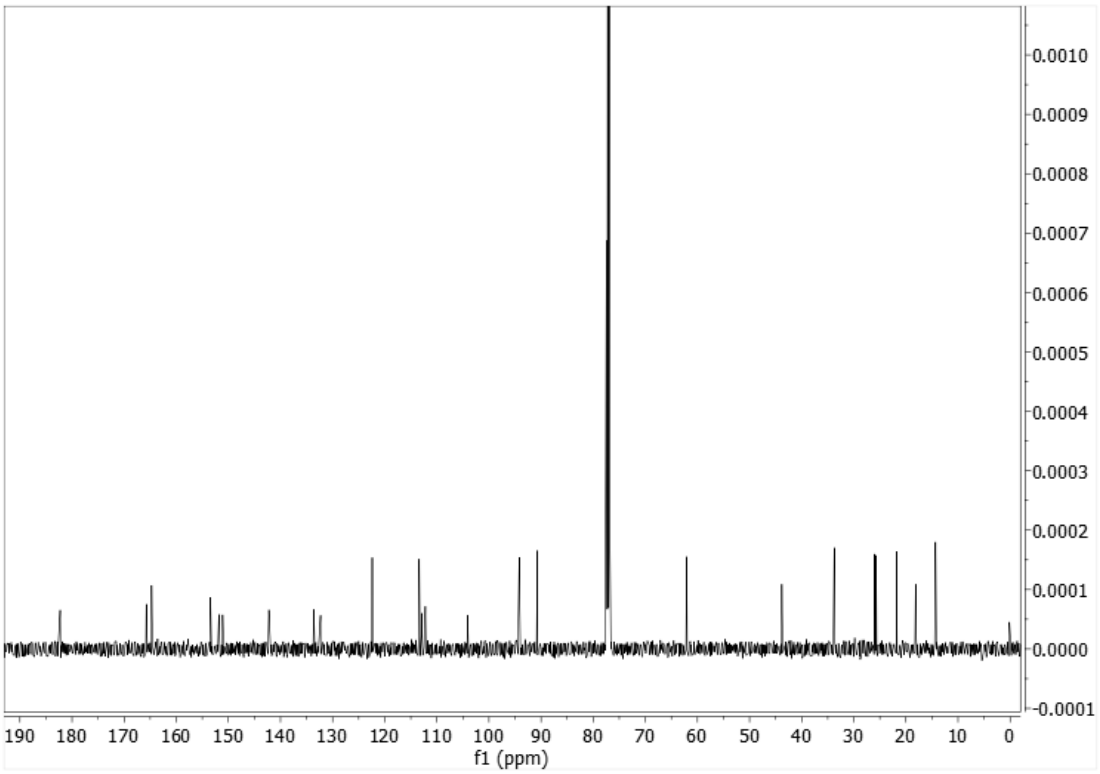

Figure A.14 ^{13}C NMR (125 MHz, $CDCl_3$) spectrum of metabolite **3**

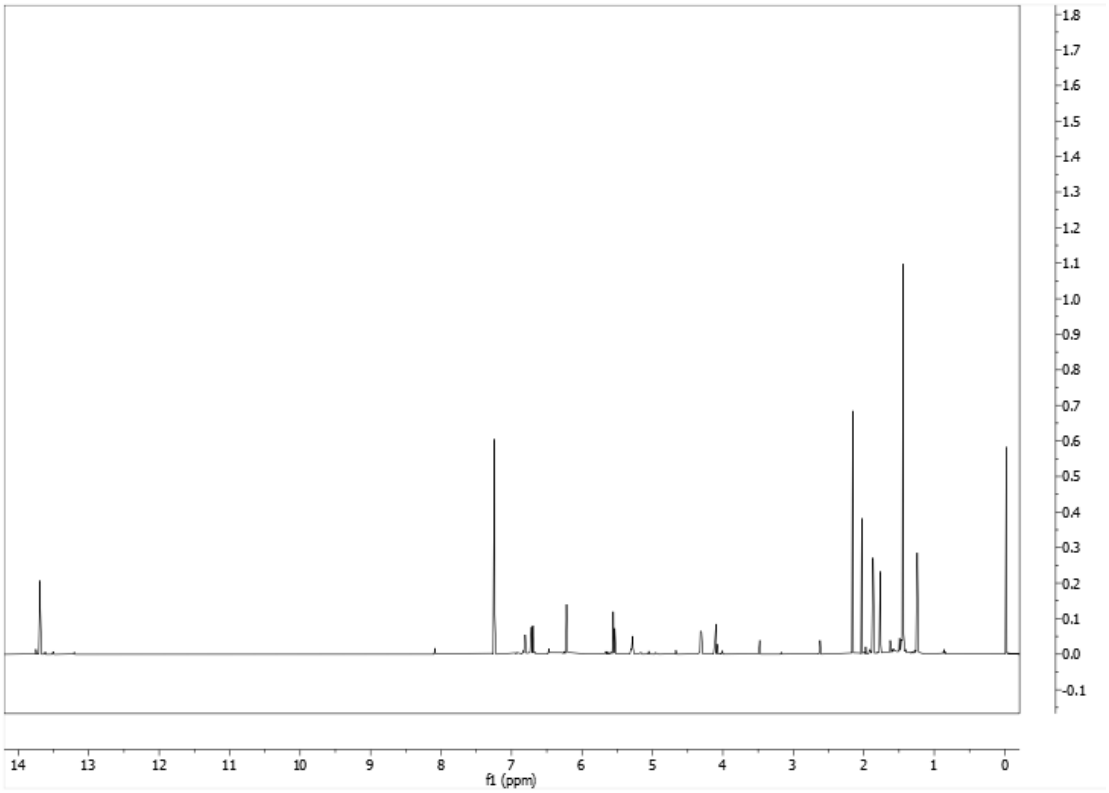

Figure A.15 ^{1}H NMR (500 MHz, $CDCl_3$) spectrum of metabolite **4**

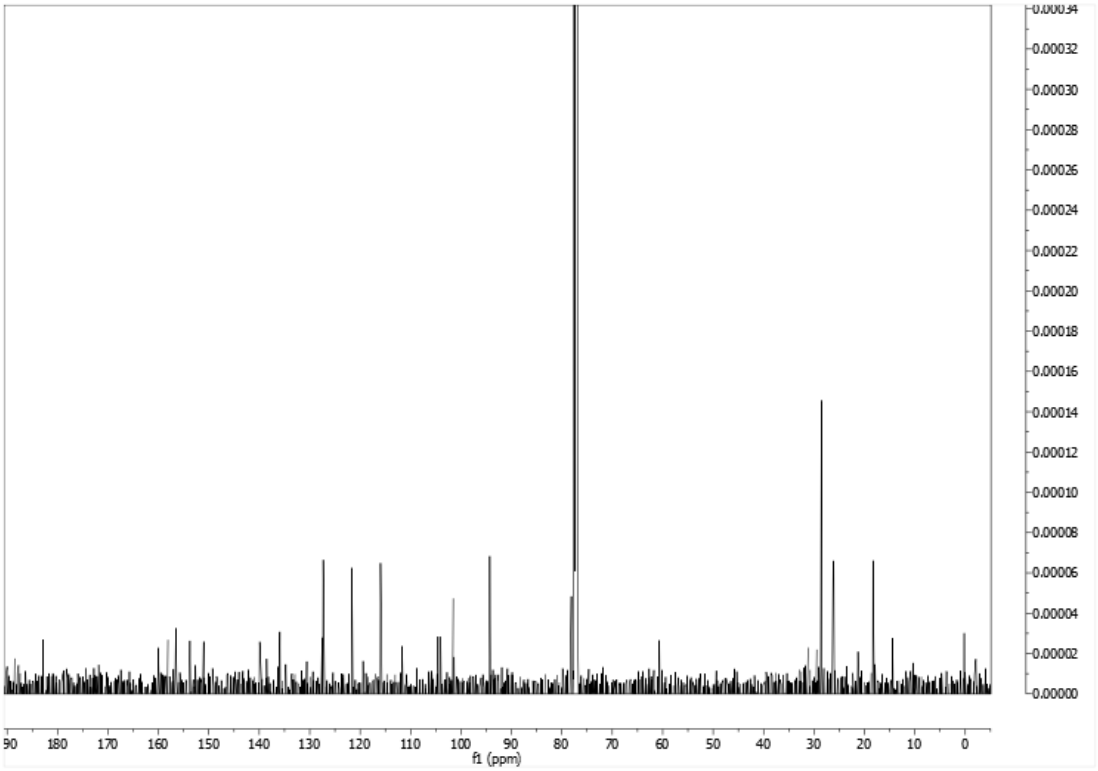

Figure A.16 ^{13}C NMR (125 MHz, $CDCl_3$) spectrum of metabolite **4**

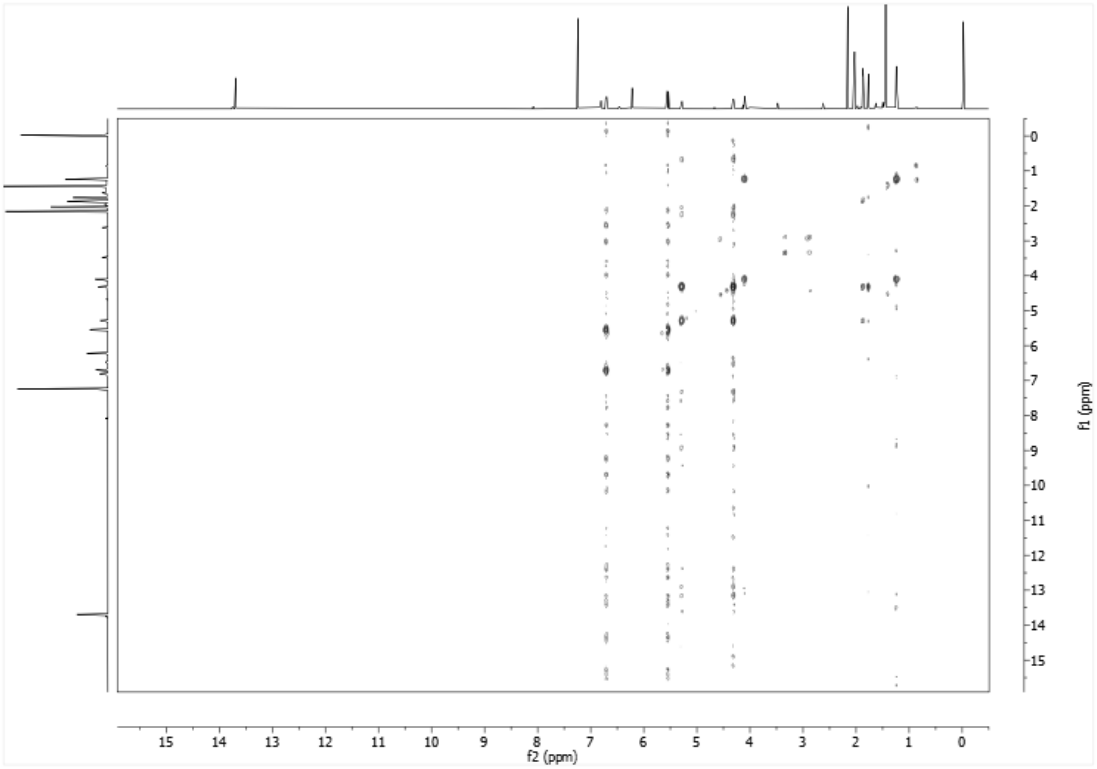

Figure A.17 ^{1}H-^{1}H COSY spectrum ($CDCl_3$) of metabolite **4**

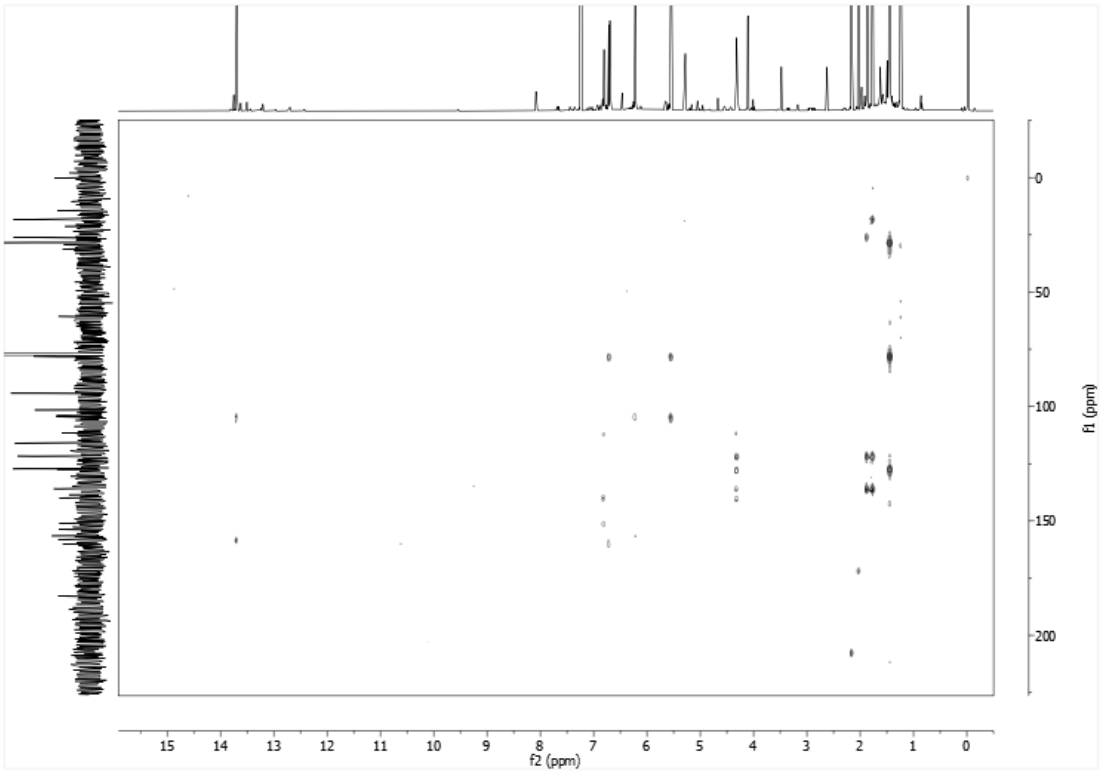

Figure A.18 HSQC spectrum ($CDCl_3$) of metabolite **4**

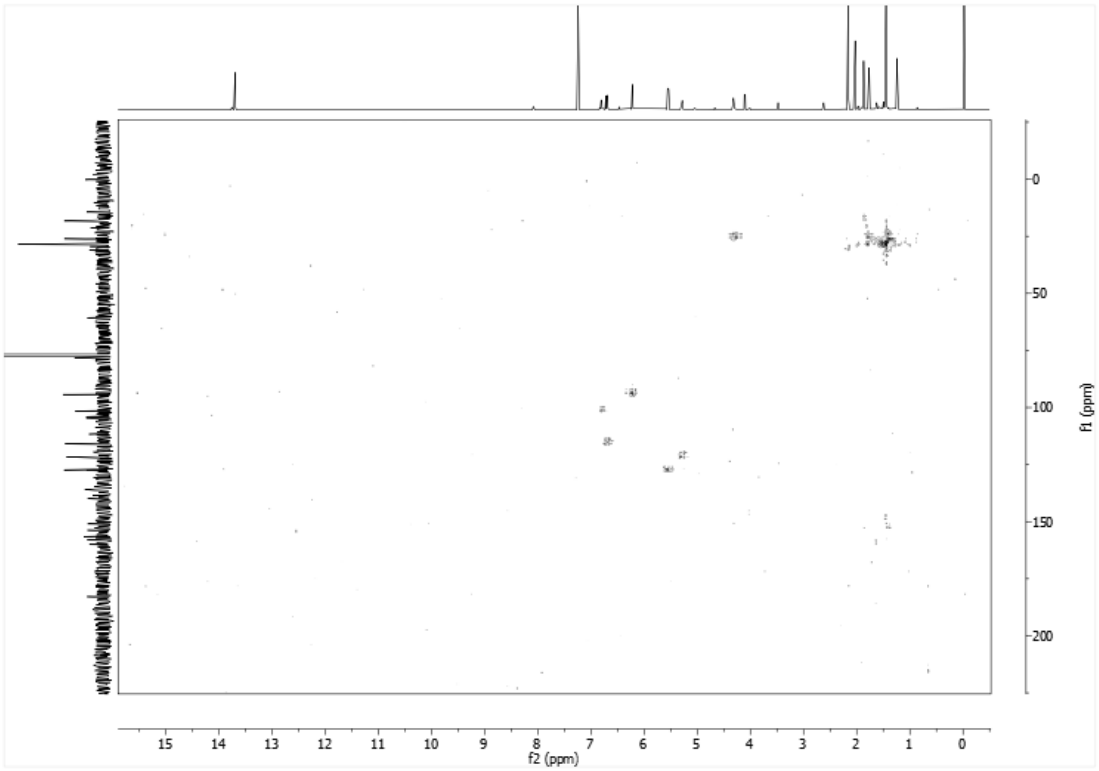

Figure A.19 HMBC spectrum ($CDCl_3$) of metabolite **4**

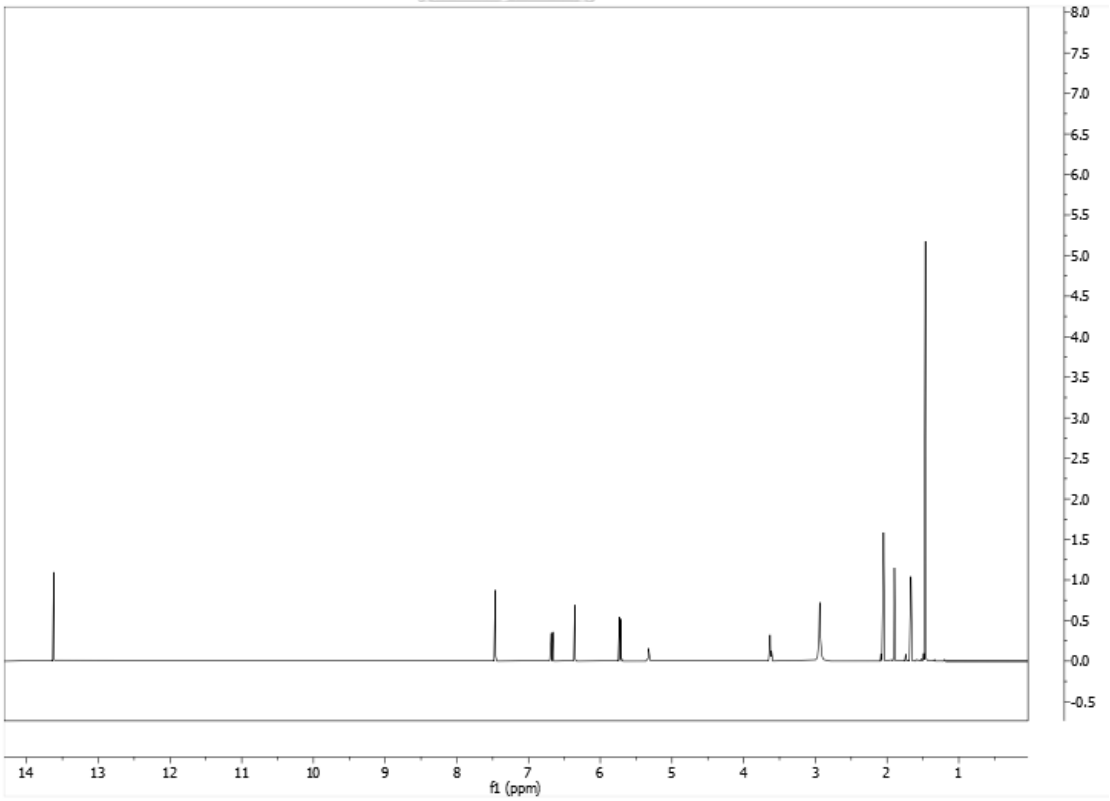

Figure A.20 ^{1}H NMR (500 MHz, acetone-d_6) spectrum of metabolite **5**

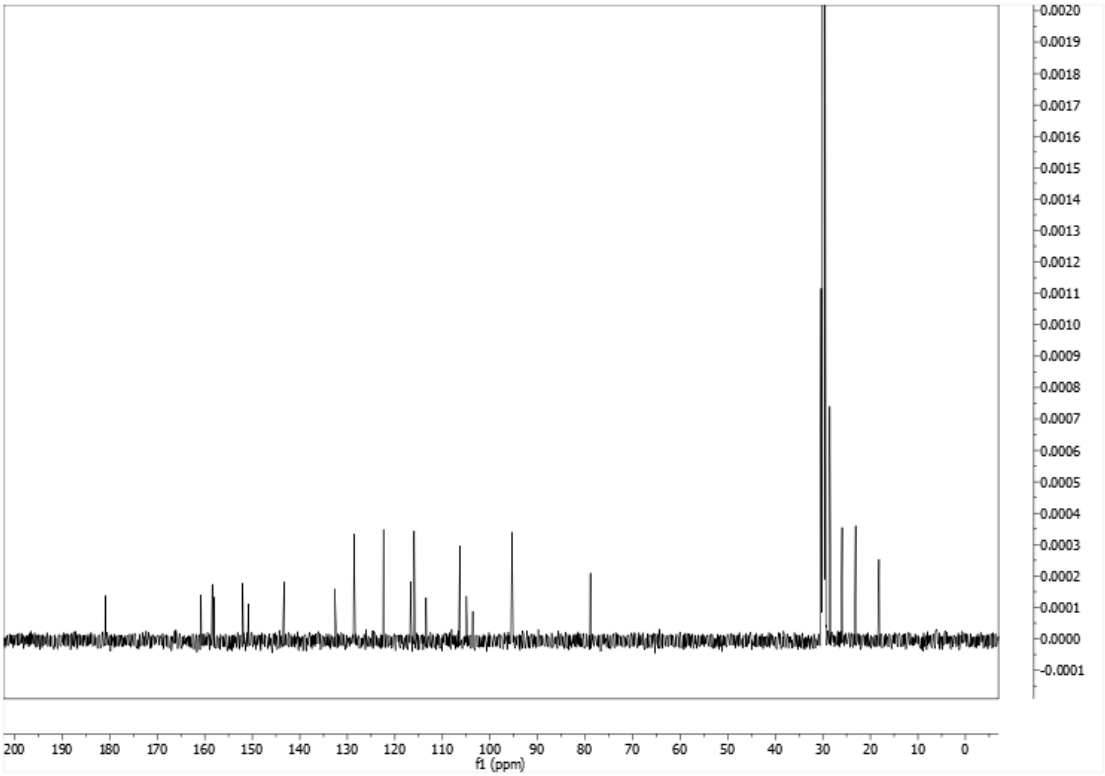

Figure A.21 ^{13}C NMR (125 MHz, acetone-d_6) spectrum of metabolite **5**

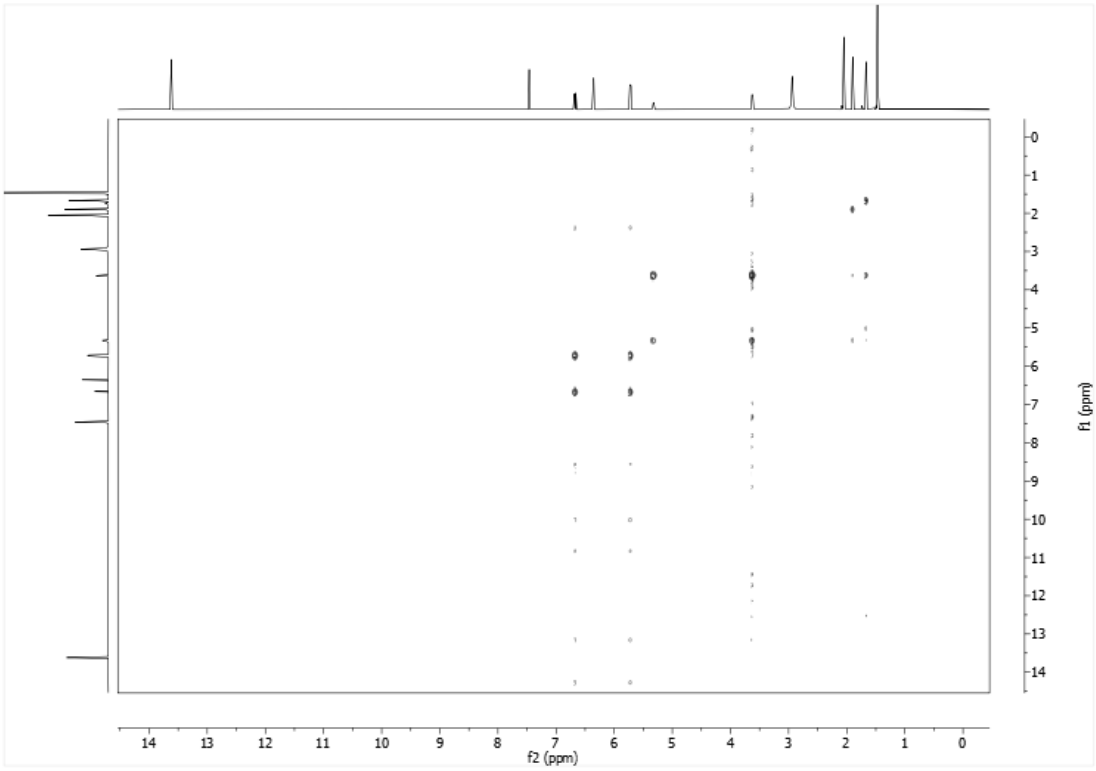

Figure A.22 ^{1}H-^{1}H COSY spectrum (acetone-d_6) of metabolite **5**

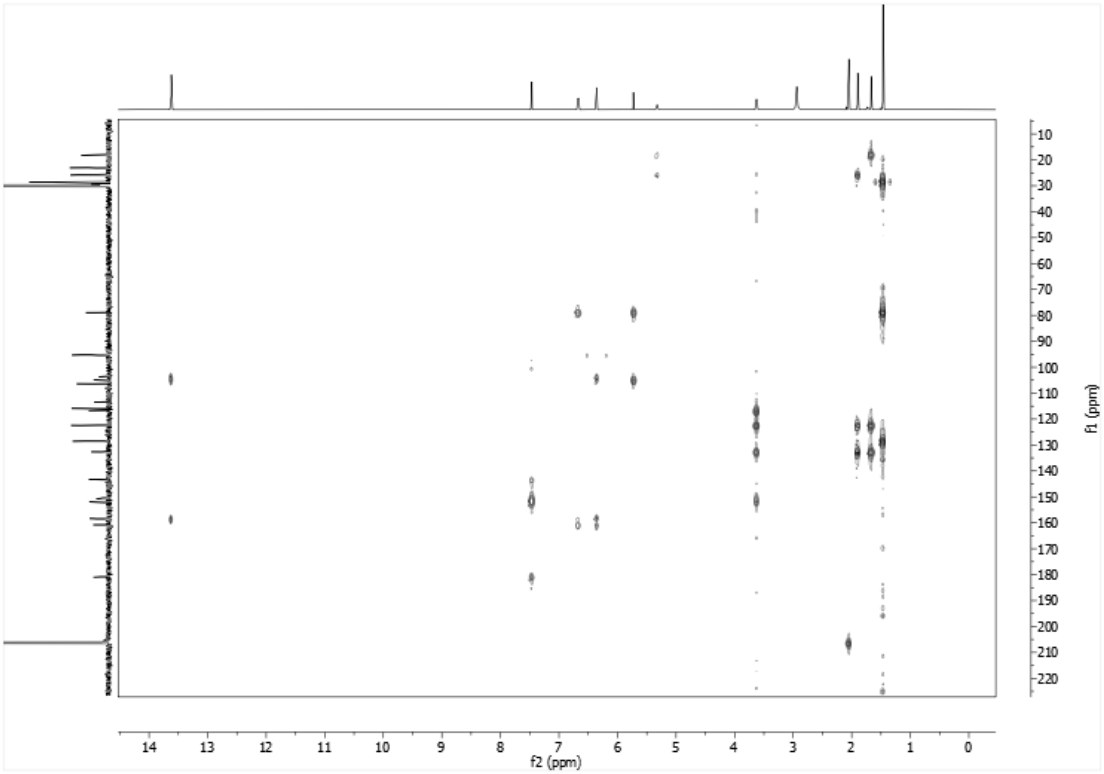

Figure A.23 HSQC spectrum (acetone-d_6) of metabolite **5**

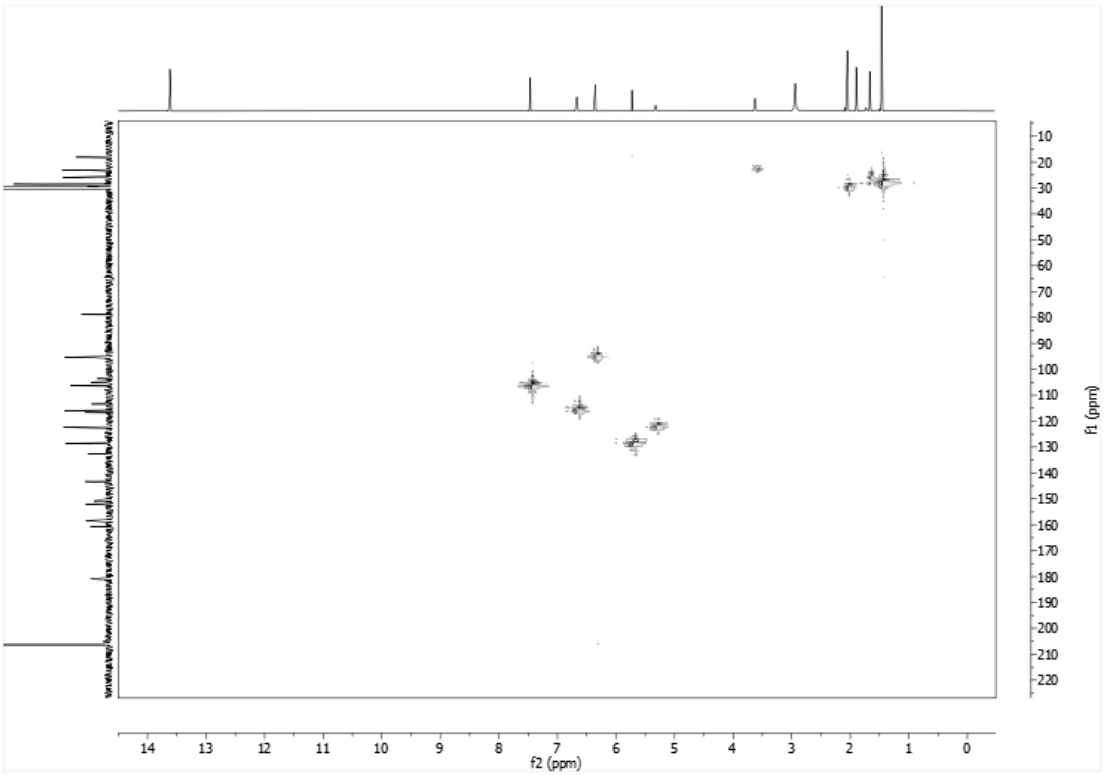

Figure A.24 HMBC spectrum (acetone-d_6) of metabolite **5**

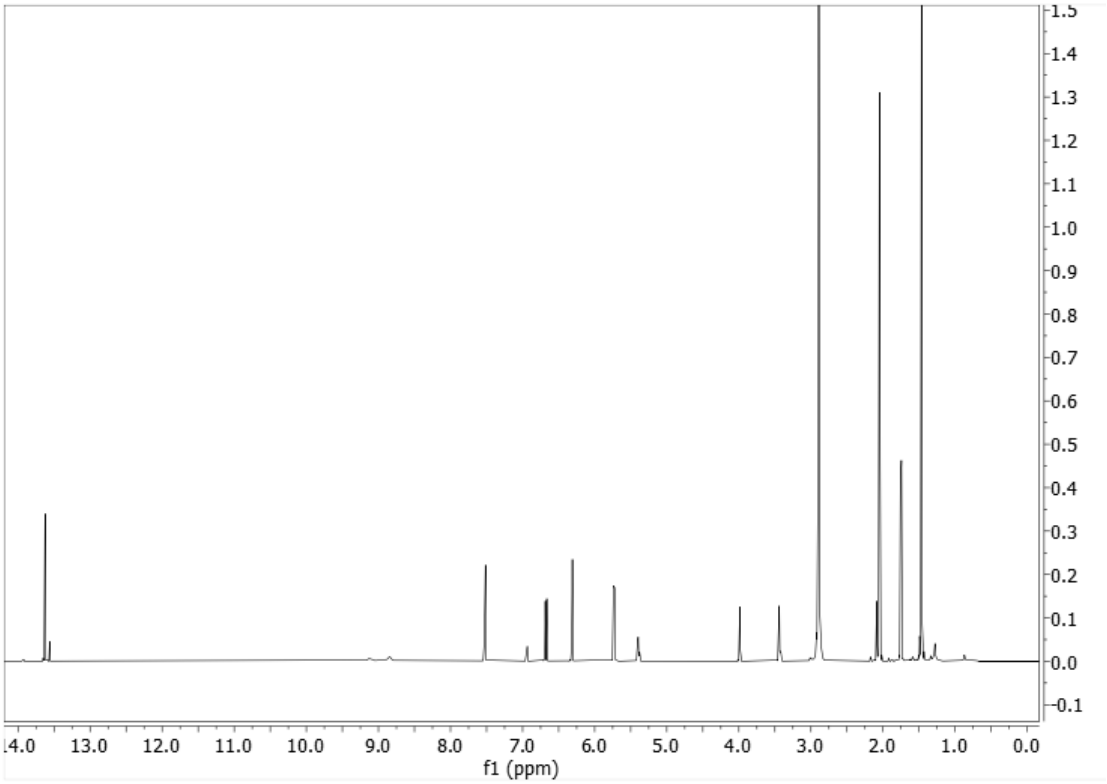

Figure A.25 ^{1}H NMR (500 MHz, acetone-d_6) spectrum of metabolite **6**

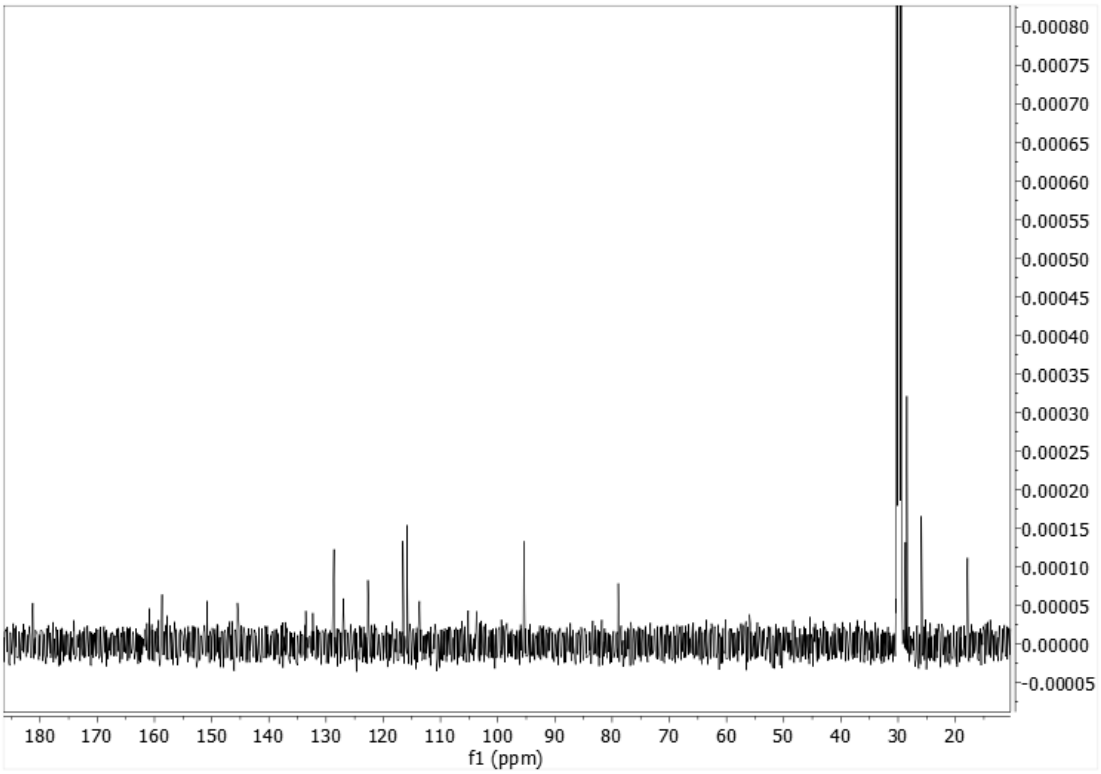

Figure A.26 ^{13}C NMR (125 MHz, acetone-d_6) spectrum of metabolite **6**

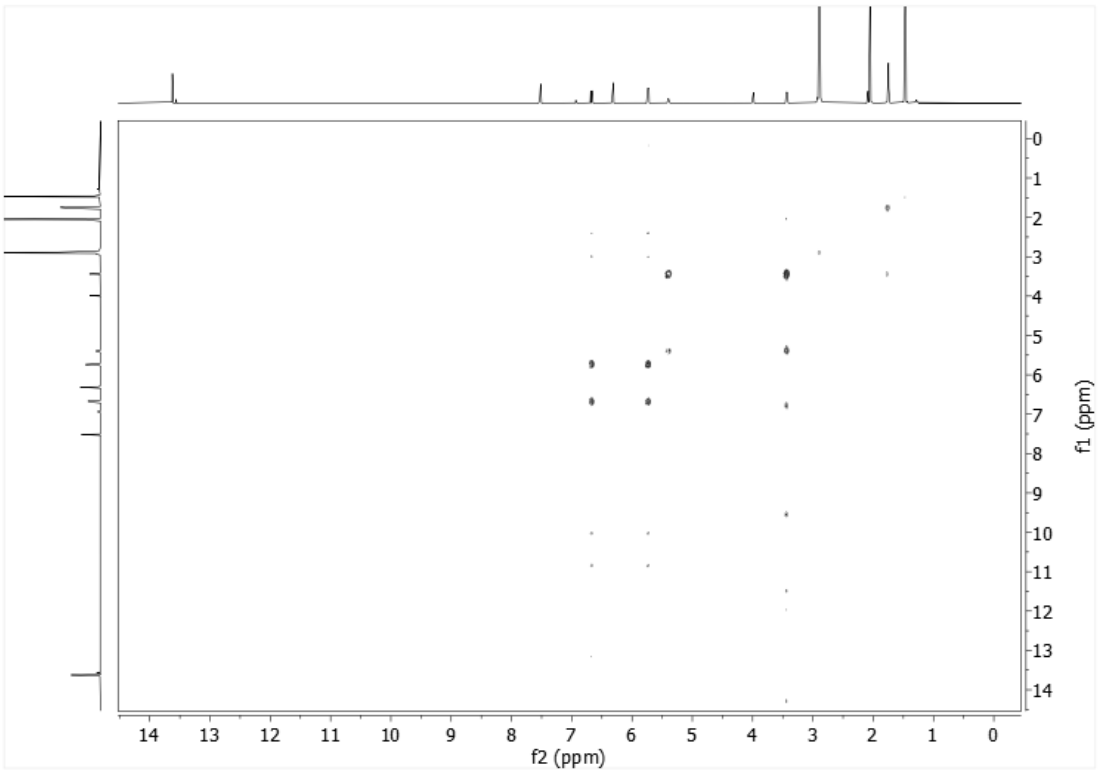

Figure A.27 ^{1}H-^{1}H COSY spectrum (acetone-d_6) of metabolite **6**

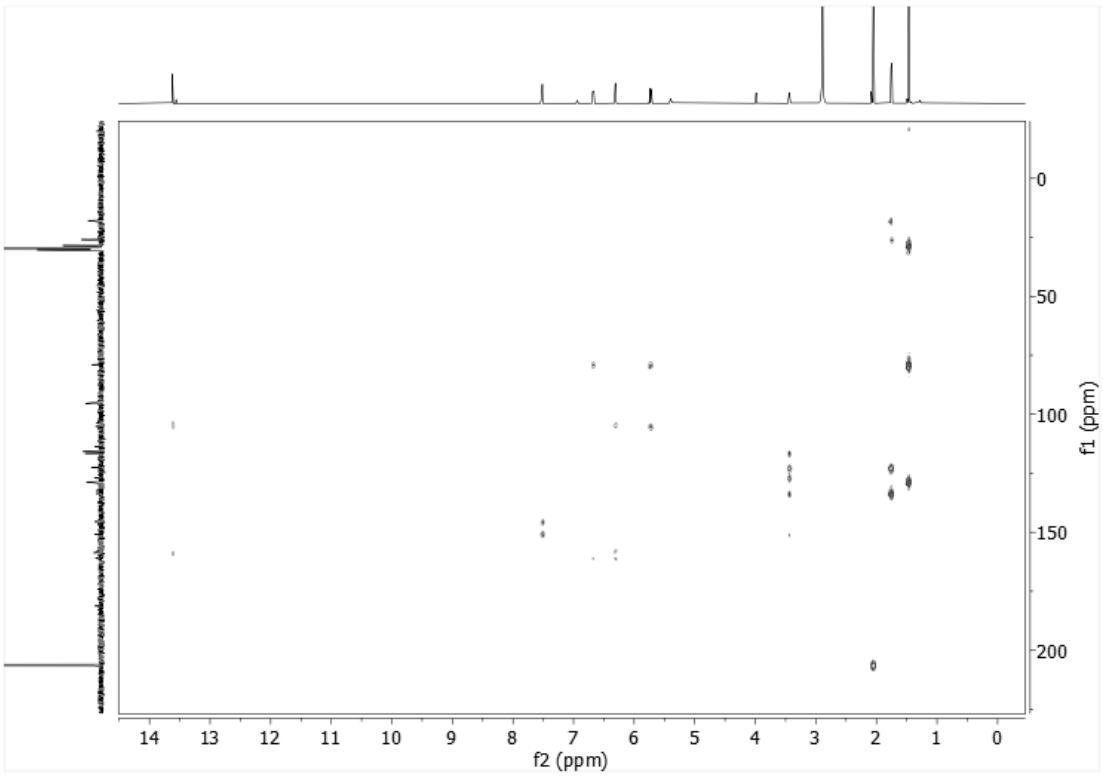

Figure A.28 HSQC spectrum (acetone-d_6) of metabolite **6**

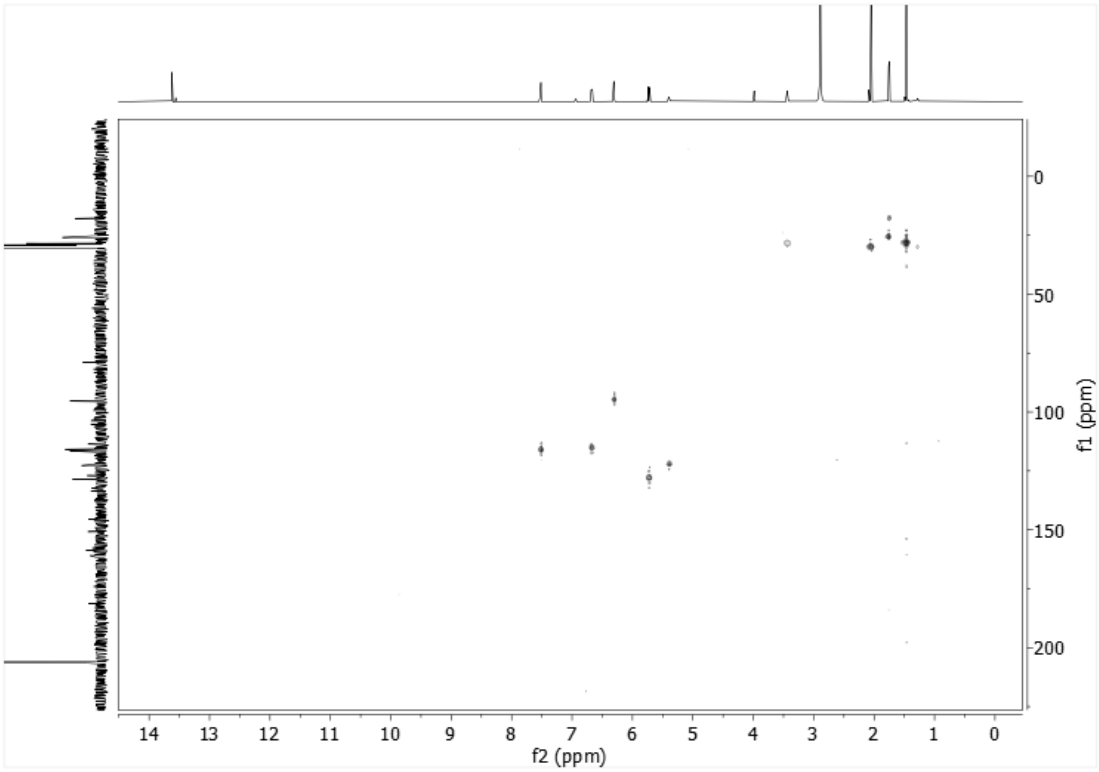

Figure A.29 HMBC spectrum (acetone-d_6) of metabolite **6**

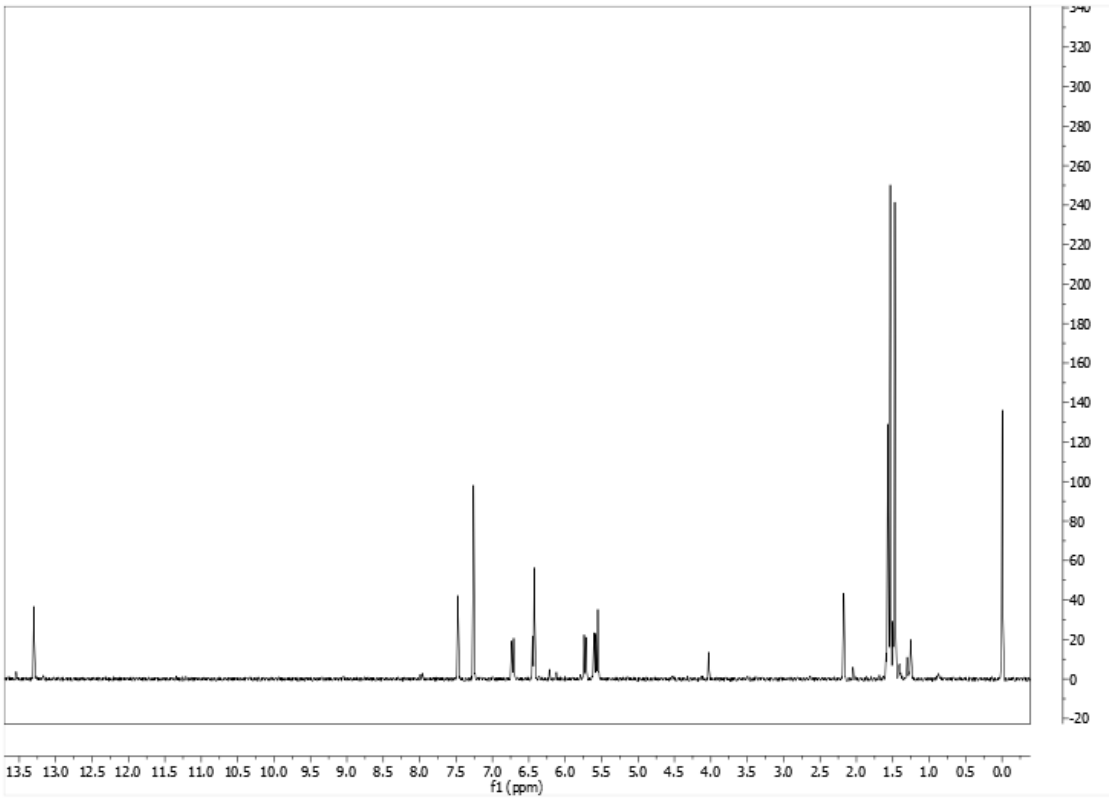

Figure A.30 ^{1}H NMR (500 MHz, $CDCl_3$) spectrum of metabolite **7**

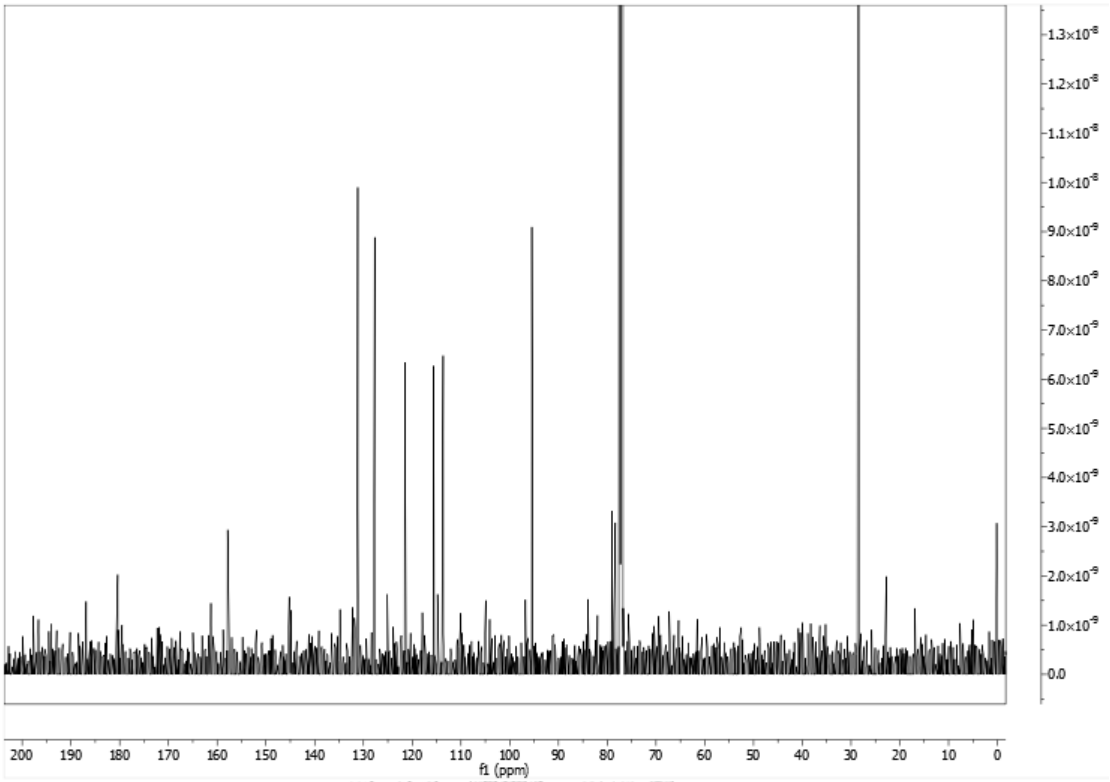

Figure A.31 ^{13}C NMR (125 MHz, $CDCl_3$) spectrum of metabolite **7**

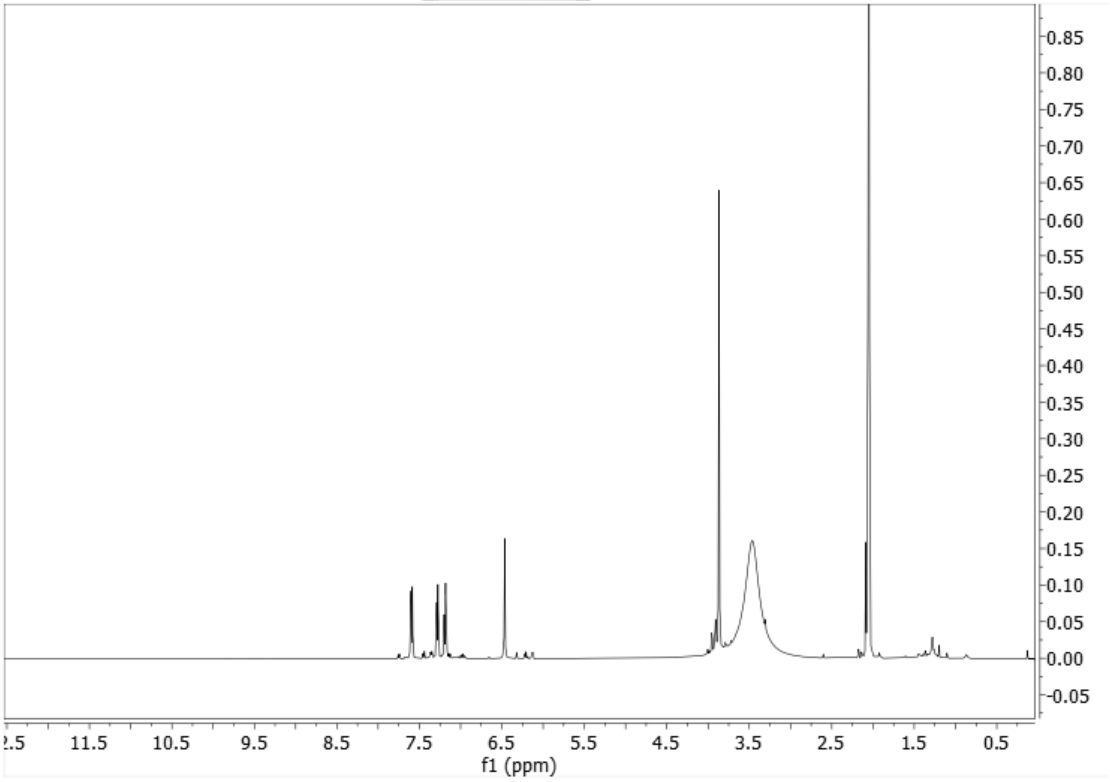

Figure A.32 ^{1}H NMR (500 MHz, acetone-d_6) spectrum of metabolite **8**

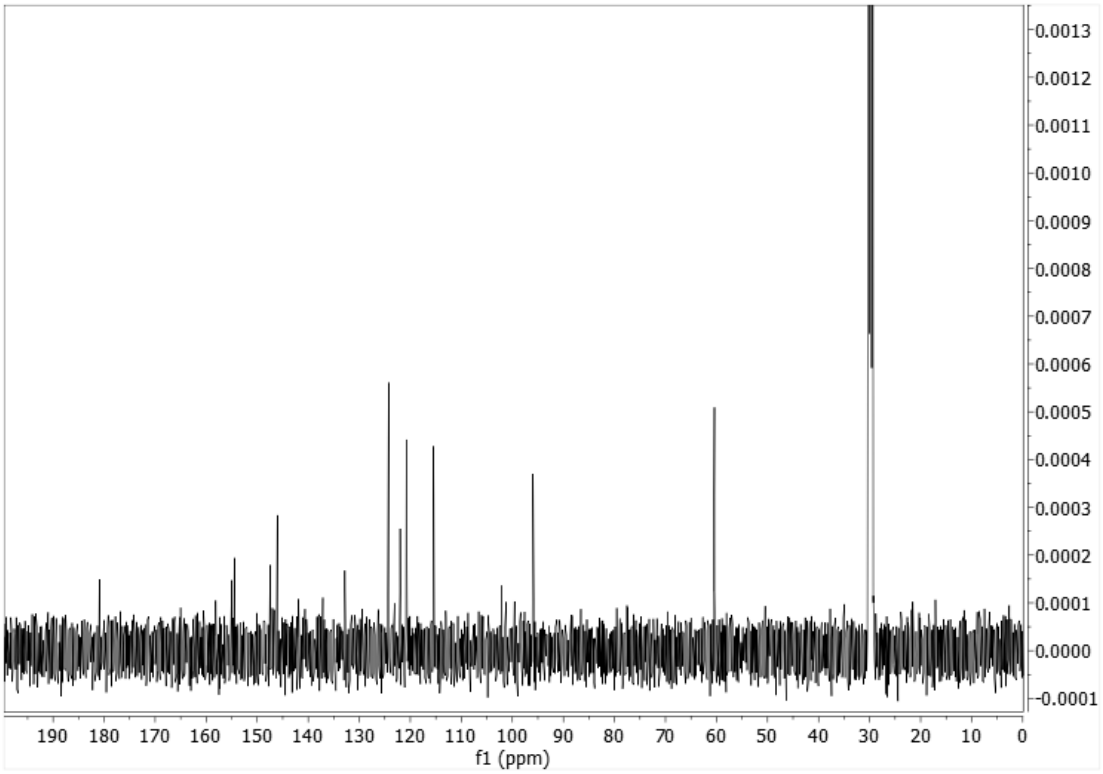

Figure A.33 ^{13}C NMR (125 MHz, acetone-d_6) spectrum of metabolite **8**

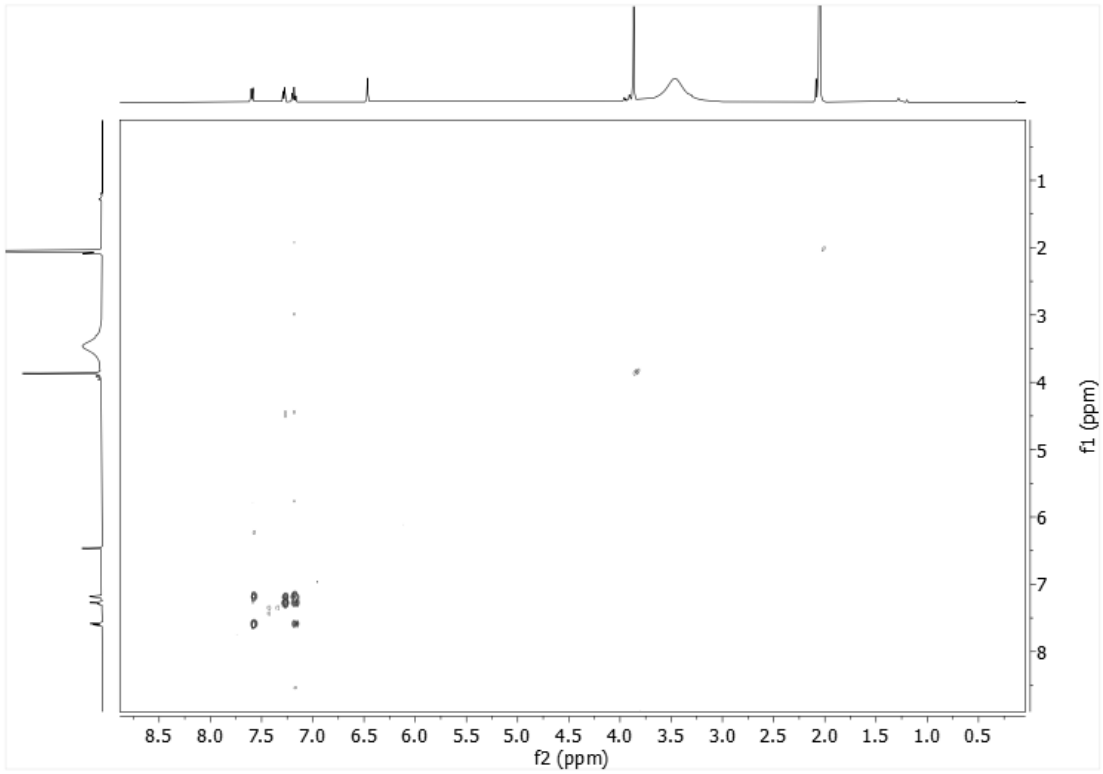

Figure A.34 ^{1}H-^{1}H COSY spectrum (acetone-d_6) of metabolite **8**

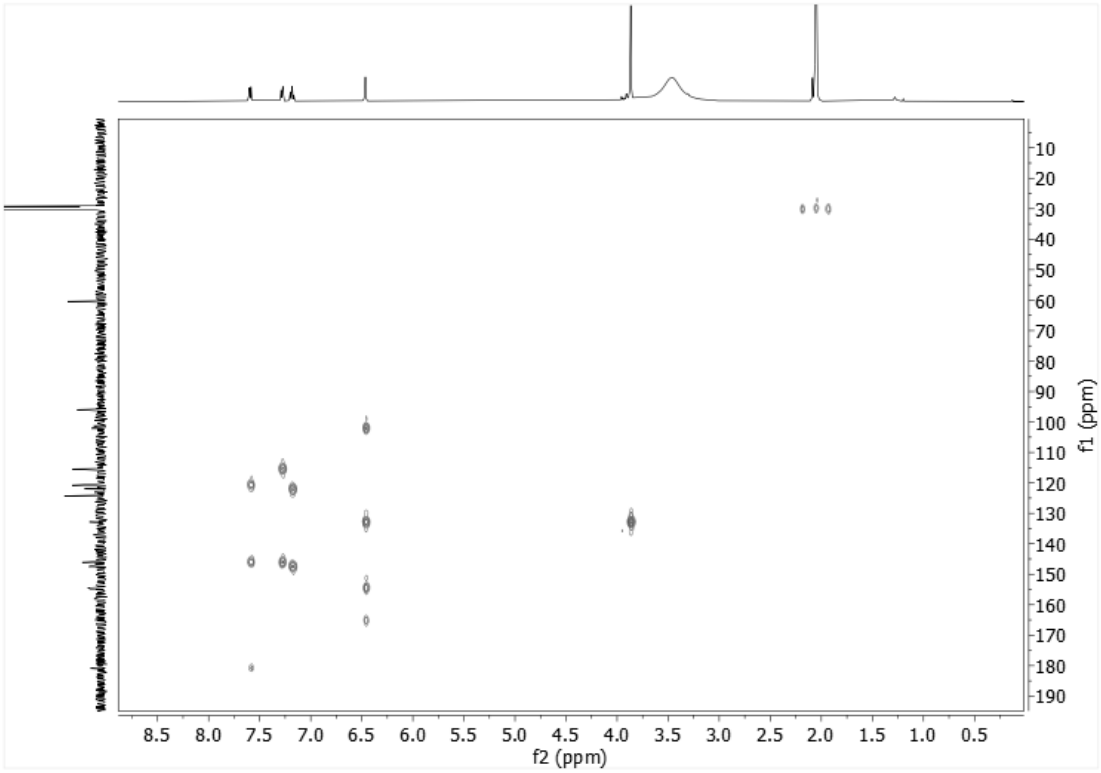

Figure A.35 HSQC spectrum (acetone-d_6) of metabolite **8**

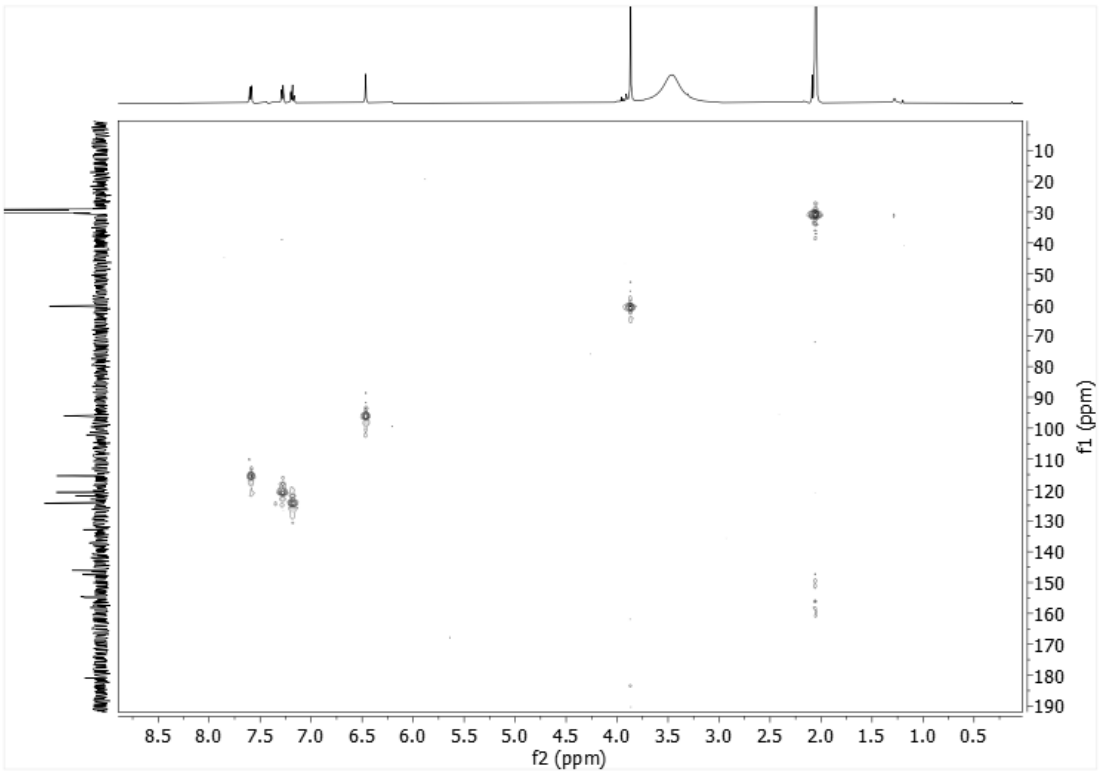

Figure A.36 HMBC spectrum (acetone-d_6) of metabolite **8**

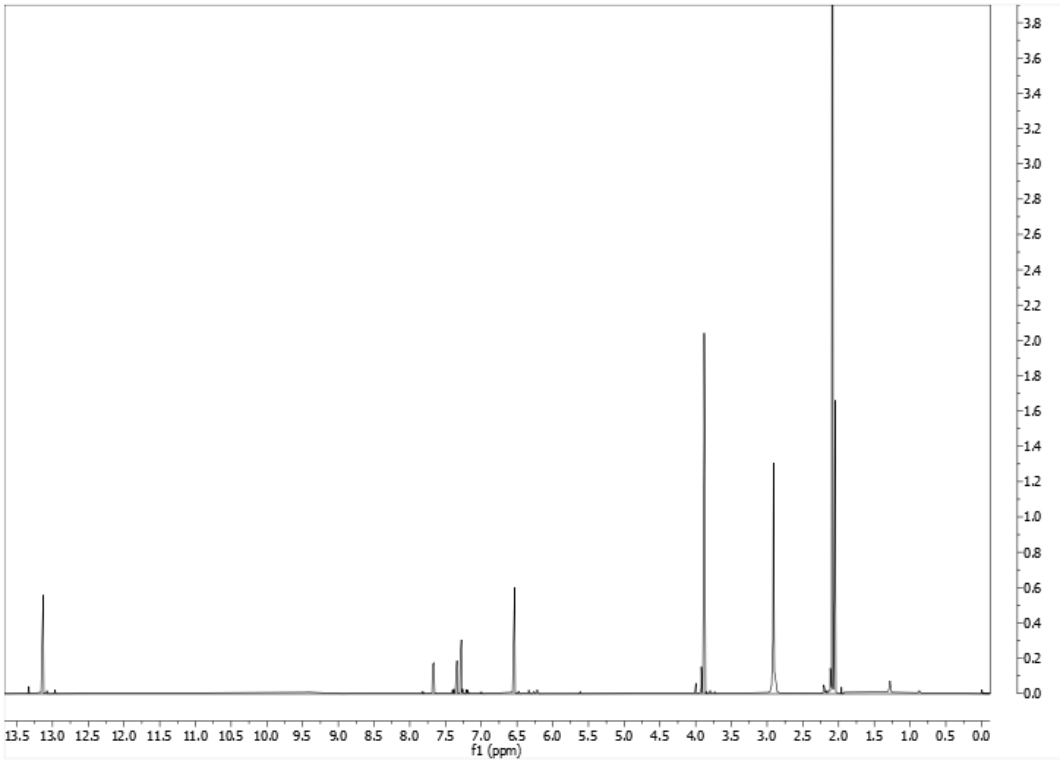

Figure A.37 ^{1}H NMR (500 MHz, acetone-d_6) spectrum of metabolite **9**

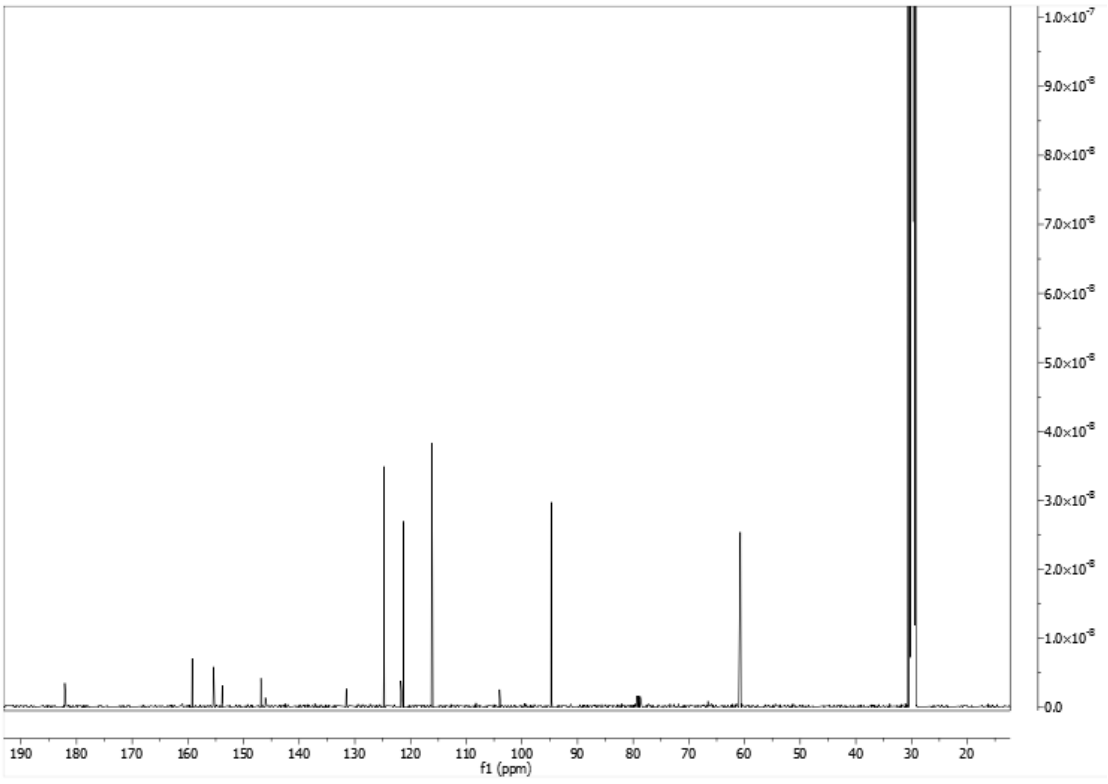

Figure A.38 ^{13}C NMR (125 MHz, acetone-d_6) spectrum of metabolite **9**

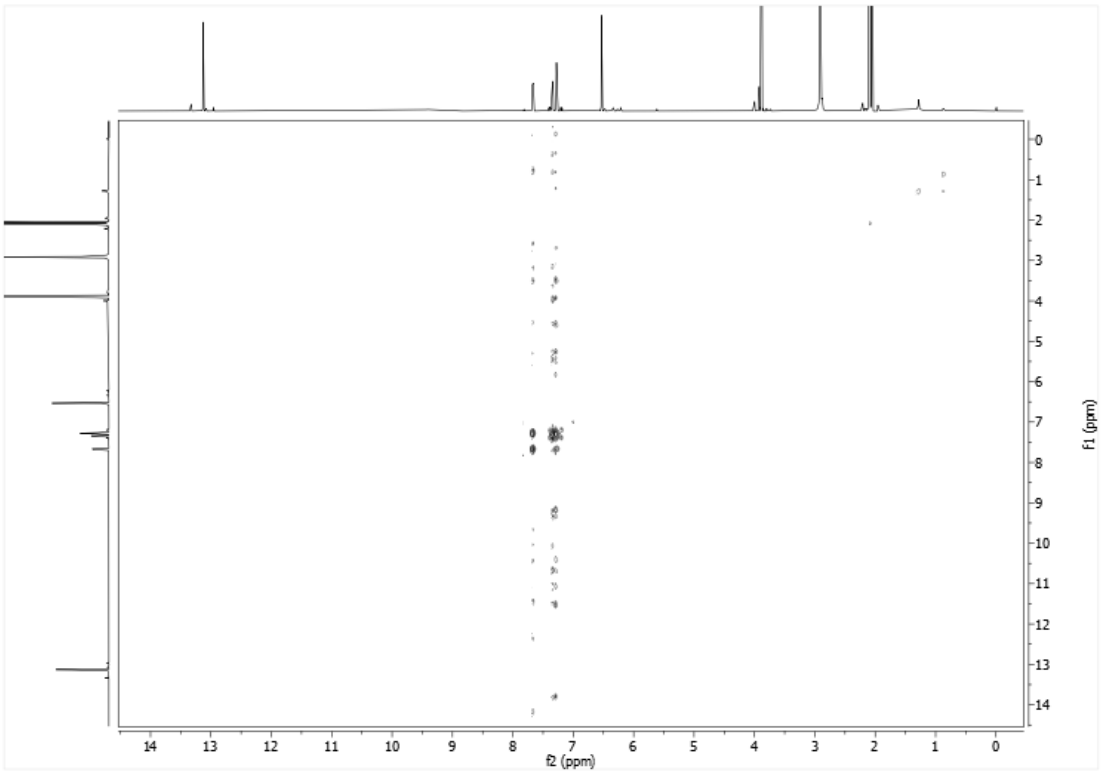

Figure A.39 ^{1}H-^{1}H COSY spectrum (acetone-d_6) of metabolite **9**

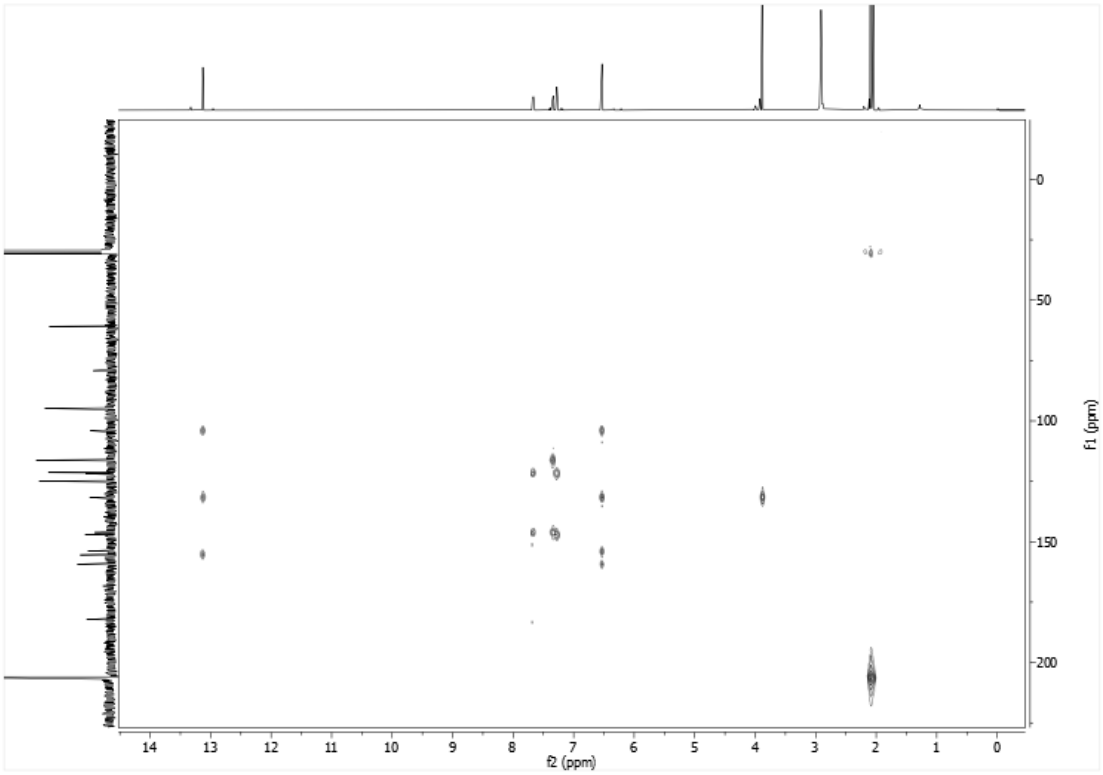

Figure A.40 HSQC spectrum (acetone-d_6) of metabolite **9**

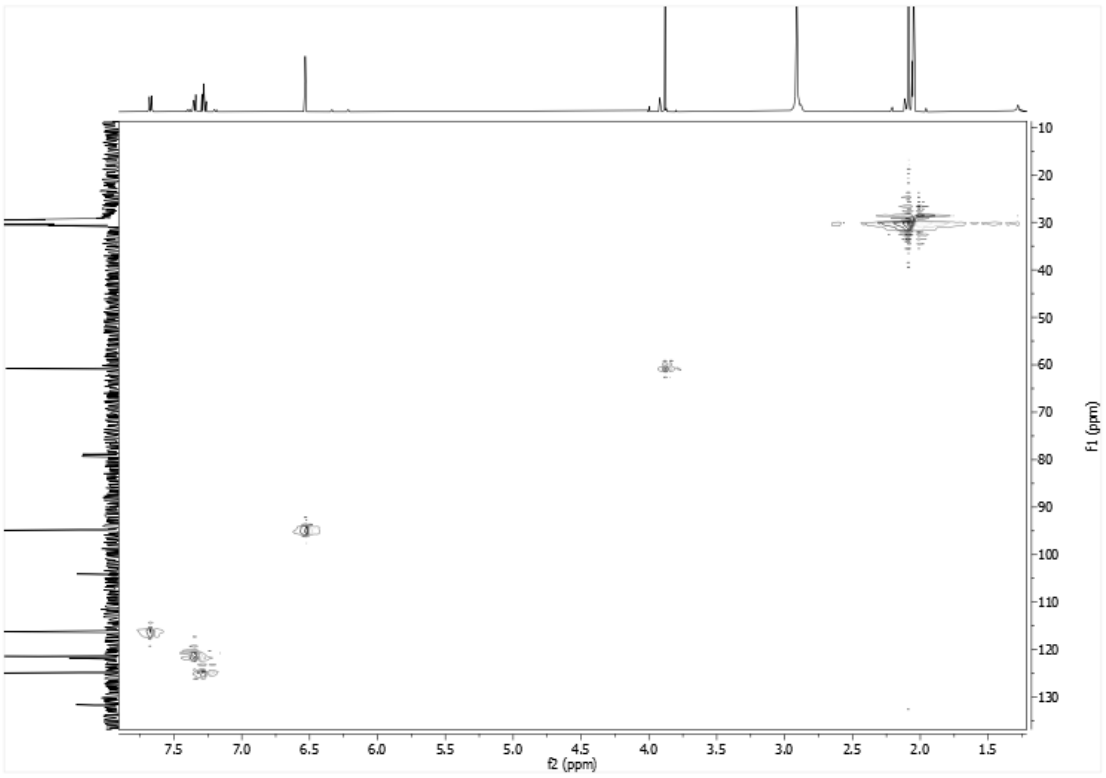

Figure A.41 HMBC spectrum (acetone-d_6) of metabolite **9**

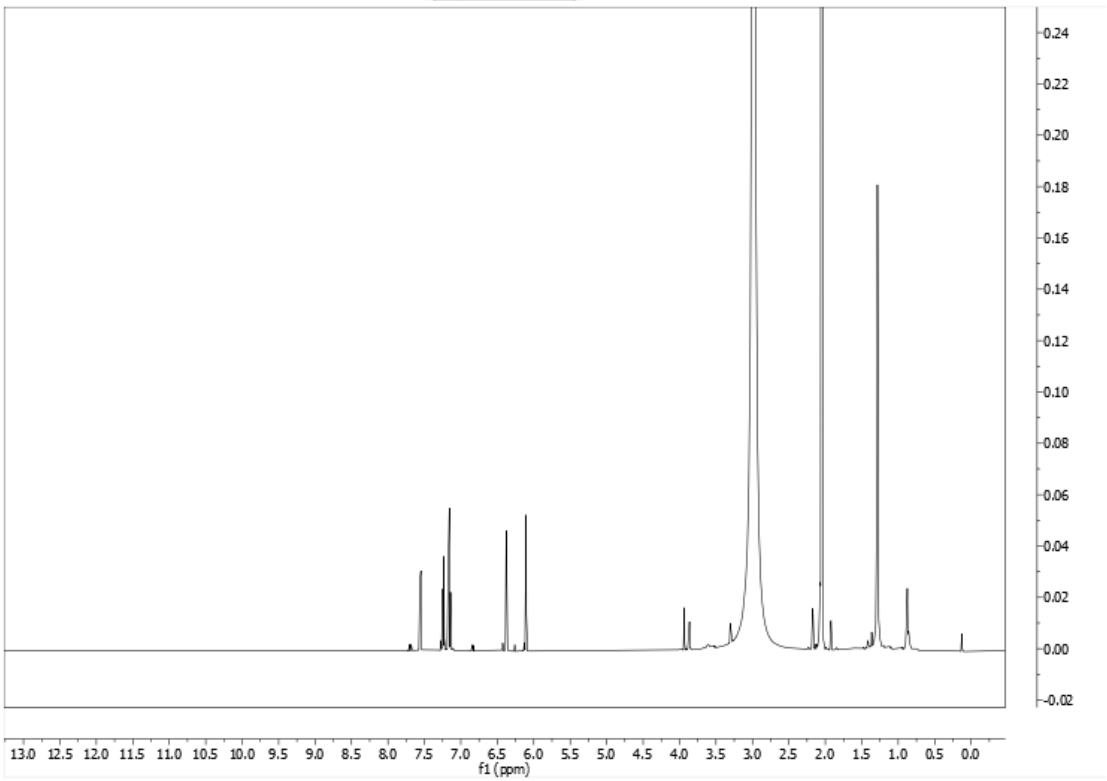

Figure A.42 ^{1}H NMR (500 MHz, acetone-d_6) spectrum of metabolite **10**

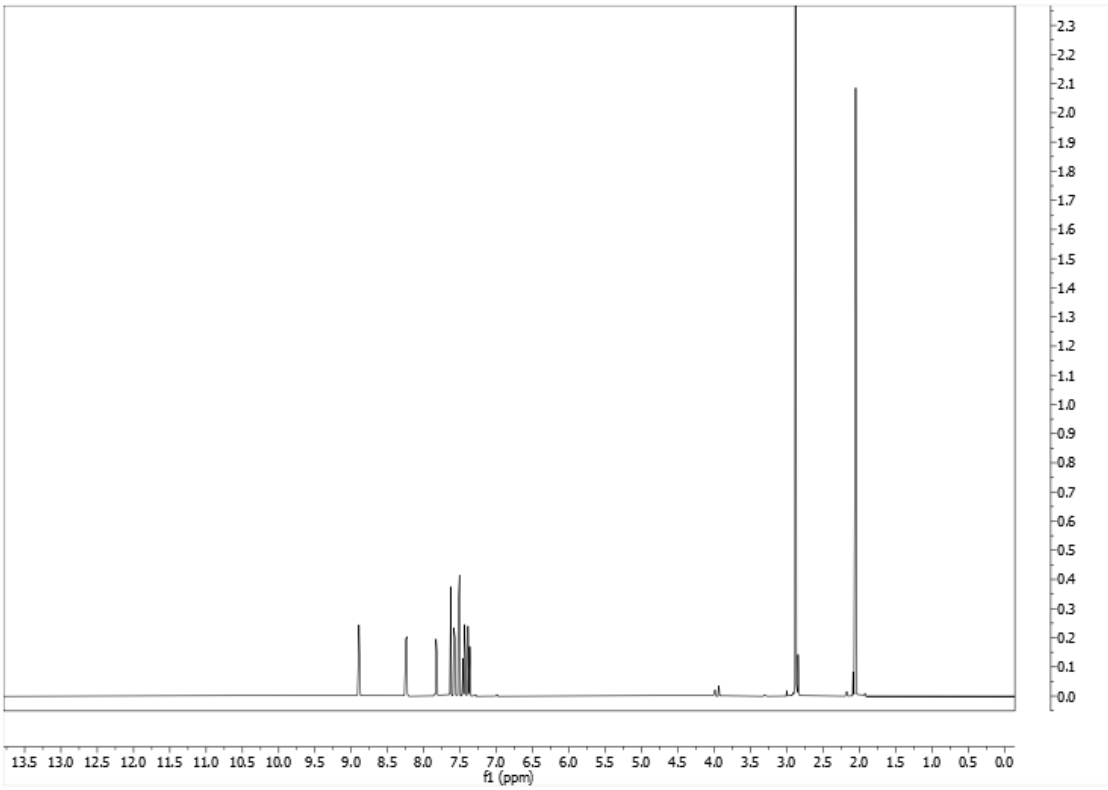

Figure A.43 ^{1}H NMR (500 MHz, acetone-d_6) spectrum of metabolite **11**

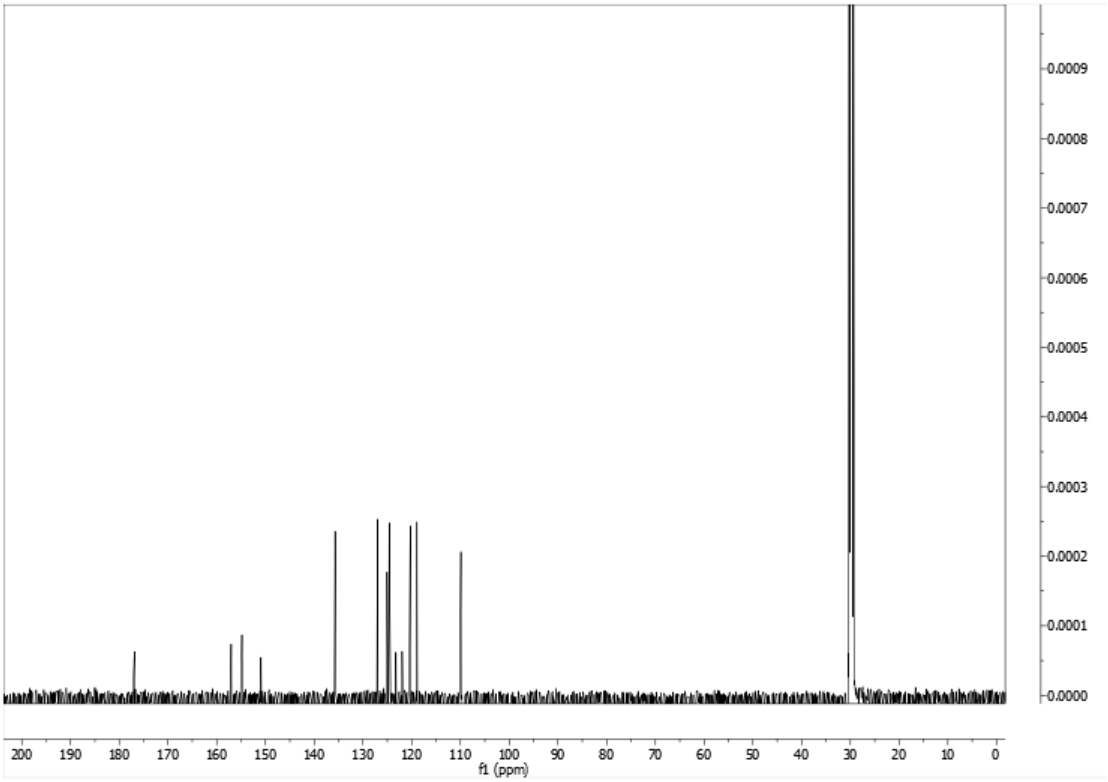

Figure A.44 ^{13}C NMR (125 MHz, acetone-d_6) spectrum of metabolite **11**

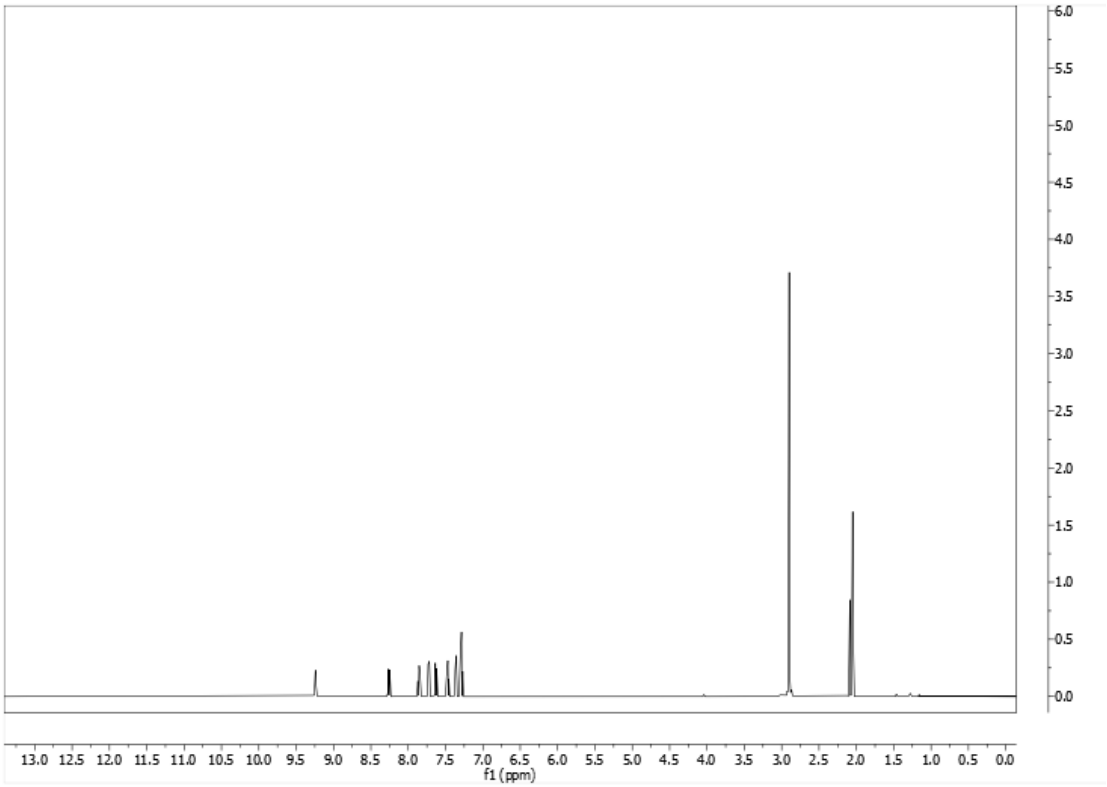

Figure A.45 ^{1}H NMR (500 MHz, acetone-d_6) spectrum of metabolite **12**

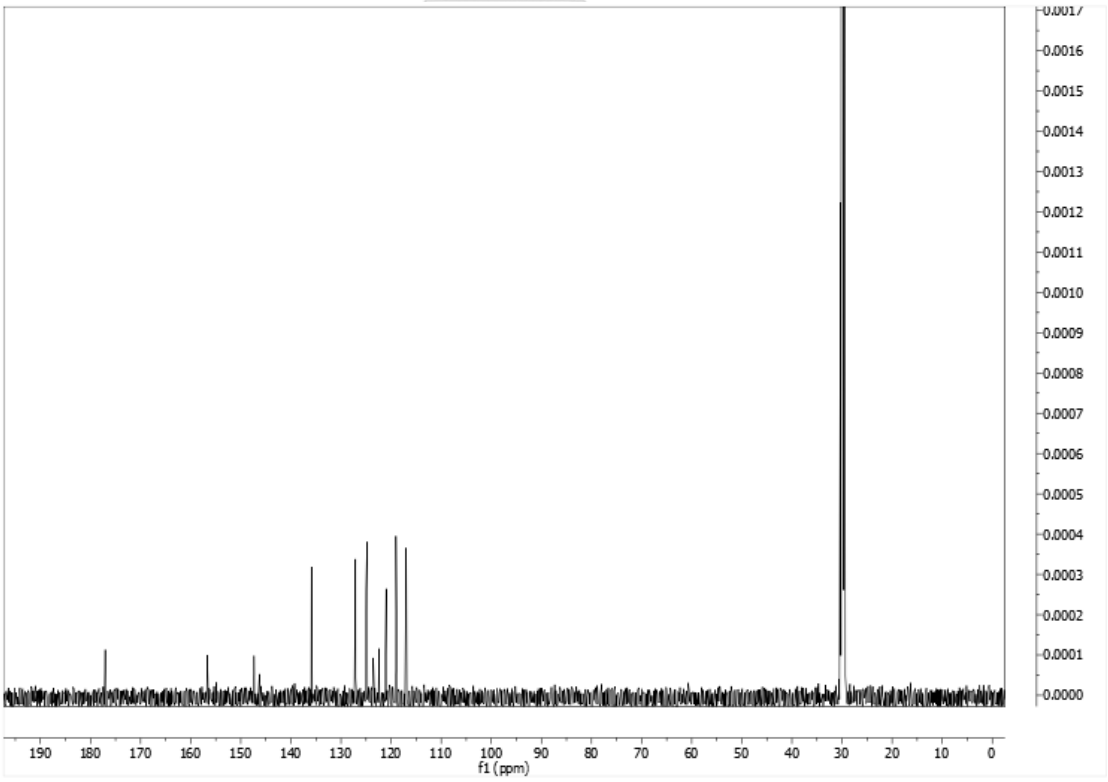

Figure A.46 ^{13}C NMR (125 MHz, acetone-d_6) spectrum of metabolite **12**

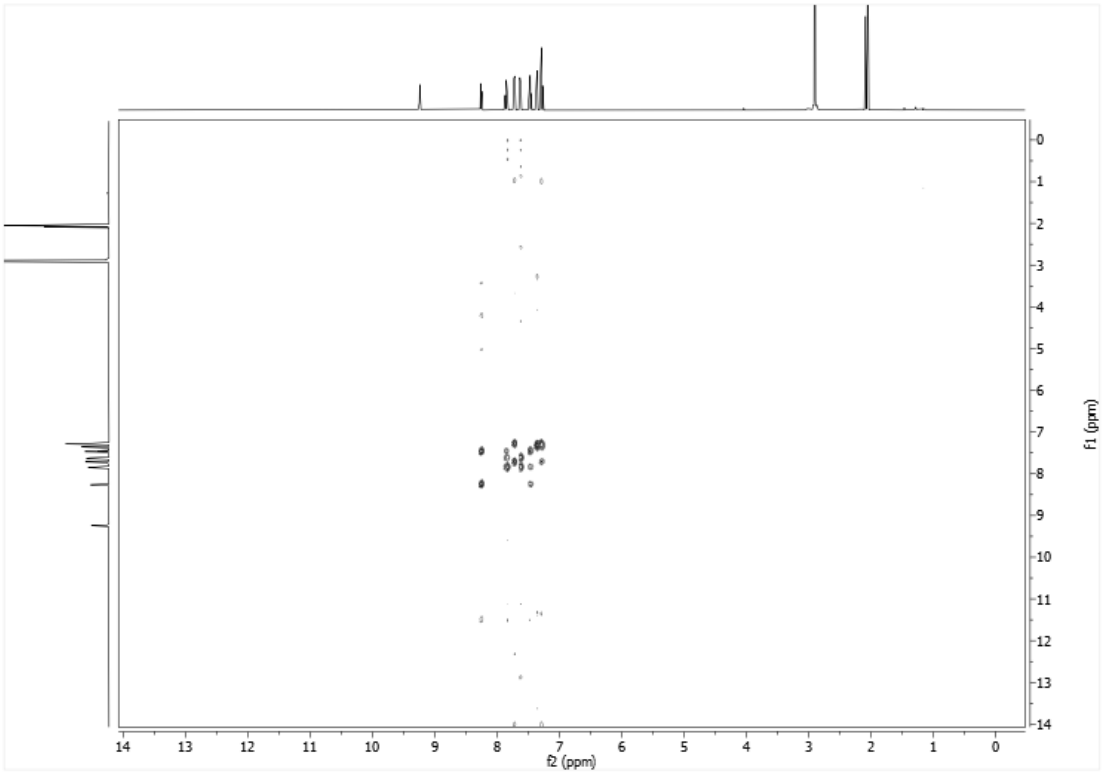

Figure A.47 ^{1}H-^{1}H COSY spectrum (acetone-d_6) of metabolite **12**

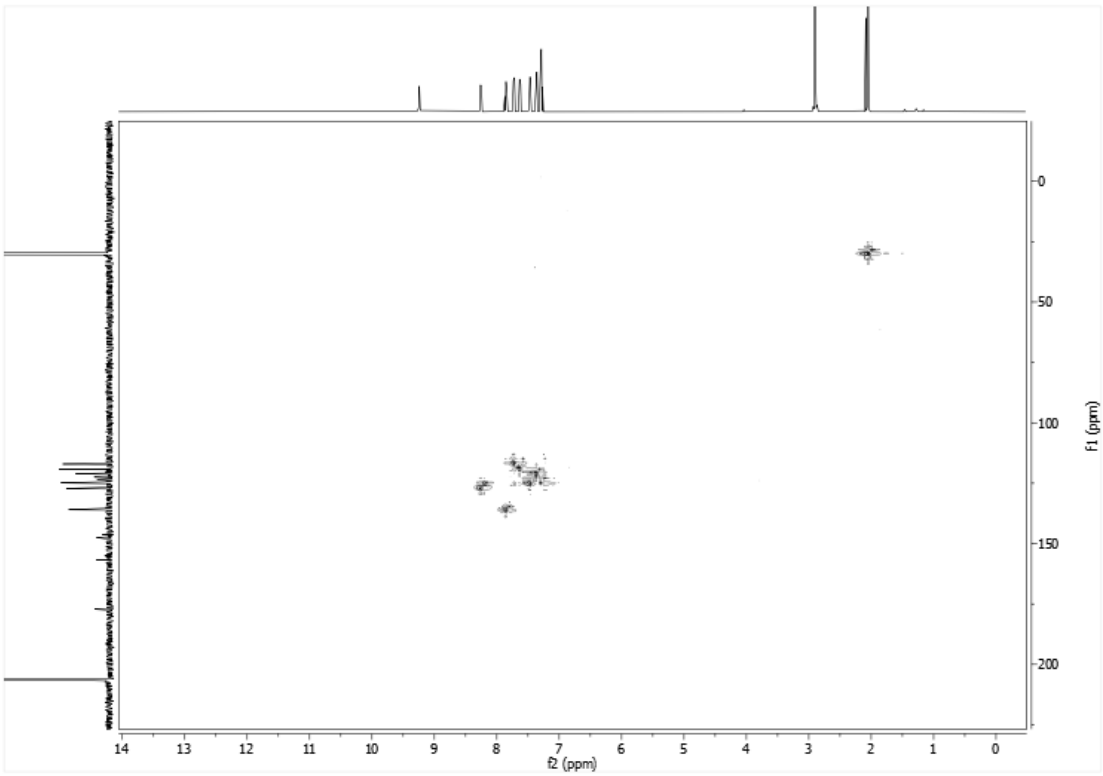

Figure A.48 HSQC spectrum (acetone-d_6) of metabolite **12**

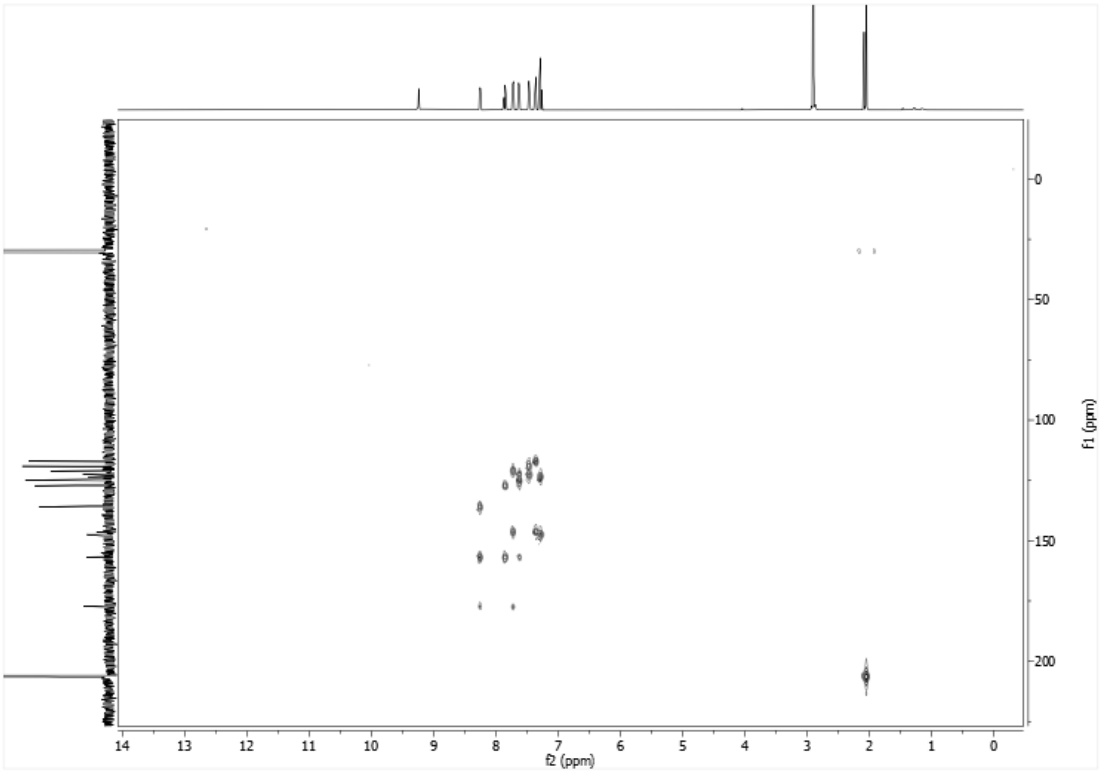

Figure A.49 HMBC spectrum (acetone-d_6) of metabolite **12**

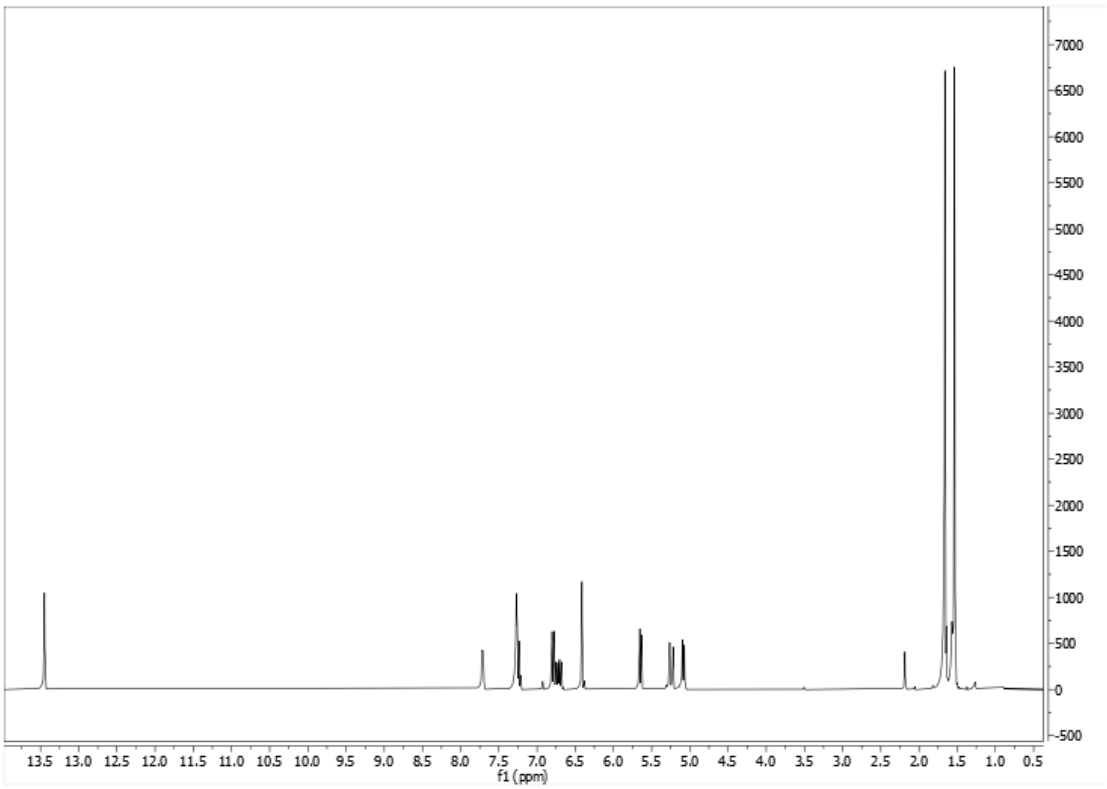

Figure A.50 ^{1}H NMR (400 MHz, $CDCl_3$) spectrum of metabolite **13**

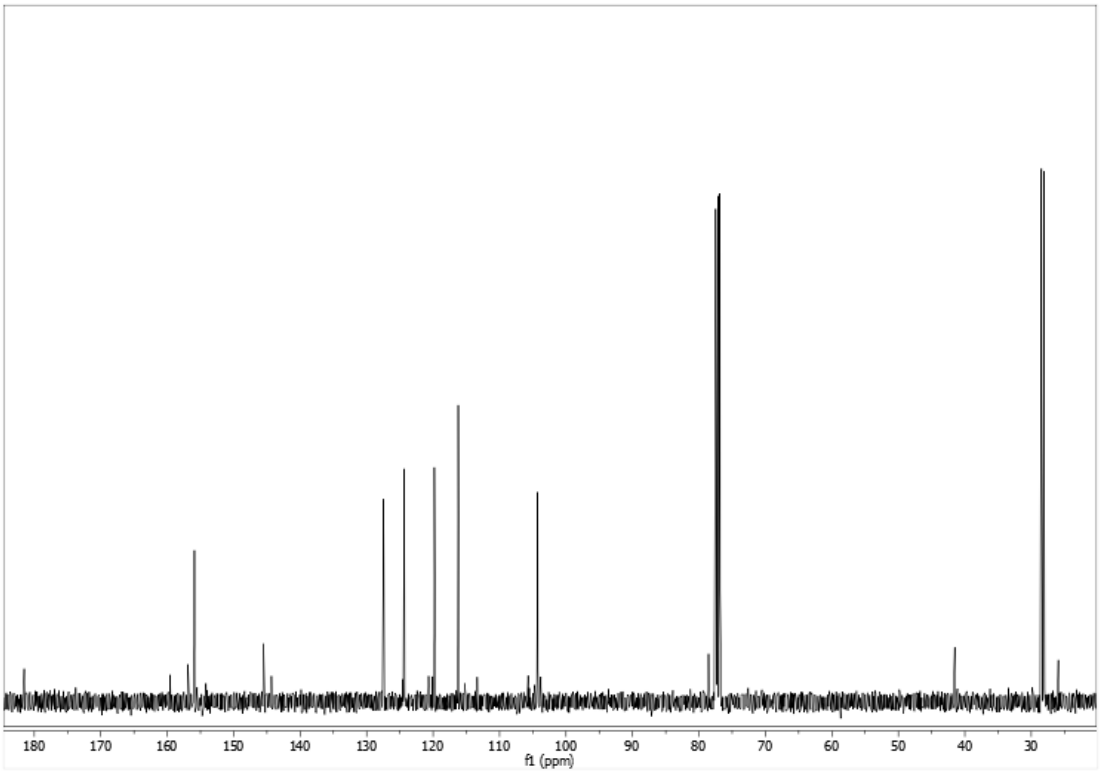

Figure A.51 ^{13}C NMR (100 MHz, $CDCl_3$) spectrum of metabolite **13**

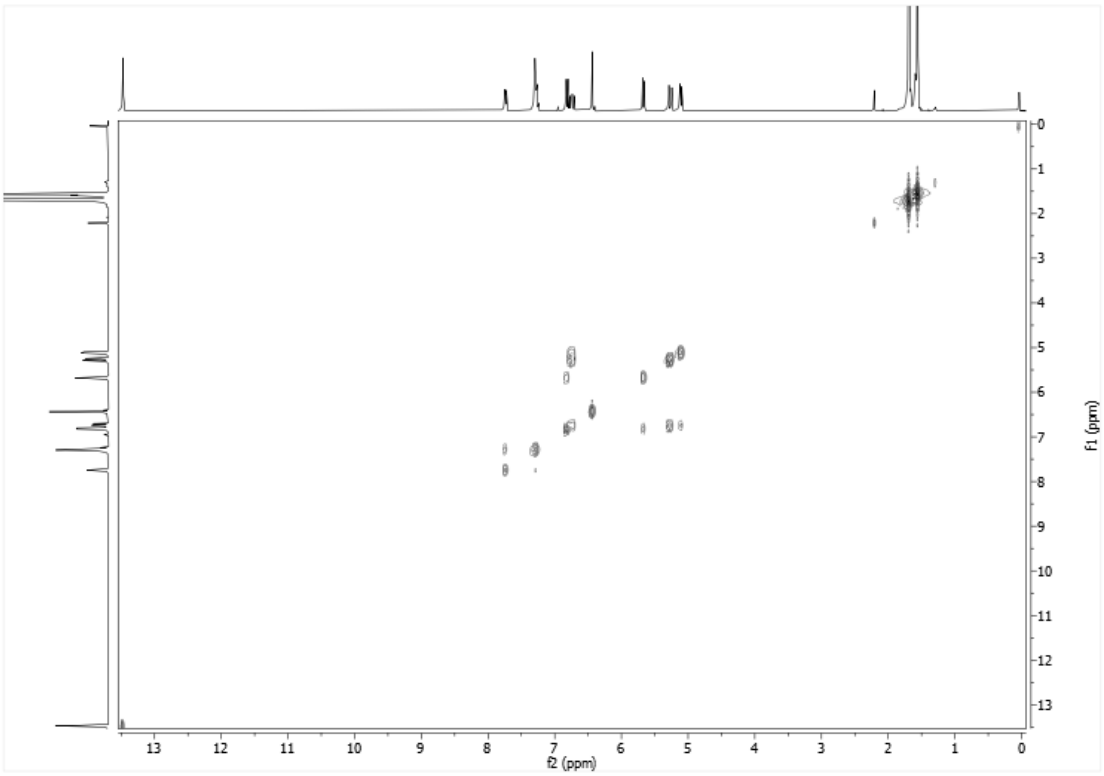

Figure A.52 ^{1}H-^{1}H COSY spectrum ($CDCl_3$) of metabolite **13**

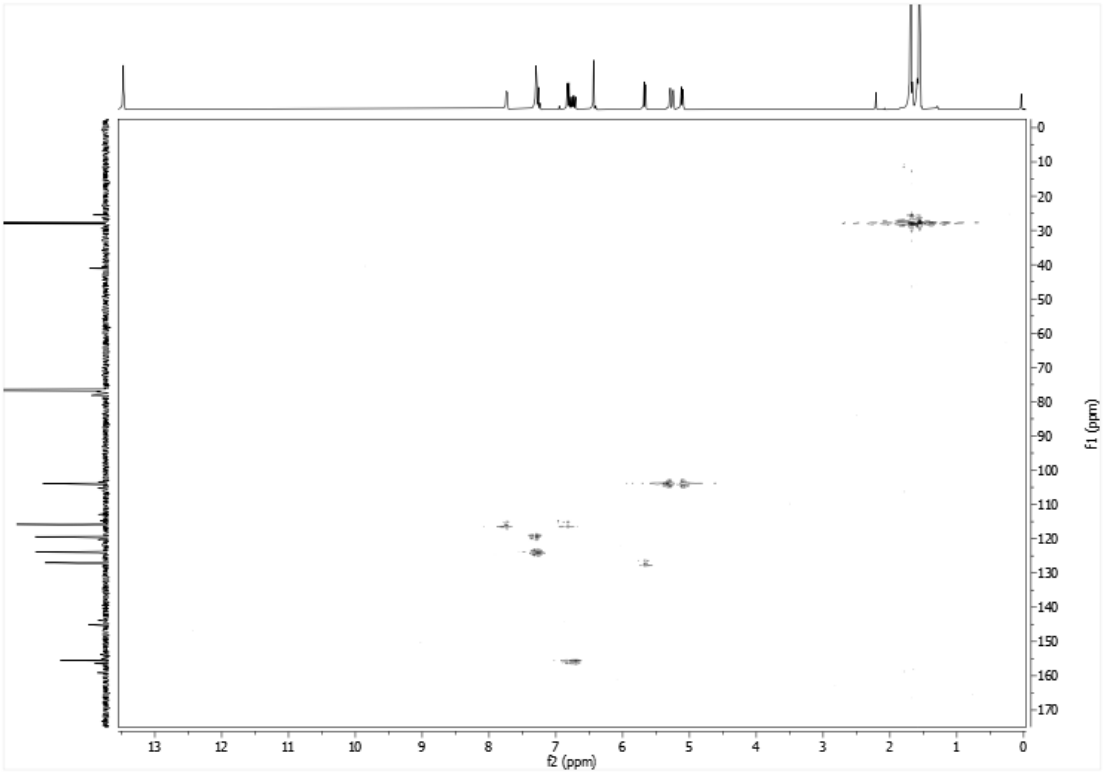

Figure A.53 HSQC spectrum ($CDCl_3$) of metabolite **13**

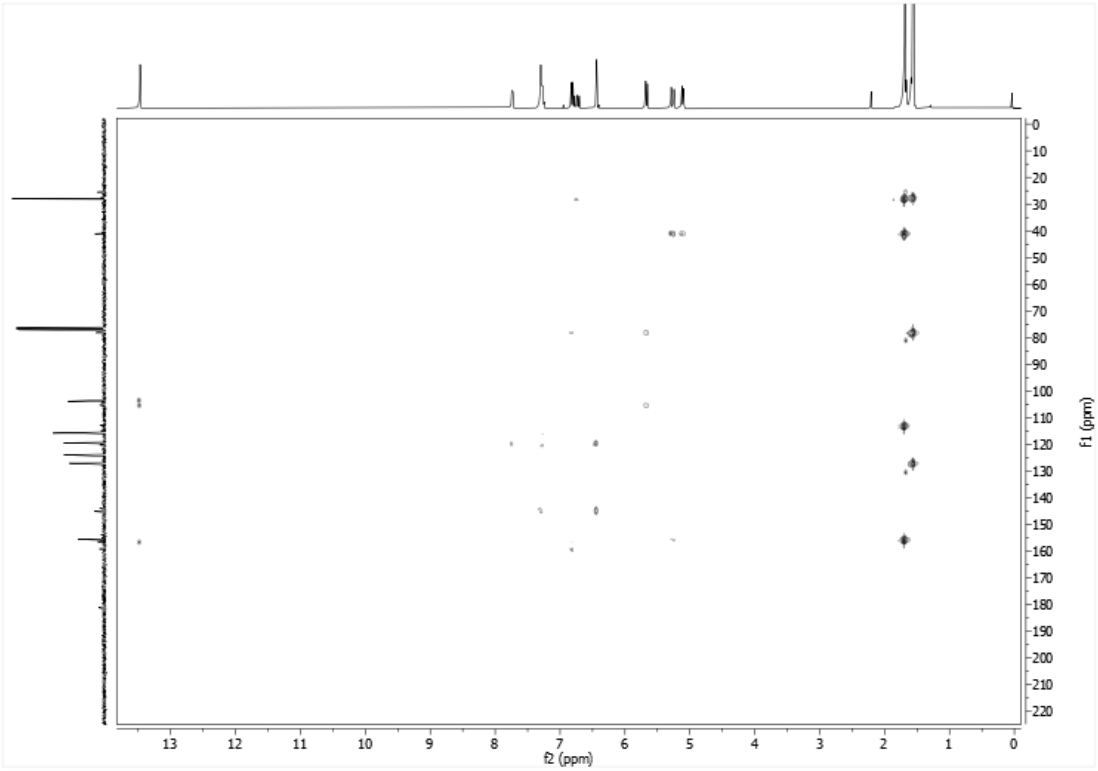

Figure A.54 HMBC spectrum ($CDCl_3$) of metabolite **13**

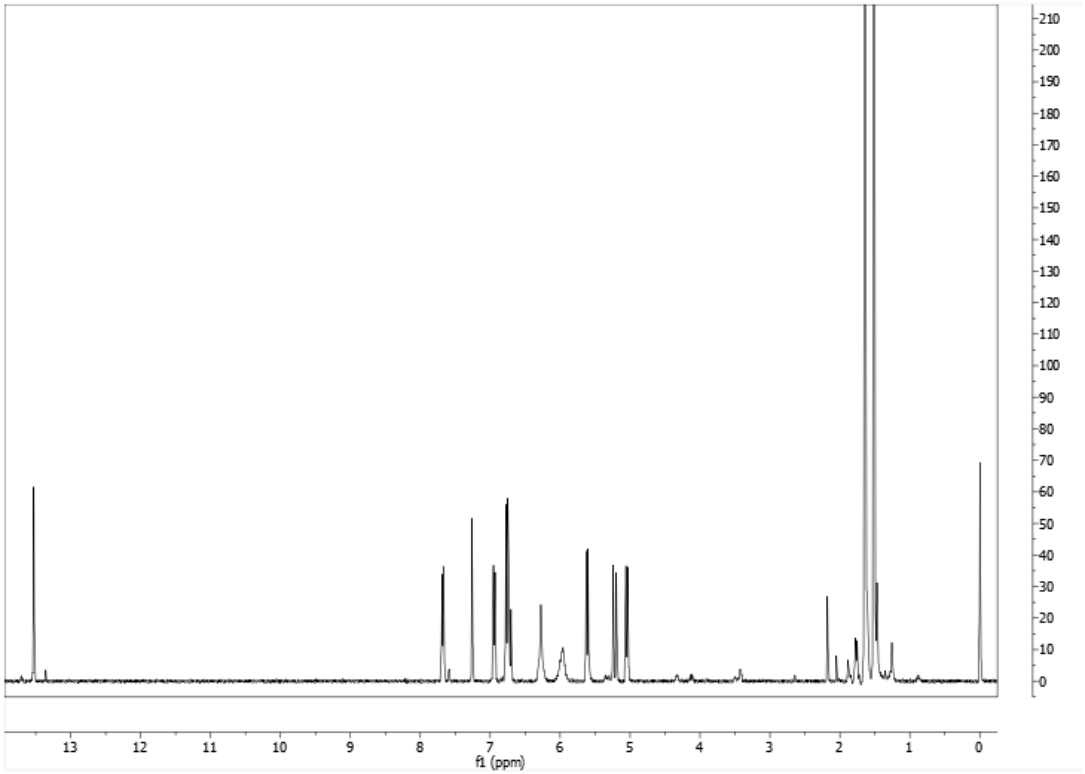

Figure A.55 ^{1}H NMR (400 MHz, $CDCl_3$) spectrum of metabolite **14**

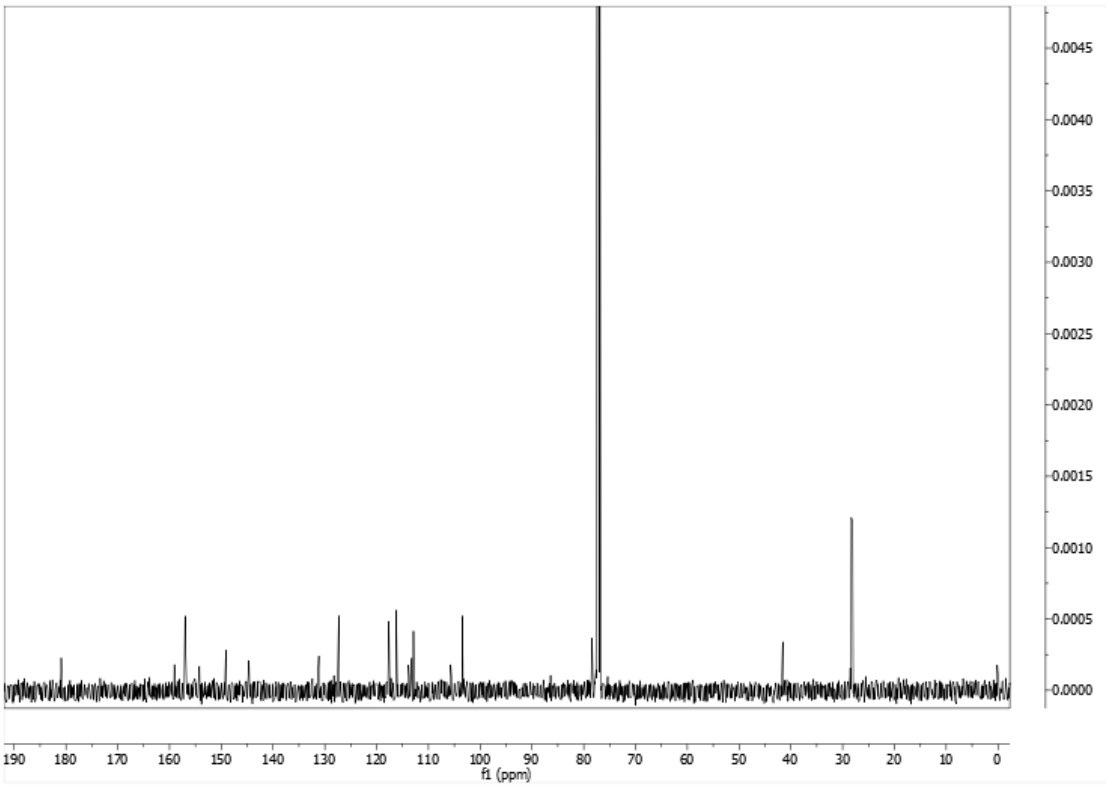

Figure A.56 ^{13}C NMR (125 MHz, $CDCl_3$) spectrum of metabolite **14**

VITA

NAME	Syahadatain Nor Haerani
DATE OF BIRTH	22 August 1994
PLACE OF BIRTH	Klaten, Central Java, Indonesia
INSTITUTIONS ATTENDED	B.Sc (Chemistry), Universitas Gadjah Mada
HOME ADDRESS	S.K. Apartment Charoenpol, 557/3 Banthattong Rd, Wangmai, Pathumwan, Bangkok 10330

จุฬาลงกรณ์มหาวิทยาลัย
CHULALONGKORN UNIVERSITY